LBL-20712
UC-45

Lawrence Berkeley Laboratory
UNIVERSITY OF CALIFORNIA

APPLIED SCIENCE DIVISION

RECEIVED
LAWRENCE
BERKELEY LABORATORY
JAN 31 1986
ARY AND
DOCUMENTS SECTION

ON THE IGNITION AND COMBUSTION OF FUEL DROPLETS AND THE IGNITION OF PREMIXED FUELS BY HOT CYLINDRICAL SURFACES

R.H. Rangel, A.C. Fernandez-Pello,
and A.K. Oppenheim

November 1985

TWO-WEEK LOAN COPY
This is a Library Circulating Copy
which may be borrowed for two weeks

APPLIED SCIENCE
DIVISION

Prepared for the U.S. Department of Energy under Contract DE-AC03-76SF00098

LBL-20712
c.2

DISCLAIMER

This document was prepared as an account of work sponsored by the United States Government. While this document is believed to contain correct information, neither the United States Government nor any agency thereof, nor the Regents of the University of California, nor any of their employees, makes any warranty, express or implied, or assumes any legal responsibility for the accuracy, completeness, or usefulness of any information, apparatus, product, or process disclosed, or represents that its use would not infringe privately owned rights. Reference herein to any specific commercial product, process, or service by its trade name, trademark, manufacturer, or otherwise, does not necessarily constitute or imply its endorsement, recommendation, or favoring by the United States Government or any agency thereof, or the Regents of the University of California. The views and opinions of authors expressed herein do not necessarily state or reflect those of the United States Government or any agency thereof or the Regents of the University of California.

ON THE IGNITION AND COMBUSTION OF FUEL DROPLETS AND THE IGNITION OF PREMIXED FUELS BY HOT CYLINDRICAL SURFACES

R.H. Rangel, A.C. Fernandez-Pello, and A.K. Oppenheim

Department of Mechanical Engineering
University of California, Berkeley
Berkeley, CA 94720

and

Applied Science Division
Lawrence Berkeley Laboratory
University of California
Berkeley, CA 94720

This work was partially supported by the U.S. Army Tank-Automotive Command under contract No. DAAE07-85-R025, by the National Science Foundation under Grants CPE-8502114 and INT. 8115965, and by the Director, Office of Energy Research, Office of Basic Energy Science, Engineering, and Geosciences Division, and the Office of Utilization Technology of the U.S. Department of Energy under contract No. DE-AC-03-76SF00098.

ABSTRACT

Two types of combustion problems relevant to the gasification, ignition and combustion of fuels in combustion chambers using sprays are theoretically analyzed using mathematical and numerical techniques. The problem of the vaporization, ignition and subsequent combustion of a fuel droplet in a hot convective flow at atmospheric or moderately elevated pressures is analyzed using boundary layer theory around a spherical fuel droplet. The preliminary stages leading to the onset of ignition are treated as a perturbation of the boundary-layer non-reacting flow using the method of matched asymptotic expansions. The quasi-steady laminar combustion regime of the fuel droplet is analyzed using the flame-sheet approximation. The internal circulation of the liquid phase is also included in the analysis. The results show that ignition occurs towards the rear of the droplet where the residence time is longer. The droplet burning rate, however, is maximum at the forward stagnation point where the boundary layer is thinner. Liquid internal motion has only a minor influence on the burning characteristics of the droplet. A second group of problems studied is the quasi-steady thermal ignition of a premixed combustible gas flowing in mixed-convective conditions past a hot cylindrical, inert or catalytic, surface. The laminar boundary-layer equations including finite-rate kinetics are solved and the location of the ignition region is determined using the method of matched asymptotic expansions for large activation energies. Ignition is shown to occur very close to the surface where the temperatures are higher and downstream of the forward stagnation point where the heat losses are smaller.

Table of Contents

Table of Contents iii

Nomenclature iv

INTRODUCTION 1

Chapter 1: LITERATURE REVIEW..... 3

1.1 Premixed Gas-phase Ignition by Inert Surfaces..... 3

1.2 Premixed Gas-phase Ignition by Catalytic Surfaces 5

1.3 Droplet Ignition 6

1.4 Droplet Combustion 8

Chapter 2: GAS-PHASE THERMAL IGNITION OF PREMIXED FUELS BY CATALYTIC AND INERT CYLINDRICAL SURFACES 11

2.1 Introduction 11

2.2 Analysis 13

2.3 Results 24

2.4 Concluding Remarks 31

Chapter 3: MIXED-CONVECTION THERMAL IGNITION OF DROPLETS AND OTHER CONDENSED FUELS 33

3.1 Introduction 33

3.2 Analysis 35

3.3 Results 45

3.4 Concluding Remarks 49

Chapter 4: MIXED-CONVECTION DROPLET COMBUSTION WITH INTERNAL CIRCULATION 51

4.1 Introduction 51

4.2 Theoretical Model 53

4.3 Analysis 55

4.4 Results 64

4.5 Concluding Remarks 71

Chapter 5: CONCLUSIONS 75

References 80

Appendix A 88

Appendix B 91

Appendix C 94

List of Figures 97

Figures 101

Introduction

Studies of the ignition and combustion of gasified fuels are traditionally classified according to whether the fuel and oxidizer are premixed or not (Williams, 1965; Kanury, 1975; Glassman, 1977). The processes of ignition and combustion of single droplets and sprays belong to the latter case, and are controlled primarily by the convective and diffusive mixing of the fuel and oxidizer. The resulting chemical reaction, if it occurs, is referred to as a diffusion flame. Studies of single and spray droplet combustion are relevant for the improvement of the combustion efficiencies using spray injection (Chigier, 1976; Blazowski, 1978) When the fuel and oxidizer are thoroughly mixed prior to their exposure to an ignition source, the mixture is referred to as a premixed combustible and the resulting chemical reaction, if it occurs, is referred to as a premixed flame. Studies of the ignition and combustion of premixed combustibles are relevant to a variety of engineering applications such as auto-ignition of combustible mixtures in diesel engines, flame stabilization in combustors, improvement of combustion efficiencies, explosions, and catalytic pollutant-control devices. (Blazowski and Walsh, 1975; Pfefferle, 1978).

In the present work, several diffusion and premixed combustion problems relevant to the gasification, ignition and combustion of fuels in combustion chambers using sprays are analyzed theoretically. The problems include the quasi-steady

thermal ignition of a premixed combustible gas flowing past a hot, cylindrical, inert or catalytic surface, and the gasification, ignition and combustion of single fuel droplets in a hot convective environment. In what follows, a literature review of studies related to the above subjects and a description of this work are presented.

Chapter 1

Literature Review

1.1 Premixed Gas-phase Ignition by Inert Surfaces

Several theoretical and experimental studies have been published of the thermal ignition of a premixed combustible gas by hot catalytic and inert surfaces. These theoretical studies, however, have been restricted to the simpler geometries of stagnation-point flows, flat-plate boundary layer, and spherically symmetric flows. Sharma and Sirignano (1969) and (1970) performed numerical analyses of the ignition of a premixed gas by a hot inert surface in a stagnation point and in a flat-plate and wake flow respectively. A very complete review of the existing literature up to 1970 was presented by Merzhanov and Averson (1971). Alkidas and Durbetaki (1971) and (1973) used numerical methods to integrate the boundary layer equations for the reacting flow in plane and axisymmetric stagnation points respectively.

Liñan (1974) introduced the technique of matched asymptotic expansions for large activation energies in a study of counterflow diffusion flames. Using first-order matched asymptotic expansions, Law (1978a) and (1978b) analyzed the stagnation point and the spherically symmetric ignition of a premixed gas by an inert surface. Su and Sirignano (1981) improved the results of the spherically symmetric ignition case by using second-order matched asymptotic expansions. Using first-order asymptotics, Berman and Ryazantser (1978), and Law

and Law (1979) studied the gas-phase thermal ignition by a hot inert flat plate. In their numerical analyses, Treviño and Sen, (1981a), (1981b), and (1982), studied the effect of the plate thermal resistance and of the Prandtl number on the ignition of a premixed gas by an inert flat plate. Treviño and Fernandez-Pello (1983) used matched asymptotic expansions to study the effect of the plate thickness in the gas-phase thermal ignition process. Law and Law (1981) used a combined perturbation/numerical procedure and included the effect of reactant consumption in their study of ignition by a hot flat plate. The transient ignition process of a stagnant fuel has been studied for the cases of a flat plate and a spherical particle by Law (1979) using matched asymptotic expansions. The same spherical case was analyzed by Su et al (1979) using numerical integration. Transient ignition in boundary layer flows past a flat plate has been studied by Treviño and Sen (1980) and (1981a) with the use of the finite-difference technique.

An experimental study of gas-phase ignition in the free-convective flow past a hot vertical surface was conducted by Cairnie et al (1981). Their results show the inadequacy of the Arrhenius model when the ignition temperatures are below 1000 K. Stout and Jones (1949) measured the amount of energy necessary to ignite fuel-air mixtures. Experimental studies of gas-phase ignition by heated cylindrical rods have been presented by Mullen et al (1949) and by Adomeit (1965). The first authors found that ignition was more readily accomplished for larger rod diameters and higher initial gas temperature. The authors indicated that the most likely ignition locations were the downstream stagnation

point and the region located about 70° from that point. In his work, Adomeit relates the ignition delay to the initial heat conduction process in the gas. A very complete review of experimental works has been presented by Laurendeau (1982).

1.2 Premixed Gas-phase Ignition by Catalytic Surfaces

Theoretical studies of the thermal ignition of a premixed combustible gas by a catalytic surface have also been limited to the geometries described above. Mory et al (1977) performed experimental and theoretical calculations of low temperature combustion of hydrogen-air mixtures. The catalytic active regions were observed to be non-uniformly distributed. Ablow et al (1980) studied the relative contribution of surface and gas phase reactions in a stagnation point flow by means of experimental, analytical and numerical models. Schefer et al. (1980) presented experimental results of both, surface and gas-phase reactions in catalytic flat-plate flows of hydrogen-air mixtures. Schefer (1982) used a numerical model including seventeen reactions to solve the boundary-layer equations for laminar flow of a hydrogen/air mixture past catalytic and inert flat plates. Treviño and Fernandez-Pello (1981) and Treviño (1983) used matched asymptotic expansions to study the gas-phase ignition in flat-plate and stagnation point flows respectively. Law and Chung (1983) considered the inhibition of the gas-phase ignition

through reactant depletion by the surface catalytic reaction. Fakhery and Bucckius (1983) studied the transient catalytic combustion of a fuel mixture at a flat plate neglecting the effects of gas-phase reactions.

1.3 Droplet Ignition

The ignition process of a fuel droplet exposed to a large temperature environment was studied experimentally and theoretically by El-Wakil and Abdou (1966). Temperature, diameter, and total ignition delay of the droplet were obtained under a variety of operating conditions. They found that total ignition delays were shorter for more volatile fuels, smaller initial diameters and higher initial droplet and air temperatures. In an experimental study, Polymeropoulos (1973) measured the vaporization rates and ignition temperatures of liquid drops in free convection using porous spheres coated with a film of fuel. A theoretical and experimental investigation was performed by Sangiovanni and Kesten (1975) using furfuryl alcohol droplets of 300 μm in diameter. Their theoretical model considered the unsteady ignition of a spherically symmetric droplet. Saitoh et al (1982) studied the problem of droplet ignition near the ignitable limit. In their experiments they found that under those conditions, ignition time delays were longer for initially smaller droplet diameters due to the

reduction of the local Damköhler number.

An analysis for ignition and extinction of condensed fuels in axisymmetric stagnation flow was presented by Fendell (1965) using pertubation theory for small and large values of the Damköhler number. Numerical integration was employed for moderate values of the Damköhler number and the characteristic S-shaped ignition-extintion curve was obtained. Matched asyptotic expansions for large activation energies were used by Law (1975) to study the quasi-steady, spherically-symmetric ignition and extintion of a fuel drop based on the solution by Liñan (1974) of the problem of counterflow diffusion flames. The mathematical correspondence between the two problems was discussed and ignition and extinction criteria were obtained. Asymptotic expansions for large activation energies were also used by Krishnamurthy (1976) in a study of ignition in the stagnation-point boundary layer. An ignition theory for spherically-symmetric droplets was presented by Law (1978c) accounting for the transient heating of the droplet. A study of unsteady ignition and extinction of spherically symmetric droplets was performed by Pindera and Brzustowski (1984) using stability theory. Their analysis yields the S-shaped ignition-extintion curve as well as some information about the stability of the transitions between the different regimes.

1.4 Droplet Combustion

Theoretical and experimental investigations on the combustion of a fuel droplet were presented by Wise et al (1954) and by Hotel et al (1954). The first authors studied the effects of several parameter using a porous sphere with a controlled supply of fuel. In their study, Hottel et al. used real droplets of different sizes and measured vaporization rates of several fuels. The theoretical approaches of these authors were based on a spherically symmetric drop model. Sanchez Tarifa et al. (1960) also considered a spherically symmetric droplet in their steady-state analysis of combustion of monopropellants and bipropellants. The unsteady behavior of the flame-to-drop diameter ratio was shown by Nuruzzaman and Beér (1971) in their experimental study using monosized droplet streams. Waldman (1974), employed the method of matched asymptotic expansions using the ratio of the droplet radius to the diffusion field radius as the small parameter. In his spherically symmetric model, the outer region was shown to be dominated by unsteady diffusion while the inner region was quasi-steady and convective-diffusive in nature. Experimental observations of droplet burning in the absence of gravity were made by Knight and Williams (1980) using a freely-falling chamber which provided 2.2 seconds of negligible gravity. A quasi-steady analysis of droplet combustion including the effect of fuel vapor accumulation in the inner region was presented by Law (1979). The neglect of such accumulation was shown to yield inaccurate estimates on the rate

of chemical heat release. Complete reviews of droplet combustion theories were presented by Williams (1973), Faeth (1977), and Law (1982a) and (1982b).

Free-convective effects on the burning of a droplet were sudied by Potter and Riley (1980) using numerical techniques, and by Fernandez-Pello and Law (1982b) using power-series expansions. Fernandez-Pello and Law (1982a) studied the gasification, ignition, steady burning and extinction in the stagnation point of a fuel particle under mixed-convective conditions. Explicit expressions were derived for the mass burning rate and for the critical ignition and extinction Damköhler numbers. The forced and mixed-convective burning of a particle was analyzed by Fernandez-Pello, (1982a) and (1982b) respectively, using power-series expansions valid up to the point of boundary-layer separation. Information on the drag experienced by a vaporizing droplet has been obtained by Yuen and Chen (1976) and the motion of the liquid inside an inviscid droplet was studied by Harper and Moore (1968). This internal circulation has a strong effect on the heating rate of the droplet as shown by Prakash and Sirignano (1978) and (1980). These authors considered the quasi-steady gas phase and thermally-unsteady liquid phase for a droplet in a forced-convective environment using an integral approach for the gas-phase solution. Tong and Sirignano (1982a) showed that the one-dimensional unsteady core region can be extended to the droplet surface with a small correction due to the existence of a liquid-phase boundary layer. Approximate analytical solutions were developed by Tong and Sirignano (1982b) and (1983) for the liquid region which are matched with the gas

phase solution at every instant of time.

Chapter 2

Gas-Phase Thermal Ignition of Premixed Fuels by Catalytic and Inert Cylindrical Surfaces

2.1 Introduction

The potential ignition of a premixed combustible gas flowing over a hot inert or catalytic surface is of relevance to the study of several combustion problems such as flame stabilization in combustors, catalytic pollutant-control devices, explosions and initiation of fires. The thermal-ignition process is primarily the result of the transfer of heat to the surrounding gas by the hot surface which initiates the chemical reaction. Because of the sensitivity of the chemical reaction to temperature, the ignition of the gas would probably occur in the boundary layer adjacent to the solid surface, where the temperatures are higher. The temperature of a catalytic surface is expected to be higher than that of an inert surface because of the heat released by the catalytic reaction. Thus, ignition of the combustible gas should more likely occur if the surface is catalytic than if it is non-catalytic. This situation would have a positive effect in the case of a flame holder as it would stabilize the gas-phase reaction. On the other hand, it may have a negative impact if the surface is that of a catalytic combustor as the role of the catalytic combustor would become unimportant once a fast gas-phase reaction is established.

In this chapter the process of gas-phase quasi-steady

thermal ignition of a premixed combustible gas by hot catalytic and inert cylindrical surfaces is analyzed for the case of a uniform and constant surface temperature. In the case of a catalytic surface it is assumed that the surface catalytic reaction is infinitely fast so that a state of thermal equilibrium exists along the surface. In the gas phase a finite-rate reaction of the Arrhenius type with a large activation energy is considered. First-order matched asymptotic methods for large activation energy are used to predict ignition. The gas flow past the cylinder is considered to be of the mixed (free and forced) convection type. It is assumed that the Reynolds and Grashof numbers are large enough so that the boundary-layer approximation is applicable to describe the flow and that the thickness of the boundary layer is small compared with the radius of the cylinder. The critical gas-phase Damköhler number for ignition will be deduced and the ignition distance along the cylindrical surface will be obtained. The gas-phase ignition distances for the inert and catalytic surfaces will be compared and it will be shown that although the catalytic surface tends to inhibit the gas-phase ignition process through the mechanism of reactant consumption, the larger surface temperatures expected in this case will favor the onset of ignition.

2.2 Analysis

The problem to be analyzed and the coordinate system used in the analysis are shown schematically in Fig. 2.1. A mixture of a gaseous fuel and oxidizer with velocity U_∞, temperature T_∞, and concentrations $Y_{i\infty}$ (i = F, O), flows over a hot catalytic or inert cylinder which has a uniform temperature T_w. The acceleration of gravity g is in the direction opposite that of the flow. In the case of a catalytic surface, the combustible gas is assumed to undergo an infinitely fast catalytic reaction at the cylinder surface where the fuel is instantaneously consumed. In both cases a finite-rate homogeneous quasi-steady ignition reaction of the Arrhenius type is considered to occur in the gas phase. It is also assumed that the Reynolds and Grashof numbers are large enough so that the boundary-layer approximation holds, and that the thickness of the boundary layer is small compared with the radius of the cylinder. A one-step, irreversible chemical reaction is assumed of the form:

$$\nu_F[F] + \nu_O[O] \longrightarrow \nu_P[P] \tag{2.1}$$

where ν_i is the stoichiometric coefficient and [I] represent the species (F = fuel, O = oxidant, P = products).

The equations that govern the process are the mass, momentum in the x-direction, energy and species boundary-layer equations for a reacting flow past a cylinder. These are neglecting curvature:

$$\frac{\partial(\rho u)}{\partial x} + \frac{\partial(\rho v)}{\partial y} = 0 \tag{2.2}$$

$$\rho u \frac{\partial u}{\partial x} + \rho v \frac{\partial u}{\partial y} = \rho_e U_e \frac{dU_e}{dx} + g(\rho_\infty - \rho)\sin\sigma + \frac{\partial}{\partial y}\left(\mu \frac{\partial u}{\partial y}\right) \tag{2.3}$$

$$\rho u c_p \frac{\partial T}{\partial x} + \rho v c_p \frac{\partial T}{\partial y} = \frac{\partial}{\partial y}\left(\lambda \frac{\partial T}{\partial y}\right) - Q\,\omega_F \tag{2.4}$$

$$\rho u \frac{\partial Y_i}{\partial x} + \rho v \frac{\partial Y_i}{\partial y} = \frac{\partial}{\partial y}\left(\rho D \frac{\partial Y_i}{\partial y}\right) + \gamma_i\,\omega_F \tag{2.5}$$

where i = F, O, P. In the above equations ρ, T, c_p, λ, D, and μ are respectively the density, temperature, specific heat at constant pressure, thermal conductivity, diffusion coefficient and viscosity of the mixture. Q is the heat of reaction per unit mass of fuel, u and v are the velocities in the x and y directions respectively, Y_i is the mass fraction of species i, and γ_i is the mass ratio between species i and fuel. For a second-order Arrhenius type reaction, the production term ω_F is given by:

$$\omega_F = -A\,W_F \nu_F \rho^2 T\, Y_F\, Y_O \exp(-E/\bar{R}\,T) \tag{2.6}$$

where A is the pre-exponential factor, W_F is the molecular weight of the fuel, E is the activation energy, and R is the universal gas constant. For an infinitely fast surface reaction, the boundary conditions for the above equations are:

At $y = 0$:

$u = 0$, $v = 0$, $T = T_w$,

catalytic surface: $Y_F = 0$, $Y_O = Y_{O\infty} - \gamma_s Y_{F\infty}$,

inert surface: $Y_F = Y_{F\infty}$, $Y_O = Y_{O\infty}$. (2.7)

At $y \to \infty$:

$u = 2\, U_\infty \sin(x/R)$, $T = T_\infty$, $Y_F = Y_{F\infty}$, $Y_O = Y_{O\infty}$. (2.8)

where γ_s is the stoichiometric mass ratio between oxidant and fuel.

Defining a stream function ψ, such that the mass conservation equation is satisfied:

$$\rho u = \mu_\infty \frac{\partial \psi}{\partial y} \quad , \quad \rho v = - \mu_\infty \frac{\partial \psi}{\partial x} \tag{2.9}$$

assuming that the quantities ρT, $\rho\lambda$, $\rho\mu$, ρD^2, and c_p are constant, and introducing the dimensionless independent variables:

$$\eta = (Re^4 + Gr^2)^{1/8} \int_0^y \frac{\rho}{\rho_\infty} \frac{dy}{R} \quad , \quad \sigma = \frac{x}{R} \tag{2.10}$$

and the functions:

$$f = \frac{\psi}{\sigma (Re^4 + Gr^2)^{1/8}} \quad , \quad \tilde{T} = \frac{c_p T}{Q} \quad , \quad \tilde{Y}_i = \frac{\nu_F W_F}{\nu_i W_i} Y_i \tag{2.11}$$

in the boundary layer equations [Eqs.(2.2)-(2.5)], these become:

$$\left(\frac{\partial f}{\partial \eta}\right)^2 + \sigma \frac{\partial f}{\partial \eta}\frac{\partial^2 f}{\partial \sigma \partial \eta} - f\frac{\partial^2 f}{\partial \eta^2} - \sigma \frac{\partial f}{\partial \sigma}\frac{\partial^2 f}{\partial \eta^2} = \frac{\sin(2\sigma)}{2\sigma(1+\varphi^2)^{1/2}} + \frac{\tilde{T}-\tilde{T}_\infty}{\tilde{T}_w-\tilde{T}_\infty}\frac{\varphi \sin\sigma}{\sigma(1+\varphi^2)^{1/2}} + \frac{\partial^3 f}{\partial \eta^3} \qquad (2.12)$$

$$\sigma \frac{\partial f}{\partial \eta}\frac{\partial \tilde{T}}{\partial \sigma} - f\frac{\partial \tilde{T}}{\partial \eta} - \sigma \frac{\partial f}{\partial \sigma}\frac{\partial \tilde{T}}{\partial \eta} = \frac{1}{Pr}\frac{\partial^2 \tilde{T}}{\partial \eta^2} + D_a \tilde{Y}_F \tilde{Y}_0 \exp(-\tilde{T}a/\tilde{T}) \qquad (2.13)$$

$$\sigma \frac{\partial f}{\partial \eta}\frac{\partial \tilde{Y}_j}{\partial \sigma} - f\frac{\partial \tilde{Y}_j}{\partial \eta} - \sigma \frac{\partial f}{\partial \sigma}\frac{\partial \tilde{Y}_j}{\partial \eta} = \frac{1}{Sc}\frac{\partial^2 \tilde{Y}_j}{\partial \eta^2} - D_a \tilde{Y}_F \tilde{Y}_0 \exp(-\tilde{T}a/\tilde{T}) \qquad (2.14)$$

where Re, Gr, Pr, Sc are the Reynolds, Grashof, Prandtl and Schmidt numbers, T_a is the nondimensional activation energy, and ϕ is the mixed convection ratio, respectively defined as:

$$Re = \frac{2RU_\infty \rho_\infty}{\mu_\infty} \qquad Gr = \frac{gR^3 \rho_\infty^2 (T_w - T_\infty)}{\mu_\infty T_\infty}$$

$$Pr = \frac{c_p \mu_\infty}{\lambda_\infty} \qquad Sc = \frac{\mu_\infty}{\rho_\infty D_\infty}$$

$$\tilde{T}_a = \frac{c_p E}{\bar{R} Q} \qquad \varphi = Gr/Re^2$$

The transformation of Eqs.(2.3)-(2.5) into Eqs.(2.12)-(2.14) is given in detail in Appendix A. The parameter:

$$Da = \frac{A\, W_0\, \nu_0\, R^2\, P_\infty\, \rho_\infty}{Re\,(1+\varphi^2)^{1/4}\, \bar{W}\, \bar{R}\, \mu_\infty} \qquad (2.15)$$

is the ratio of the residence time and the chemical time, p_∞ is the mixture pressure, and W is the mean molecular weight of the mixture. The formulation of the problem using the nondimensional parameter $(Re^4+Gr^2)^{1/8}$ permits the continuous solution of the problem of mixed-convection flow from the forced-flow limit ($\phi = 0$) to the free-flow limit ($\phi = \infty$) (Fernandez-Pello and Law, 1982).

The nondimensional boundary conditions are:

At $\eta = 0$:

$$\partial f/\partial\eta = 0 \ , \quad f = 0 \ , \quad T = T_w \ ,$$

$$\text{catalytic surface:} \quad Y_F = 0 \ , \quad Y_O = Y_{O\infty} - (\gamma_s/\gamma_O)Y_{F\infty} \ ,$$

$$\text{inert surface:} \quad Y_F = Y_{F\infty} \ , \quad Y_O = Y_{O\infty} \ . \tag{2.16}$$

At $\eta \rightarrow \infty$:

$$\partial f/\partial\eta = (1+\phi^2)^{-1/4}(\sin\sigma)/\sigma \ , \ T = T_\infty \ , \ Y_F = Y_{F\infty} \ , \ Y_O = Y_{O\infty} . \tag{2.17}$$

We now introduce a more convenient transverse independent variable defined as:

$$\xi = 1 - \frac{\int_\eta^\infty \exp(-h)\, d\eta}{Ap} \ , \quad h = Pr\int_0^\eta f\, d\eta \ , \quad Ap = \int_0^\infty \exp(-h)\, d\eta \tag{2.18}$$

in the energy and species equations [Eqs. (2.13)-(2.14)]. These become:

$$\frac{1}{Pr}\frac{\partial^2\tilde{T}}{\partial\xi^2} + \sigma\left(\exp(h)Ap\frac{\partial f}{\partial\sigma}\frac{\partial\tilde{T}}{\partial\xi} - \exp(2h)Ap^2\frac{\partial f}{\partial\eta}\frac{\partial\tilde{T}}{\partial\sigma}\right) +$$

$$D_a\tilde{Y}_F\tilde{Y}_0\exp(-\tilde{T}a/\tilde{T}) = 0 \qquad (2.19)$$

$$\frac{1}{Sc}\frac{\partial^2\tilde{Y}_i}{\partial\xi^2} + \sigma\left(\exp(h)Ap\frac{\partial f}{\partial\sigma}\frac{\partial\tilde{Y}_i}{\partial\xi} - \exp(2h)Ap^2\frac{\partial f}{\partial\eta}\frac{\partial\tilde{Y}_i}{\partial\sigma}\right) -$$

$$D_a\tilde{Y}_F\tilde{Y}_0\exp(-\tilde{T}a/\tilde{T}) = 0 \qquad (2.20)$$

The onset of ignition in the gas phase will be analyzed under the conditions when the activation energy is large. Similar analyses were performed by Law and Law (1979) and by Treviño and Fernandez-Pello (1981) in their respective studies of the thermal ignition in the boundary layer over an inert and a catalytic flat plate.

Before the establishment of the ignition reaction, the gas flow is assumed to be chemically frozen and consequently only the surface catalytic reaction is present in the catalytic case, whereas no reaction occurs on the inert surface. Under these conditions, which correspond to the limit $T_a \to \infty$, Equations (2.19) and (2.20) reduce to:

$$\frac{1}{Pr}\frac{\partial^2\tilde{T}}{\partial\xi^2} + \sigma\left(\exp(h)Ap\frac{\partial f}{\partial\sigma}\frac{\partial\tilde{T}}{\partial\xi} - \exp(2h)Ap^2\frac{\partial f}{\partial\eta}\frac{\partial\tilde{T}}{\partial\sigma}\right) = 0 \qquad (2.21)$$

$$\frac{1}{Sc}\frac{\partial^2\tilde{Y}_i}{\partial\xi^2} + \sigma\left(\exp(h)Ap\frac{\partial f}{\partial\sigma}\frac{\partial\tilde{Y}_i}{\partial\xi} - \exp(2h)Ap^2\frac{\partial f}{\partial\eta}\frac{\partial\tilde{Y}_i}{\partial\sigma}\right) = 0 \qquad (2.22)$$

with boundary conditions:

At $\xi = 0$:

$T = T_w$,

catalytic surface: $Y_F = 0$, $Y_O = Y_{O\infty} - (\gamma_S/\gamma_O) Y_{F\infty}$,

inert surface: $Y_F = Y_{F\infty}$, $Y_O = Y_{O\infty}$, (2.23)

At $\xi = 1$:

$T = T_\infty$, $Y_F = Y_{F\infty}$, $Y_O = Y_{O\infty}$. (2.24)

Equations (2.12) and (2.13) with their respective boundary conditions are solved numerically to obtain the value of the Nusselt number at the cylinder surface. This parameter will be needed later in the determination of the ignition conditions.

If the physical conditions are sufficient for the ignition of the gas, the homogeneous gas-phase chemical reaction will be initiated near the cylinder surface where the temperature is higher. Although in the case of the catalytic cylinder the fuel concentration near the surface is small due to the existence of the fast chemical reaction, the gas-phase reaction will still occur near the surface. This is due to the stronger dependence of the reaction rate on temperature, particularly for large activation energy [Eq.(2.6)]. However, the effect of reactant consumption is very important in the case of the catalytic surface and must be taken into account. At the onset of ignition, the temperature and concentration profiles will be perturbed by a small quantity of order ε from the corresponding

profiles in the homogeneous frozen flow. Therefore, a solution in this region (inner zone) is proposed of the form:

$$T = T_f + \varepsilon\theta \quad ,$$

$$Y_i = Y_{if} - \beta_i \varepsilon\theta \tag{2.25}$$

where θ is the perturbed temperature and β_i is a function of the Lewis number and is equal to one for the case Le = 1.

An order of magnitude analysis of the temperature and species concentrations near the cylinder surface shows that the proper stretched transverse independent variable for this zone should be of the form $\chi \sim \xi/\varepsilon$. Furthermore, by selecting:

$$\chi = - Ap\left[\frac{\partial \tilde{T}_f}{\partial \eta}\bigg|_w\right]\frac{\xi}{\epsilon} \tag{2.26}$$

the differential equation for the perturbed temperature is transformed into one that is identical to that obtained for a flat plate. In terms of χ the temperature and concentration profiles become:

$$T = T_w + \varepsilon(\theta - \chi),$$

catalytic surface: $Y_F = - \varepsilon(r_F\, \chi + \beta_F\theta)$, $Y_O = Y_{Ow} + 0(\varepsilon)$,

inert surface: $Y_F = Y_{F\infty} + 0(\varepsilon)$, $Y_O = Y_{O\infty} + 0(\varepsilon)$. (2.27)

where $Y_{Ow} = Y_{O\infty} - (\gamma_s/\gamma_O)\, Y_{F\infty}$.

Substitution of the above relations into Eqs.(2.19) and (2.20) shows the convective terms to be of order ε^3 while the diffusion and reaction terms are of order ε^2 for the catalytic surface and of order ε for the inert surface (See Appendix B for details of this analysis). The small parameter is found to be given by $\varepsilon = T_w^2/T_a$. This order of magnitude analysis shows the inhibitory character of the catalytic reaction which is seen to reduce the gas-phase reaction by an order of magnitude through the mechanism of fuel depletion. Moreover, in the case of a stoichiometric mixture, the gas-phase reaction term in the catalytic-surface case is reduced by two orders of magnitude from its value in the inert-surface case. In such a case, the reaction, diffusion, and convective terms are all of the same order of magnitude and the full equation (reactive-diffusive-convective) has to be solved. Physically this means that, due to the low concentration of reactants near the surface, the gas-phase reaction is initiated further away from the surface where the velocities are higher. Since most catalytic combustion applications operate with lean mixtures this case is not considered here. For the lean-mixture catalytic-surface case the resulting equation for the perturbed temperature is:

$$\frac{\partial^2\theta}{\partial\chi^2} + \frac{\Delta_1}{2}(\chi - \alpha\theta)\exp(\theta - \chi) = 0 \qquad (2.28)$$

where:

$$\alpha = - \left.\frac{\partial \tilde{T}_f}{\partial \eta}\right|_w \Big/ \left.\frac{\partial \tilde{Y}_{Ff}}{\partial \eta}\right|_w = \frac{c_p (T_w - T_\infty)}{Q\, Y_{F\infty}} \tag{2.29a}$$

and:

$$\Delta_1 = \frac{2\, Q\, T_w^4\, Y_{F\infty} Y_{Ow} Pr\, Da \exp(-Ta/T_w)}{\gamma_0\, c_p\, Ta^2\, (T_w - T_\infty)^3 \left[Nu_f^2 / Re(1+\varphi^2)^{1/4} \right]} \tag{2.29b}$$

is the relevant Damköhler number for the catalytic-surface case.

For the inert-surface case the perturbed equation results:

$$\frac{\partial^2 \theta}{\partial \chi^2} + \frac{\Delta_2}{2} \exp(\theta - \chi) = 0 \tag{2.30}$$

where:

$$\Delta_2 = \frac{2\, Q\, T_w^2\, Y_{F\infty} Y_{O\infty} Pr\, Da \exp(-Ta/T_w)}{\gamma_0\, c_p\, Ta\, (T_w - T_\infty)^2 \left[Nu_f^2 / Re(1+\varphi^2)^{1/4} \right]} \tag{2.31}$$

is the relevant Damköhler number for the inert-surface case.

In the above equations, $Nu_f = q_w R / [\lambda_\infty (T_w - T_\infty)]$ is the frozen-flow local Nusselt number, which contains the dependence on the angular location of the Damköhler numbers Δ_1 and Δ_2. The boundary conditions for Eqs. (2.28) and (2.30) are $\theta(0) = 0$ and $(\partial\theta/\partial\chi)|_\infty = 0$. The latter boundary condition is obtained through the matching of the inner and outer solutions as discussed by Law and Law (1979).

The heat flux at the cylinder surface is a parameter that

has the potential of being indicative of the onset of ignition. The general expression for the heat transfer at the cylinder surface is:

$$q_w = -\lambda \left.\frac{\partial T}{\partial y}\right|_w - \rho D \left.\frac{\partial Y}{\partial y}\right|_w Q \qquad (2.32)$$

where the first term is due to the temperature gradient at the cylinder surface and the second term is due to the heat released by the catalytic reaction, if this is present, at the cylinder surface. The nondimensional form of Eq. (2.32) for unity Lewis number is:

Catalytic cylinder:

$$\tilde{q}_{w1} = \frac{q_w\, R\, c_p}{Re^{1/2}(1+\varphi^2)^{1/8}\lambda_\infty Q\, Y_{F\infty}} = \frac{Nu_f}{Re^{1/2}(1+\varphi^2)^{1/8}}(\alpha - 1) \qquad (2.33)$$

Inert cylinder:

$$\tilde{q}_{w2} = \frac{q_w\, R}{Re^{1/2}(1+\varphi^2)^{1/8}\lambda_\infty(T_w - T_\infty)} = \frac{Nu_f}{Re^{1/2}(1+\varphi^2)^{1/8}}\left[1 - \left.\frac{\partial\theta}{\partial\chi}\right|_w\right] \qquad (2.34)$$

Equation (2.33) shows that the net heat flux at the surface of the catalytic cylinder is independent of the onset of the gas phase reaction. This is due to the fact that variations of the two terms in Eq. (2.32) exactly oppose each other. As the gas phase reaction develops, the heat released by the catalytic reaction decreases with the increased reactant consumption in

the gas-phase reaction. However, the corresponding increase in the gas-phase temperature results in the decrease of the temperature gradient at the surface and consequently in the reduction of the heat flux from the surface to the gas. The condition of zero heat transfer at the catalytic surface only occurs for the case of $\alpha=1$. On the other hand, Eq. (2.34) indicates that the heat flux at the surface of the inert cylinder decreases during the onset of ignition from its frozen value to zero at the moment of ignition when $\partial\theta/\partial\chi|_w = 1$. This is due to the increased generation of heat by the gas-phase reaction, which results in the increase of the gas temperature and consequently in the decrease of the temperature gradient at the surface. The above effects are scaled by the value of the Nusselt number at the corresponding angular location. The general trend of these results is similar to that predicted for a flat plate (Law and Law, 1979; and Treviño and Fernandez-Pello, 1981).

2.3 Results

The variation of the frozen-flow Nusselt number along the cylinder surface is presented in Fig. 2.2 for values of the mixed-convection ratio of $\phi = 0$ (forced flow), $\phi = 1$ (mixed flow), and $\phi = \infty$ (free flow). It is seen that the surface Nusselt number (heat flux) decreases from a maximum at the forward stagnation point to a minimum at the point of boundary layer separation. This is due to the growth of the boundary

layer with the angular coordinate.

Information about the gas-phase ignition process is obtained from the integration of Eqs. (2.28) and (2.30). The numerical integration of these equations shows that there is a critical value of the Damköhler number $\Delta = \Delta^c$ for which a unique solution of the corresponding equation exists. For $\Delta > \Delta^c$ there are no solutions of the equations and for $\Delta < \Delta^c$ there are to solutions of each equation, one of which has no physical meaning. The critical Damköhler number Δ^c indicates the thermal runaway and therefore determines the onset of ignition in the gas phase.

The maximum value of the perturbed temperature occurs at $\chi \rightarrow \infty$. Fig. 2.3 shows this maximum value, $\theta(\infty)$, as a function of the Damköhler number Δ_1 for different values of the parameter α. The upper branches correspond the physically meaningless solution. The critical Damköhler numbers $\Delta_1{}^c$ correspond to the points of infinite slope $(\partial\theta(\infty)/\partial\Delta_1 = \infty)$. The values of the critical Damköhler numbers $\Delta_1{}^c$ obtained from Fig. 2.3 are presented in Fig. 2.4 as functions of α. It is observed that the critical Damköhler number $\Delta_1{}^c$ increases as

the parameter α increases, that is, as the fuel mixture becomes leaner, the fuel temperature T_∞ becomes lower or the gas-phase heat of reaction Q is reduced. The effect of the parameter α on the initiation of the gas-phase reaction is not readily apparent from Fig. 2.4 as the combination of variables forming this parameter also appears in the denominator of the expression for the Damköhler number Δ_1 (Eq. 2.29). With only one exception, an increase in α produces a negative effect on the onset of the gas-phase reaction as will be explained now. A decrease in the mixture temperature T_∞, the fuel concentration $Y_{F\infty}$, or the gas-phase heat of reaction Q, yields an increase in the critical Damköhler number $\Delta_1{}^c$, as Fig 2.4 indicates, and also produces a decrease in the particular current value of the Damköhler number Δ_1 (Eq. 2.29). The result is a reduction in the possibility of ignition in the gas phase. An exception to this trend corresponds to an increase in the surface temperature T_w. This also produces an increase in the parameter α and consequently an increase in the critical Damköhler number $\Delta_1{}^c$ (Fig. 2.4). However, due to the very high sensitivity to temperature of the exponential in the expression for the

Damköhler number Δ_1, the effect is a substantial increase in the latter, possibly beyond the critical value and therefore promoting ignition in the gas phase.

Integration of Eq. (2.30) for the inert cylinder results in the ignition curve presented in Fig. 2.5. It is seen that in this case a unique critical Damköhler number $\Delta_2{}^c = 1$ is obtained. This result is similar to that obtained by Law and Law (1979) for a non-catalytic flat plate.

The dependence of the ignition process on the problem physical variables is obtained by equating the Damköhler numbers Δ_1 and Δ_2 to their corresponding critical values $\Delta_1{}^c$ and $\Delta_2{}^c$. The location along the cylinder surface at which ignition occurs is found through the angular dependence of the frozen-flow Nusselt number Nu_f appearing in Eqs. (2.29) and (2.30). In order to facilitate the graphic representation of the ignition angular location, it is convenient to define two Damköhler numbers $\Delta_{1\sigma}$ and $\Delta_{2\sigma}$ which are independent of the polar angle σ. The new Damköhler numbers are defined by:

$$\Delta_{n\sigma} = \left[\frac{Nu_f}{Nu_{f0}}\right]^2 \Delta_n \quad , \qquad n = 1 , 2 \qquad (2.35)$$

where Nu_{f0} is the frozen-flow Nusselt number at the forward

stagnation point. When the maximum perturbed temperature $\theta(\infty)$ is plotted against the Damköhler number $\Delta_{n\sigma}$, different curves are obtained for different values of the angular location σ as can be seen in Fig. 2.6 for a representative case. The critical values of the two new Damköhler numbers defined by Eq. (2.35) can be found by setting Δ_1 and Δ_2 in Eq. (2.35) equal to their respective critical values given in Figs. 2.4 and 2.5, that is:

$$\Delta^c_{n\sigma} = \left[\frac{Nu_f}{Nu_{f0}}\right]^2 \Delta^c_n \quad , \qquad n = 1 , 2 \qquad (2.36)$$

These critical Damköhler numbers are functions of the angular coordinate σ, as can be seen in Eq. (2.36), and their variation with σ obtained with the aid of Figs. 2.2, 2.4, and 2.5 is shown in Figs. 2.7, 2.8, and 2.9 for values of the mixed-convection ratio of $\phi = 0$, $\phi = 1$, and $\phi = \infty$, respectively. As in the results presented before, the critical Damköhler number $\Delta_{1\sigma}{}^c$ for the catalytic case, has a parametric dependence on α, whereas a unique curve is obtained for $\Delta_{2\sigma}{}^c$. It is also seen that for all flow conditions, the critical Damköhler numbers decrease as the angular coordinate increases, indicating that ignition occurs more easily with increasing

distance downstream from the front stagnation point. The dependance of the ignition location on the variables of the problem is obtained by substituting the expression for Da (Eq. 2.15) into Eq. 2.29 for the catalytic surface and Eq. (2.31) for the inert surface and then equating Δ_1 and Δ_2 in these equations to their corresponding critical values given in Figs. (2.4) and (2.5). It is deduced that the ignition angular coordinate increases as the activation energy increases, or as the initial gas temperature, the fuel concentration or the surface temperature decreases. These results agree with a phenomenological description of the problem in terms of the respective variations of the physical and chemical times with the above variables. As the initial gas or plate temperature decreases, the physical time decreases and in order to balance the fixed chemical time, the reaction must occur further downstream where the boundary layer is thicker, heat losses are smaller, and consequently, the physical time is larger. As the activation energy increases or the initial fuel concentration decreases, the chemical time increases and in order to balance the chemical and physical times, the ignition process must occur further downstream, where the physical time is larger.

The ratio of ignition angular locations between catalytic and inert cylindrical surfaces provides interesting information about the differences between the ignition processes in both cases. For the same fluid properties, excess oxidizer and activation energy, but different plate temperatures, the

following relation between both ignition locations is obtained:

$$\frac{\sigma_1}{\sigma_2} \sim \frac{(T_{w_1} - T_\infty)^3 \, Ta \, T_{w_2}^2 \, \exp(-Ta/T_{w_2})}{(T_{w_2} - T_\infty)^2 \, T_{w_1}^4 \, \exp(-Ta/T_{w_1})} \tag{2.37}$$

In a practical case, it is expected that the surface temperature of the catalytic cylinder would be larger than the temperature of the inert cylinder because of the generation of heat by the catalytic reaction. From Eq.(2.37) it is seen that in this case $\sigma_1 < \sigma_2$ due to the strong temperature dependence of the exponentials. This result suggests the advantage of using a catalytic surface in flame holders instead of an inert one since gas ignition will occur closer to the forward stagnation point. For the same plate temperature, however, Eq. (2.37) gives:

$$\frac{\sigma_1}{\sigma_2} \sim \frac{1}{\epsilon} \Delta_1^c \, \alpha \tag{2.38}$$

which indicates that under these circumstances ignition occurs further downstream for the catalytic than for the inert surface. For example, in a free-convection flow ($\phi \rightarrow \infty$) with $\alpha = 0.1$ and $\varepsilon = 0.002$, if the ignition location is the front stagnation point for an inert cylinder, the corresponding ignition location for a catalytic cylinder would be $\sigma = 170^\circ$, close to the rear of the cylinder. This result shows the inhibitory character of the catalytic surface reaction on the

gas-phase reaction because of the reduction of the fuel concentration near the wall.

2.4 Concluding Remarks

An analysis has been performed of the gas-phase thermal ignition of a premixed combustible gas flowing over a hot catalytic or inert cylindrical surface. The analysis shows that if gas-phase ignition is intended, the use of a catalytic surface is recommendable because the higher temperature generated by the catalytic surface reaction will favor the ignition of the gas. On the other hand, if the catalytic and inert surfaces have the same temperature, gas-phase ignition will occur later with the catalytic surface because the consumption of fuel at the surface reaction inhibits the chemical reaction in the gas phase. The analysis also shows that in both cases gas-phase ignition conditions are more favorable as the flow approaches the separation point. Since the analysis is not applicable once the boundary layer separates, it cannot predict the exact location where ignition will be initiated. For natural convection, however, separation does not occur until practically the rear stagnation point, thus, it appears that this would be the location where ignition occurs under this flow condition. For mixed and forced convection flow, boundary-layer separation occurs somewhere along the rear portion of the cylinder depending on the mixed-flow intensity and it is not possible to identify the

initial location of ignition. For an inert cylinder it appears that ignition would be initiated in the wake region at the rear of the cylinder since there the residence time should be large. In the case of a catalytic cylinder, however, the products of the surface reaction may accumulate in the wake region in which case gas-phase ignition may not occur in this zone. If this is the case, ignition will most likely occur at the point of boundary-layer separation. The present analysis can be easily applied with minor modifications to the case of spherical surfaces. If the sphere has a catalytic surface its surface temperature will reach the adiabatic flame temperature because the heat released by the surface catalytic reaction cannot be evacuated. Thus in this case ignition will likely occur uniformly on the sphere surface and a flame will immediately surround the sphere. In the case of an inert sphere it will not be possible to keep its temperature constant since convective cooling of the surface would occur prior to ignition. However, the case of a constant-temperature sphere has little practical importance.

Chapter 3

Mixed-Convection Ignition of a Droplet or a Cylindrical Fuel

3.1 Introduction

The thermal ignition of condensed and liquid fuels has been the subject of many theoretical and experimental investigations due to the relevance that this phenomenon has in an important number of combustion processes such as droplet and spray combustion in engineering applications, and initiation and propagation of fires. When a liquid fuel droplet or other condensed ignitable material is introduced in a high-temperature oxidizing environment, the resulting temperature gradient at the surface of the fuel will produce a heat flux from the ambient toward the droplet. This heat flux will in general serve two purposes: Part of the heat flux will be further transmitted toward the interior of the fuel and will result in an increase of the liquid temperature. The rest of the heat flux will be used to overcome the latent heat of vaporization of the fuel and will therefore result in the evaporation of the liquid at the surface. The fuel vapors produced at the gas-liquid interface will be diffused outwards and convected downstream and outwards into the high-temperature oxidizing region. Under the appropriate conditions, which will be identified later, the fuel and oxidizer will combine and initiate a reaction process which may lead to a temperature runaway and to a fully established diffusion flame. In the case of a droplet that has been injected into a combustion chamber,

the objective of the combustor designer is to promote and accelerate the onset of the ignition process described above. On the other hand, in fire-prevention studies one is interested in suppressing or at least delaying the ignition process. As it will be shown in the analysis, there are several factors that affect the initiation of the gas-phase reaction, among which we may mention the convective conditions, the ambient temperature and oxidizer concentration, and the activation energy.

In this chapter, an analysis is presented of the quasi-steady ignition of a constant-temperature, spherical or cylindrical, liquid or condensed fuel that is exposed to a high-temperature oxidizing gas. It is assumed that the oxidizing gas is flowing with a velocity U_∞ which is parallel to the direction of gravity. As a result of this, a mixed-convection flow pattern is established in the vicinity of the droplet or cylindrical fuel. Moreover, it is assumed that either the Reynolds or Grashof number is large enough so that the boundary-layer approximation is validated and that the thickness of the boundary layer is small compared with the radius of the droplet or cylindrical fuel. The droplet or cylindrical fuel is assumed to be in equilibrium vaporization at a uniform and constant vaporization temperature. The weakly initiating gas-phase reaction is assumed to be a one-step process governed by an Arrhenius-type expression with a large activation energy. First-order matched asymptotic expansions for large activation energy are used to describe the ignition process. The analysis yields the critical Damköhler number for ignition as well as the location on the droplet surface at

which ignition is likely to begin.

3.2 Analysis

Figure 3.1 shows a schematic of the model to be analyzed as well as the coordinate system employed. A single-component fuel droplet or condensed cylindrical fuel of radius R at its vaporization temperature T_w is in equilibrium vaporization in an oxidizing gas of high temperature T_∞, oxygen concentration $Y_{O\infty}$, and velocity U_∞. The acceleration of gravity g is in the direction of the flow. The appearance of a chemical reaction in the gas phase will be directly related to the values of the residence and chemical times. If the chemical time is much larger than the residence time, ignition is not possible. On the other hand, if the ratio of the residence time to the chemical time is large enough, an ignition reaction is considered to take place in the gas phase. Since the chemical reaction is very sensitive to temperature, the ignition process will occur near the outer edge of the boundary layer where the temperatures are higher. This reaction is assumed to be irreversible and to consist of one step:

$$\nu_F[F] + \nu_O[O] \longrightarrow \nu_P[P] \tag{3.1}$$

where ν_i is the stoichiometric coefficient of species i and [I] represents the species (F = fuel, O = oxidizer, P = products).

Under the assumption of a large Grashof or Reynolds number,

the process is governed by the boundary-layer conservation equations of mass, momentum in the x direction, energy, and species. These equations are, neglecting curvature:

$$\frac{\partial(a^n \rho u)}{\partial x} + \frac{\partial(a^n \rho v)}{\partial y} = 0 \tag{3.2}$$

$$\rho u \frac{\partial u}{\partial x} + \rho v \frac{\partial u}{\partial y} = \rho_e U_e \frac{dU_e}{dx} + g(\rho_\infty - \rho)\sin\sigma + \frac{\partial}{\partial y}\left(\mu \frac{\partial u}{\partial y}\right) \tag{3.3}$$

$$\rho u c_p \frac{\partial T}{\partial x} + \rho v c_p \frac{\partial T}{\partial y} = \frac{\partial}{\partial y}\left(\lambda \frac{\partial T}{\partial y}\right) - Q\,\omega_F \tag{3.4}$$

$$\rho u \frac{\partial Y_i}{\partial x} + \rho v \frac{\partial Y_i}{\partial y} = \frac{\partial}{\partial y}\left(\rho D \frac{\partial Y_i}{\partial y}\right) + \gamma_i\,\omega_F \tag{3.5}$$

where the last equation actually represents as many equations as species are to be considered (i = F, O, P). In the above equations, the constant n is equal to 0 for cylindrical geometry and 1 for spherical geometry. The fluid properties are: density ρ, viscosity μ, specific heat at constant pressure c_p, thermal conductivity λ, and diffusion coefficient D. Q is the heat of reaction per unit mass of fuel, γ_i is the mass ratio between the species i and the fuel, u and v are respectively the velocities in the x and y directions, T is the temperature and Y_i is the mass fraction of the species i. The production term ω_F is given by an Arrhenius-type expression:

$$\omega_F = - A W_F \nu_F \rho^2 T Y_F Y_0 \exp(-E/\bar{R} T) \tag{3.6}$$

where A is the pre-exponential factor, W_F is the molecular weight of the fuel, E is the activation energy per mol, and R is the universal gas constant.

The boundary conditions to be met by the above equations are the requirements of no-slip at the surface, equilibrium evaporation and mass conservation at the surface; and the conditions at the free stream. In mathematical form these requirements are:

At $y = 0$:

$$u = 0 \quad , \quad \rho v h_{fg} = \lambda \partial T/\partial y \quad , \quad T = T_w \quad ,$$

$$\rho v = \rho v Y_F - \rho D(\partial Y_F/\partial y) \quad ,$$

$$0 = \rho v Y_i - \rho D(\partial Y_i/\partial y) \quad , \quad i \neq F. \tag{3.7}$$

At $y \to \infty$:

$$u = U_e = (2-n/2) U_\infty \sin(x/R), \quad T = T_\infty, \quad Y_F = 0, \quad Y_O = Y_{O\infty}. \tag{3.8}$$

The next step is the introduction of a stream function defined by:

$$a^n \rho u = \mu_\infty \frac{\partial(a^n \psi)}{\partial y} \quad , \quad a^n \rho v = - \mu_\infty \frac{\partial(a^n \psi)}{\partial x} \tag{3.9}$$

so that the continuity equation is immediately satisfied.

It is convenient to define dimensionless variables for the temperature, activation temperature, and mass fractions as:

$$\tilde{T} = \frac{c_p T}{Q} \quad , \quad \tilde{T}_a = \frac{c_p E}{\bar{R} Q} \quad , \quad \tilde{Y}_i = \frac{\nu_F W_F}{\nu_i W_i} Y_i \tag{3.10}$$

and appropriate dimensionless independent variables as:

$$z = \int_0^y \frac{\rho}{\rho_\infty} \frac{dy}{R} \quad , \quad \sigma = \frac{x}{R} \tag{3.11}$$

Assuming that the quantities ρT, $\rho\mu$, $\rho\lambda$, $\rho^2 D$, and c_p are constant and introducing more appropriate boundary-layer independent and dependent variables given by:

$$\eta = (Re^4 + Gr^2)^{1/8} z = Re^{1/2}(1 + \phi^2)^{1/8} z ,$$

$$f = (Re^4 + Gr^2)^{-1/8} \psi/\sigma = Re^{1/2}(1 + \phi^2)^{1/8} \psi/\sigma. \tag{3.12}$$

in the boundary-layer equations [Eqs.(3.2)-(3.5)], these become:

$$\left(\frac{\partial f}{\partial \eta}\right)^2 + \sigma \frac{\partial f}{\partial \eta}\frac{\partial^2 f}{\partial \sigma \partial \eta} - \left(f + \sigma \frac{\partial f}{\partial \sigma} + n\, f\, \sigma \cot\sigma\right)\frac{\partial^2 f}{\partial \eta^2} =$$

$$\frac{\sin(2\sigma)}{2\sigma(1+\varphi^2)^{1/2}} + \frac{\tilde{T} - \tilde{T}_\infty}{\tilde{T}_w - \tilde{T}_\infty}\,\frac{\varphi \sin\sigma}{\sigma(1+\varphi^2)^{1/2}} + \frac{\partial^3 f}{\partial \eta^3}. \qquad (3.13)$$

$$\frac{\partial f}{\partial \eta}\frac{\partial \tilde{T}}{\partial \sigma} - \left(f + \sigma\frac{\partial f}{\partial \sigma} + n f \sigma \cot\sigma\right)\frac{\partial \tilde{T}}{\partial \eta} = \frac{1}{Pr}\frac{\partial^2 \tilde{T}}{\partial \eta^2} + D_a \tilde{Y}_F \tilde{Y}_0 \exp(-\tilde{T}a/\tilde{T}). \qquad (3.14)$$

$$\frac{\partial f}{\partial \eta}\frac{\partial \tilde{Y}_i}{\partial \sigma} - \left(f + \sigma\frac{\partial f}{\partial \sigma} + n f \sigma \cot\sigma\right)\frac{\partial \tilde{Y}_i}{\partial \eta} = \frac{1}{Sc}\frac{\partial^2 \tilde{Y}_i}{\partial \eta^2} - D_a \tilde{Y}_F \tilde{Y}_0 \exp(-\tilde{T}a/\tilde{T}). \qquad (3.15)$$

where the dimensionless parameters are:

$$Re = \frac{(2-\frac{n}{2})RU_\infty \rho_\infty}{\mu_\infty}, \quad Gr = \frac{gR^3 \rho_\infty^2 (T_\infty - T_w)}{\mu_\infty T_\infty}$$

$$Pr = \frac{c_p \mu_\infty}{\lambda_\infty}, \quad Sc = \frac{\mu_\infty}{\rho_\infty D_\infty} \qquad (3.16)$$

and the mixed-convection ratio is defined as:

$$f = Gr/Re^2 \qquad (3.17)$$

A detailed derivation of Eqs. (3.13)-(3.15) is given in Appendix C. The parameter Da represents an appropriate Damköhler number, or the ratio of the residence time and the chemical time. It is given by:

$$Da = \frac{A\, W_0\, \nu_0\, R^2\, P\, \rho_\infty}{Re\,(1+\varphi^2)^{1/4}\, \overline{W}\, \overline{R}\, \mu_\infty} \qquad (3.18)$$

where p is the pressure and W is the mean molecular weight of the mixture. If this Damköhler number is too small the reaction term is negligible and the flow is said to be frozen.

Under the preceding variable transformation, the boundary conditions given by Eqs. (3.7) and (3.8) become:

At $\eta = 0$:

$$\frac{\partial f}{\partial \eta} = 0 \ , \quad -\left(f + \sigma\frac{\partial f}{\partial \sigma} + nf\sigma\cot\sigma\right) = \frac{Q}{Pr\, h_{fg}}\frac{\partial \tilde{T}}{\partial \eta} \ , \quad \tilde{T} = \tilde{T}_w \ ,$$

$$\left(f + \sigma\frac{\partial f}{\partial \sigma} + nf\sigma\cot\sigma\right)(1-\tilde{Y}_F) = \frac{1}{Sc}\frac{\partial \tilde{Y}_F}{\partial \eta} \ , \tag{3.19}$$

$$-\left(f + \sigma\frac{\partial f}{\partial \sigma} + nf\sigma\cot\sigma\right)\tilde{Y}_i = \frac{1}{Sc}\frac{\partial \tilde{Y}_i}{\partial \eta} \ .$$

At $\eta \to \infty$:

$$\frac{\partial f}{\partial \eta} = \frac{\sin\sigma}{\sigma(1+\psi^2)^{1/4}} \ , \quad \tilde{T} = \tilde{T}_\infty \ , \quad \tilde{Y}_F = 0 \ , \quad \tilde{Y}_O = \tilde{Y}_{O\infty} \tag{3.20}$$

It has been recognized above that the ignition process must be initiated towards the outer edge of the gaseous boundary layer because it is there where the temperature is high enough to compensate for the retarding effect of the large activation energy. It is then convenient to introduce a coordinate transformation that will translate the origin to the outer edge of the boundary layer. The coordinate η, which goes from 0 at

the fuel surface to ∞ at the outer edge of the boundary layer, is replaced by the coordinate ξ, which goes from 0 at the outer edge of the boundary layer to 1 at the fuel surface. A similar transformation has been used by Krishnamurthy (1976) in a study of ignition at the stagnation-point boundary layer. The variable ξ is defined by:

$$\xi = 1 - \frac{\int_0^\infty \exp(-h)\, d\eta}{Ap} \quad , \qquad (3.21)$$

$$h = Pr \int_0^\eta \left(f + \sigma \frac{\partial f}{\partial \sigma} + n f \sigma \cot\sigma\right) d\eta \quad , \quad Ap = \int_0^\infty \exp(-h)\, d\eta$$

As a result of this transformation, the boundary-layer equations for conservation of energy and species [Eqs.(3.14) and (3.15)] become:

$$\frac{1}{Pr}\left[\frac{\partial \xi}{\partial \eta}\right]^2 \frac{\partial^2 \tilde{T}}{\partial \xi^2} - \sigma\left[\frac{\partial \xi}{\partial \eta}\right]\frac{\partial f}{\partial \xi}\frac{\partial \tilde{T}}{\partial \sigma} + D_a \tilde{Y}_F \tilde{Y}_0 \exp(-\tilde{T}a/\tilde{T}) = 0 \qquad (3.22)$$

$$\frac{1}{Pr}\left[\frac{\partial \xi}{\partial \eta}\right]^2 \frac{\partial^2 \tilde{Y}_i}{\partial \xi^2} - \sigma\left[\frac{\partial \xi}{\partial \eta}\right]\frac{\partial f}{\partial \xi}\frac{\partial \tilde{Y}_i}{\partial \sigma} - D_a \tilde{Y}_F \tilde{Y}_0 \exp(-\tilde{T}a/\tilde{T}) = 0 \qquad (3.23)$$

When the activation energy is large, $Ta \gg 1$ and the temperature T is low, the reaction term becomes negligible and Equations (3.22) and (3.23) simplify further to:

$$\frac{1}{Pr}\left[\frac{\partial \xi}{\partial \eta}\right] \frac{\partial^2 \tilde{T}}{\partial \xi^2} - \sigma \frac{\partial f}{\partial \xi} \frac{\partial \tilde{T}}{\partial \sigma} = 0 \tag{3.24}$$

$$\frac{1}{Pr}\left[\frac{\partial \xi}{\partial \eta}\right] \frac{\partial^2 \tilde{Y}_i}{\partial \xi^2} - \sigma \frac{\partial f}{\partial \xi} \frac{\partial \tilde{Y}_i}{\partial \sigma} = 0 \tag{3.25}$$

which corresponds to the frozen-flow or non-reactive vaporization solution.

Near the outer edge of the boundary layer ($\xi \rightarrow 0$), the temperature is sufficiently high and therefore a chemical reaction will be initiated. Due to the very high sensitivity to temperature of the exponential reaction term, the chemical reaction will be confined to a very narrow zone at the outer edge of the boundary layer. The temperature and species-concentration profiles in this region will be slightly perturbed as a consequence of the weakly-proceeding reaction. The temperature and species concentrations in the ignition zone are therefore proposed of the form:

$$T = T_f + \varepsilon\theta \tag{3.26}$$

$$Y_i = Y_{if} - \varepsilon\theta \tag{3.27}$$

where θ is the perturbed temperature. With the assumption of unity Lewis number, the equations for the perturbed temperature and concentrations are identical, which validates the use of the same perturbed variable in Equations (3.26) and (3.27).

As it was mentioned above, the ignition zone will be restricted to a narrow region in the vicinity of $\xi=0$. Consequently, stretching this coordinate seems appropriate. The

stretched coordinate can be shown to be of the form $\chi \sim \xi/\varepsilon$, and, following the arguments used in Chapter 2 for the ignition of a premixed fuel, the stretched transverse variable is selected as:

$$\chi = -\left[\frac{\partial \tilde{T}}{\partial \xi}\bigg|_{\xi=0}\right]\frac{\xi}{\epsilon} \tag{3.28}$$

because this choice will permit the evaluation of the solution in terms of an already solved problem. In terms of χ, the temperature and concentration profiles in the vicinity of $\xi=0$ become:

$$T = T_\infty + \varepsilon(\theta - \chi) \tag{3.29}$$

$$Y_F = -\varepsilon(\theta + r_F\,\chi) \tag{3.30a}$$

$$Y_O = Y_{O\infty} - \varepsilon(\theta + r_O\chi) \tag{3.30b}$$

where:

$$r_F = \frac{\partial \tilde{Y}_{Ff}}{\partial \xi}\bigg|_0 \Big/ \frac{\partial \tilde{T}_f}{\partial \xi}\bigg|_0 \quad , \quad r_O = \frac{\partial \tilde{Y}_{Of}}{\partial \xi}\bigg|_0 \Big/ \frac{\partial \tilde{T}_f}{\partial \xi}\bigg|_0 \tag{3.31}$$

Substitution of Equations (3.28)-(3.30) into the energy-conservation equation [Eq.(3.22)] shows that the small parameter is given by the expression $\varepsilon = T_\infty{}^2/Ta$ (the treatment of the temperature exponential term is similar to that used in Appendix B for the case of a premixed fuel. In this case,

however, the temperature is perturbed from its free-stream value) The differential equation for the perturbed temperature results:

$$\chi^2 \frac{\partial^2 \theta}{\partial \chi^2} - \Omega \frac{\partial \theta}{\partial \sigma} + \Delta(\chi - \alpha\theta) \exp(\theta - \chi) = 0 \qquad (3.32)$$

where:

$$\Delta = \frac{Pr\, \tilde{Y}_{0\infty} Da \exp(-Ta/T_\infty)}{\alpha\ H} \quad , \quad \Omega = \frac{Pr \sin\sigma}{H(1+\varphi^2)^{1/4}} \qquad (3.33)$$

and:

$$H = \left(\left[\frac{\partial}{\partial \xi} \left(\frac{\partial \xi}{\partial \eta} \right) \right]_{\xi=0} \right)^2 = Pr^2 \left(f(\infty) + \sigma \frac{\partial f}{\partial \sigma}(\infty) + n f(\infty) \sigma \cot\sigma \right)^2$$

$$\alpha = - \left. \frac{\partial \tilde{T}_f}{\partial \xi} \right|_0 \Big/ \left. \frac{\partial \tilde{Y}_{Ff}}{\partial \xi} \right|_0 = \frac{c_p (T_\infty - T_w) + h_{fg}}{Q} \qquad (3.34)$$

The three terms in Eq. (3.32) can be easily identified as diffusion, convection, and reaction, respectively. The parameter Δ represents the ratio of the residence and chemical times and is therefore the relevant Damköhler number of the problem. If this Damköhler number is too small, the reaction term drops out of the equation and the frozen case is obtained. It should be noted that the Damköhler number Δ is a function of the angular coordinate σ and that consequently the ignition process is also σ-dependent. The parameter Ω appears as a

factor in the convective term and it controls the relative importance of this term with respect to the other two. In the case of a forced or relatively mild mixed flow ($0<\phi<5$), this term must be retained and the full partial differential equation has to be solved. In the case of a free-convective flow, however, the convective term vanishes since for this case $\Omega \rightarrow 0$ as $\phi \rightarrow \infty$.

3.3 Results

Equation (3.32) has been solved numerically by Liñan (1974) for several values of the parameter α. The solution provides the Damköhler number for ignition, Δ^c, as a function of α. Those solutions are shown in Fig.3.2, where the characteristic s-shaped ignition curves can be seen. For each value of the parameter α there is one s-shaped curve. For values of Δ below the critical value Δ^c two solutions are obtained one of which has no physical meaning. For Δ larger than Δ^c no solutions of the equation exist. The point $\Delta=\Delta^c$ corresponds to the thermal runaway and indicates the transition from the incipient-ignition regime to the diffusion-flame regime. The influence of the flow parameters on the onset of ignition at the stagnation point of a fuel particle was analyzed by Fernandez-Pello and Law (1982). The analysis in this chapter is concerned with the determination of the region along the fuel surface in which ignition is likely to occur. For a given set

of physical properties and flow conditions, we seek to establish the location of the thermal runaway along the fuel periphery. The Damköhler number defined by Eq.(3.33) may be rewritten in the case of free convection as:

$$\Delta = \frac{A Y_{0\infty} P \mu_\infty \exp(-Ta/T_\infty)}{\alpha \rho_\infty Pr \bar{R} \bar{W} v_\infty^2} \tag{3.35}$$

where v_∞ is the entrainment velocity at the outer edge of the boundary layer and is a function of the angular location along the fuel surface. It is given by:

$$v_\infty = Gr^{1/4} \frac{\mu_\infty}{\rho_\infty R} \left(f(\infty) + \sigma \frac{\partial f}{\partial \sigma}(\infty) + n f(\infty) \sigma \cot\sigma \right) \tag{3.36}$$

The value of the entrainment velocity has been obtained from a numerical solution of the problem of free-convective vaporization of a spherical or cylindrical condensed fuel. The details of this solution are the following: In Equations (3.13) and (3.14), the exponential reaction term is dropped by letting $Ta \rightarrow \infty$, as corresponds to the frozen flow, and derivatives in σ are replaced by backward differences. The resulting ordinary differential equations are solved using a quasilinearization and iteration technique (Wu et al, 1982) at each axial location. Figure 3.3 is a plot of v_∞, normalized by its value at the stagnation point, versus the angular coordinate σ for a spherical fuel droplet with Ja=1 vaporizing in air (Pr=0.7).

Near the rear stagnation point of the droplet, the rapidly converging flow results in the fast thickening of the boundary layer and the formation of a downward plume. A boundary-layer solution does not exist in this region.

The location of the thermal runaway can be obtained by defining a Damköhler number based on the entrainment velocity at the front stagnation point, $v_{\infty o}$. This Damköhler number is defined as:

$$\Delta_\sigma = \frac{A Y_{0\infty} P \mu_\infty \exp(-Ta/T_\infty)}{\alpha \rho_\infty Pr \bar{R} \bar{W} v_{\infty 0}^2} \tag{3.37}$$

In terms of the Damköhler number defined in Eq.(3.33), the new Damköhler can be written as:

$$\Delta_\sigma = [v_\infty / v_{\infty o}]^2 \Delta \tag{3.38}$$

and the corresponding critical Damköhler number can be written:

$$\Delta_\sigma{}^c = [v_\infty / v_{\infty o}]^2 \Delta^c \tag{3.39}$$

The ignition distance as given by the angular coordinate σ can now be obtained from Equation (3.39) and with the aid of Figs. 3.2 and 3.3. The location σ_c of the thermal runaway as a function of the critical Damköhler number $\Delta_\sigma{}^c$ for several values of the parameter α is shown in Fig.3.4. The parameter α is expected to be small because of the large values of the heat

of combustion Q for most fuels. Fig. 3.4 shows that the critical Damköhler number $\Delta_\sigma{}^c$ decreases with increasing distance away from the front stagnation point. It can be deduced that the location of the thermal runaway is displaced downstream as the Grashof number and the activation energy increase or as the ambient temperature and oxygen concentration decrease.

The analysis shows that ignition of a vaporizing droplet in a free-convection flow is likely to occur near the rear stagnation point with the resulting diffusion flame propagating toward the front of the droplet.

3.4 Concluding Remarks

The quasi-steady thermal ignition of a condensed cylindrical or spherical fuel, including the important practical case of ignition of a vaporizing droplet, has been analyzed with the use of first-order matched asymptotic expansions. The mathematical model is based on the assumption of the existence of a thin mixed-convection boundary layer on the surface of the fuel, and on the existence of a state of equilibrium vaporization with a constant fuel temperature. The analysis shows that the weakly-proceeding ignition reaction is initiated near the edge of the boundary layer, since it is there where the temperature-dependent reaction rate [Eq.(3.6)] reaches a sufficiently large value. This occurs in spite of the fact that the fuel concentration is relatively low near the edge of the boundary layer because the dominant effect in the reaction rate is that of the temperature in the exponential Arrhenius term.

The analysis also establishes that the ignition process is directly related to a suitably defined ratio of the residence and chemical times: the Damköhler number [Eq.(3.33)]. The numerical value of this ratio indicates whether the flow is chemically frozen ($\Delta << 1$) or weakly reacting ($\Delta \approx 1$). In the case of a free-convection flow, it is demonstrated that the equation governing the process is diffusive-reactive in nature [Eq.(3.32) with Ω=0]. The absence of the convective term is explained by the fact that, in the ignition region, the flow velocity is very low and approaches a value of zero at the outer edge of the boundary layer. On the other hand, in the cases of forced or moderately-strong mixed convection, it has been shown that the governing equation is convective-diffusive-reactive in nature [Eq.(3.32)]. The presence of the convective term in this case is due to the existence of a non-zero value of the flow velocity as the edge of the boundary layer is approached. A detailed study of the free-convection case has shown that ignition is more likely to occur at locations increasingly farther away (downstream) from the front stagnation point. Although both the chemical and residence times increase with increasing distance downstream, the faster growth of the latter yields a value of the Damköhler number which increases with the downstream distance, therefore explaining the predicted behavior. Since it is assumed that a temperature runaway occurs once the ignition criterion is met, it may be concluded that ignition starts uniformly at all points downstream of the critical location σ_c (Fig.3.4). As the

global Damköhler number is increased, ignition occurs simultaneously over a larger portion of the droplet until finally, when the Damköhler number equals its critical value for ignition at the front stagnation point, the droplet is completely surrounded by an ignition reaction.

Chapter 4

Mixed-Convection Droplet Combustion with Internal Circulation.

4.1 Introduction

In most spray combustion systems the vaporization and combustion of the fuel droplets occur in a convective environment. If the convective conditions are strong enough, the shear stress at the gas-liquid droplet interface could induce internal motion within the liquid (Law et al., 1977; Prakash and Sirignano, 1978). The internal circulation will not only affect the heating rate of the droplet but could also influence its vaporization and combustion characteristics, thus affecting the rate of fuel vaporization and consequently the droplet lifetime.

In this chapter, the combustion of a single-component fuel droplet in a mixed-convection environment is analyzed once the transient heating of the droplet has been completed. The fluid-mechanical characteristics of the model are similar to those of the analyses of Harper and Moore (1968) and Prakash and Sirignano (1980); *i.e.*, the existence of liquid and gaseous boundary layers near the droplet surface bounded respectively by a liquid and a gaseous inviscid flow. The assumption here that the droplet has reached thermal equilibrium permits a simpler solution of the problem and consequently allows for a more detailed analysis of the effect of the droplet internal circulation on its burning characteristics. This analysis is applicable to most of the

lifetime of the fuel droplet whenever the difference between the initial and the vaporization temperature of the fuel is relatively small (low boiling-point fuels, low ambient pressures). This results because the initial heating time of the fuel droplet prior to the onset of evaporation is normally very short and because of the non-uniformity in the liquid temperature is reflected primarily through the magnitude of the heat flux on the liquid side of the droplet surface, which very soon becomes negligible in comparison with the heat required to evaporate the liquid. Furthermore, although the analysis is not rigorously applicable when the magnitude of the liquid heat flux is significant, its predictions are not expected to differ substantially from those that would be obtained from a model that considers transient droplet heating.

In this analysis, the series-expansion approach used by Fernandez-Pello (1982) for the burning of a solid particle in a mixed-convection environment is extended to the liquid-phase boundary layer. The result is a set of ordinary differential equations for the gas and liquid phases that are coupled by their boundary conditions at the interface. The equations are solved numerically using an iteration method and the analysis identifies two parameters related to the internal circulation of the droplet. One refers to the convective conditions of the droplet burning process and is given by a mixed-convection parameter based on the intensity of the mixed flow. The other refers to the shear stress at the gas-liquid interface and is given by the ratio of the product of viscosity and density in the gas and the liquid. The variations with these parameters of the primary variables involved in the problem are presented for

the case of droplet combustion under several convective conditions. The pure vaporization of the droplet is a particular case of the analysis and since the combustion and vaporization processes are similar, only one particular case of droplet vaporization is presented.

4.2 Theoretical Model

The model considers the steady, mixed-convection, laminar boundary-layer combustion of a fuel droplet once the initial transient heating of the liquid has been completed. The generation of liquid internal motion by shear stress at the gas-liquid interface is considered in the analysis. A particular case of this analysis is the pure vaporization of the droplet.

The general character of the model to be developed is shown schematically in Fig. 4.1. The gaseous inviscid flow surrounding the fluid droplet generates a gas-phase, mixed-convection, laminar boundary layer near the droplet surface. In this boundary layer lies a diffusion flame that establishes a uniform and approximately constant elevated droplet temperature through a balance between heat transfer from the flame and endothermic evaporation of the liquid fuel. The fuel vapors are transported outwards by convection and diffusion, reacting at the flame with the inwardly transported oxidizer gas. The heat generated by the chemical reaction is transfered both outward to the ambient and inward toward the droplet. The gaseous boundary layer generates by shear stress a liquid-phase boundary layer near the droplet surface. This boundary layer induces an inviscid circulating flow at the

droplet core. The model in the case of pure droplet evaporation is a simplified version of the above droplet combustion model: Since there is no chemical reaction, there is no generation of heat and there is no production or consumption of species. In addition, the environment consists of a high temperature infinite source of heat.

The analysis assumes that the gas and liquid Reynolds or Grashof numbers are large enough so that the boundary-layer approximation holds and that the thickness of the gaseous and liquid boundary layers are small in comparison with the droplet radius. It is also assumed that the surface tension is large enough to keep the droplet spherical and that the liquid and gas flows are axisymmetric. The gaseous inviscid flow is considered to be the potential flow over a sphere and the liquid inviscid flow is assumed to consist of a spherical Hill's vortex. The analysis is not applicable in the rear region of the droplet where separation of the gaseous boundary layer and wake-flame combustion occurs. It is assumed, however, that the separation of the boundary layer does not affect the characteristics of the Hill's vortex. The analysis also assumes that the burning droplet is in equilibrium vaporization at a constant vaporization temperature. The combustion conditions are considered to be away from ignition or extinction so that the flame-sheet approximation can be applied to describe the gas-phase reaction. A one-step, irreversible, chemical reaction is assumed to occur between fuel and oxidizer. Radiation from the flame and fuel surface is neglected. Because the characteristic transport times of the gas and liquid processes are much smaller than the characteristic time for droplet

radius variation (Prakash and Sirignano, 1980), the gas and liquid-phase phenomena are treated as quasi-steady.

4.3 Analysis

The coordinate systems adopted are indicated in Fig. 4.1. To analyze the characteristics of the boundary layer, the origin of the coordinate system is fixed at the front stagnation point on the droplet surface. The x coordinate follows the droplet surface which is assumed to be spherical. The y coordinate is normal to the droplet surface with the positive direction being outward for the gas phase and inward for the liquid phase. To describe the potential flow, the Hill's vortex, or the droplet regression rate, a polar coordinate system with origin at the center of the droplet is adopted. The polar angle is σ and the radial coordinate is r, with R being the instantaneous radius of the droplet.

The flow field is divided into four interrelated regions (Fig. 4.1). In region I a gaseous inviscid flow of uniform temperature and composition surrounds the fuel droplet. This flow is taken to be the potential flow past a sphere (Batchelor, 1970). Its stream function is given by:

$$\psi_I = \frac{1}{2}\left(r^2 - \frac{R^3}{r}\right)u_\infty \sin^2\sigma \qquad (4.1)$$

Variables without subscript refer to the gas phase and those with subscript ι refer to the liquid phase. The above stream function provides the tangential velocity at the droplet surface which is used as one of the boundary conditions for the

gaseous boundary layer.

Region II consists of a gaseous, reacting, mixed-convection, laminar boundary layer that is generated near the droplet surface. Neglecting curvature and assuming axisymmetric flow, the steady-state boundary-layer equations of conservation of mass, momentum in the x direction, energy and species for this region are respectively:

$$\frac{\partial(a\rho u)}{\partial x} + \frac{\partial(a\rho v)}{\partial y} = 0 \tag{4.2}$$

$$\rho u \frac{\partial u}{\partial x} + \rho v \frac{\partial u}{\partial y} = \rho_e U_e \frac{dU_e}{dx} + g(\rho_\infty - \rho)\sin\sigma + \frac{\partial}{\partial y}\left(\mu \frac{\partial u}{\partial y}\right) \tag{4.3}$$

$$\rho u c_p \frac{\partial T}{\partial x} + \rho v c_p \frac{\partial T}{\partial y} = \frac{\partial}{\partial y}\left(\lambda \frac{\partial T}{\partial y}\right) + \dot{q}''' \tag{4.4}$$

$$\rho u \frac{\partial Y_i}{\partial x} + \rho v \frac{\partial Y_i}{\partial y} = \frac{\partial}{\partial y}\left(\rho D \frac{\partial Y_i}{\partial y}\right) + \dot{m}''' \tag{4.5}$$

The equation of state is:

$$\rho T = \rho_\infty T_\infty \tag{4.6}$$

and chemistry:

$$\nu_F[F] + \nu_O[O] = \nu_P[P] \tag{4.7}$$

where a one-step, irreversible chemical reaction has been assumed.

Region III consists of a liquid, non-reacting, uniform-temperature and composition, laminar boundary layer generated near the droplet surface. Neglecting curvature, the constant-property equations of conservation of mass and

momentum in the x direction for this region are:

$$\frac{\partial(a u_l)}{\partial x} + \frac{\partial(a v_l)}{\partial y_l} = 0 \tag{4.8}$$

$$u_l \frac{\partial u_l}{\partial x} + v_l \frac{\partial u_l}{\partial y_l} = U_H \frac{dU_H}{dx} + \nu_l \frac{\partial^2 u_l}{\partial y_l^2} \tag{4.9}$$

The gas and liquid boundary layers are coupled at the droplet surface through their respective boundary conditions of conservation of mass and momentum.

Region IV consists of a liquid inviscid circulating flow of uniform temperature and composition generated at the droplet core. This flow consists of a Hill's spherical vortex whose stream function is given by:

$$\psi_{IV} = -\frac{A}{2} r^2 (R^2 - r^2) \sin^2\sigma \tag{4.10}$$

where A represents the strength of the vortex and is equal to $3U_\infty/2R^2$ in the case of an inviscid forced-convective flow (Harper and Moore, 1968). The presence of the boundary layers reduce the strength of the vortex to a fraction of its full inviscid value so that in general, for the forced-convection case, $A=3CU_\infty/2R^2$, where C represents that fraction. In the free-convection case there is no free-stream velocity and a characteristic free-convection velocity must appear in the expression for A. This characteristic velocity is $u_c=\sqrt{Rg\tau}$, and it may be concluded that in general, $A=3Cu_c/2R^2$, where the constant C depends on the particular flow conditions. In the

general mixed-convection case, the constant A is given by:

$$A = \frac{3}{2}Re(1+\varphi^2)^{1/4}\frac{\nu_\infty C}{R^3} \tag{4.11}$$

where the constant C has to be determined during the solution. The gas-phase Reynolds number is defined as $Re = u_\infty R/\nu_\infty$, the Grashof number as $Gr=R^2 g(T_w-T_\infty)/(T_\infty \nu_\infty{}^2)$, and the mixed-convection ratio as $\phi=Gr/(3Re/2)^2$. $\phi=0$ corresponds to the forced-convection limit and $\phi\rightarrow\infty$ to the free-convection limit.

The boundary conditions that complete the specification of the analysis are the following. In the gas, the temperature and composition approach ambient conditions as $y \rightarrow \infty$, while the tangential velocity approaches its value in the potential flow, i.e. $u_e = (3/2)u_\infty \sin\sigma$. At the liquid-gas interface, $y=0$, conservation of mass, matching of shear stresses, and conservation of energy and species provide the following conditions:

mass: $\rho v = -\rho_l v_l = m''$,

shear stress: $\mu(\partial u/\partial y) = -\mu_l(\partial u_l/\partial y_l)$,

energy: $\lambda(\partial T/\partial y) = m''L$, (4.12)

species: $\rho v = \rho v Y_F - \rho D(\partial Y_F/\partial y)$,

$\rho v Y_i = \rho D(\partial Y_i/\partial y)$, $i \neq F$.

Applied at the interface there is also the constant and known vaporization temperature of the fuel, $T = T_w$, and the non-slip condition, $u = u_l$. In the liquid, at the inner edge of the boundary layer, $y_l \rightarrow \infty$, tangential velocity and vorticity are matched with the values corresponding to the Hill's vortex. An iterative solution is required because the strength of the vortex is unknown. Finally at $x=0$, the variables must comply with the axisymmetric characteristics of the flow, i.e. $u = u_l = 0$, $\partial T/\partial x = \partial Y_i/\partial x = 0$.

The approach followed here to solve the gas phase equations [Eqs. (4.2)-(4.7)] is similar to that presented by Fernandez-Pello (1982). The problem is solved by first introducing the Shvab-Zeldovich variables:

$$\beta_1 = \frac{c_p (T - T_\infty)}{L} + \frac{(Y_0 - Y_{0\infty})\, Q}{M_0 \nu_0 L}$$
$$\beta_2 = \frac{Y_F\, Q}{M_F \nu_F L} - \frac{(Y_0 - Y_{0\infty})\, Q}{M_0 \nu_0 L} \qquad (4.13)$$

to eliminate source terms from the energy and species equations, and a stream function defined by:

$$a\rho u = \mu_\infty \frac{\partial(a\psi)}{\partial y} \quad , \quad a\rho v = -\mu_\infty \frac{\partial(a\psi)}{\partial x} \qquad (4.14)$$

such that the continuity equation is satisfied. The problem is generalized by introducing the nondimensional variables:

$$\sigma = \frac{x}{R} \quad , \quad \eta = (\tfrac{3}{2}Re)^{1/2}(1+\varphi^2)^{1/8} \int_0^y \frac{\rho}{\rho_\infty}\frac{dy}{R} \tag{4.15}$$

expanding the trigonometric terms into series of the polar angle σ:

$\sin\sigma = \sigma - \sigma^3/6 + \ldots, \cos\sigma = 1 - \sigma^2/2 + \ldots, \cot\sigma = 1/\sigma - \sigma/3 + \ldots$

and correspondingly assuming series expansions for the stream and energy-species functions of the form:

$$\begin{aligned} \psi &= (\tfrac{3}{2}Re)^{1/2}(1+\varphi^2)^{1/8}[\,\sigma\, f_0(\eta) + \sigma^3\, f_1(\eta) + \cdots\,] \\ \beta_1 &= -B\,[G_0(\eta) + \sigma^2\, G_1(\eta) + \cdots\,] \end{aligned} \tag{4.16}$$

where the mass-transfer number is defined as:

$$B = \frac{Y_{0\infty}Q}{M_0\nu_0 L} - \frac{c_p(T_w - T_\infty)}{L} \tag{4.16a}$$

For the solution of the liquid-phase equations [Eqs. (4.8) and (4.9)], an approach similar to the one used in the gas phase is followed. The continuity equation is satisfied with a stream function ψ_l, such that:

$$a\,u_l = \nu_l \frac{\partial(a\,\psi_l)}{\partial y_l} \quad , \quad a\,v_l = -\,\nu_l \frac{\partial(a\,\psi_l)}{\partial x} \tag{4.17}$$

The nondimensional variables:

$$\sigma = \frac{x}{R} \quad , \quad \eta_l = (\tfrac{3}{2}Re_l)^{1/2}(1+\varphi^2)^{1/8}\frac{y_l}{R} \tag{4.18}$$

are introduced, and a series expansion of the form:

$$\psi_l = (\tfrac{3}{2}Re_l)^{1/2}(1+\varphi^2)^{1/8}[\,\sigma F_0(\eta_l) + \sigma^3 F_1(\eta_l) + \cdots\,] \tag{4.19}$$

is assumed for the liquid stream function, where the liquid-phase Reynolds number is defined as: $Re_l = u_\infty R/\nu_l$. A more physically-meaningfull liquid Reynolds number based on some characteristic liquid velocity cannot be calculated until the strength of the vortex is known.

After introducing these series expansions in the boundary-layer equations and retaining terms up to the third power of ß, the following two sets of ordinary differential equations are obtained:

Gas phase:

$$f_0''' + 2f_0f_0'' - f_0'^2 = A_1G_0 - A_2 \tag{4.20a}$$

$$Pr^{-1}G_0'' + 2f_0G_0' = 0 \tag{4.20b}$$

$$f_1'''+2f_0f_1''-4f_0'f_1'+ 4f_1f_0''-f_0f_0''/3 = A_1G_1-A_3G_0+A_4 \tag{4.20c}$$

$$Pr^{-1}G_1'' + 2f_0G_1' - 2f_0'G_1 + 4f_1G_0' - f_0G_0'/3 = 0 \tag{4.20d}$$

Liquid phase:

$$F_0''' + 2F_0F_0'' - F_0'^2 + 4C^2/9 = 0 \tag{4.21a}$$

$$F_1''' + 2F_0F_1'' - 4F_0'F_1' + 4F_0''F_1 - F_0F_0''/3 - 8C^2/27 \tag{4.21b}$$

The coefficients A_i have the following values at each side of the flame:

for $\eta < \eta_f$:

$$A_1 = \frac{\Lambda(\tau+\varphi)}{(1+\varphi^2)^{1/2}} \quad , \quad A_2 = \frac{1+(\tau+\varphi)(1+\Lambda)}{(1+\varphi^2)^{1/2}}$$

$$A_3 = \frac{2\Lambda(\tau+\frac{1}{4}\varphi)}{3(1+\varphi^2)^{1/2}} \quad , \quad A_4 = \frac{2[1+(\tau+\frac{1}{4}\varphi)(1+\Lambda)]}{3(1+\varphi^2)^{1/2}} \tag{4.22a}$$

for $\eta > \eta_f$:

$$A_1 = \frac{(\Lambda G_f-\Lambda-1)(\tau+\varphi)}{G_f(1+\varphi^2)^{1/2}} \quad , \quad A_2 = \frac{1}{(1+\varphi^2)^{1/2}}$$

$$A_3 = \frac{2(\Lambda G_f-\Lambda-1)(\tau+\frac{1}{4}\varphi)}{3G_f(1+\varphi^2)^{1/2}} \quad , \quad A_4 = \frac{2}{3(1+\varphi^2)^{1/2}} \tag{4.22b}$$

where the parameters τ, Λ, and G_f are defined in the Nomenclature.

The boundary conditions for the above set of equations become:

$F_0(0)=-Pf_0(0)$, $F_1(0)=-Pf_1(0)$, $F_0'(0)=f_0'(0)$, $F_1'(0)=f_1'(0)$,

$F_0''(0)=-Pf_0''(0)$, $F_1''(0)=-Pf_1''(0)$, $G_0(0)=1$, $G_1(0)=0$,

$G_0'(0) = 2Prf_0(0)/B$, $G_1'(0) = Pr[4f_1(0) - f_0(0)/3]/B$,

$f_0'(\infty)=1/(1+\phi^2)^{1/4}$, $f_1'(\infty)=-(1+\phi^2)^{1/4}/6$, $G_0(\infty)=0$, $G_1(\infty)=0$,

$F_0'(\infty) = 2C/3, \qquad F_1'(\infty) = -C/9.$

In the above equations, $P = \sqrt{\mu\rho/\mu_l\rho_l}$ and C is obtained through the matching of vorticities of the liquid boundary layer as $y \to \infty$ and the Hill's vortex. The resulting expression for C is:

$$C = -\frac{(\frac{3}{2}Re_l)^{1/2}\,\nu_\infty^{1/2}(1+\varphi^2)^{1/8}[\,\sigma F_0(\infty) + \sigma^3 F_1(\infty)]}{\frac{8}{3}\nu_l^{1/2}(\sigma - \frac{1}{6}\sigma^3)} \tag{4.23}$$

Equations (4.20) and (4.21) and their boundary conditions contain seven parameters: B, τ, Λ, Pr, Re_l, and P. The first five are related to the droplet combustion process while the last two are related to the motion of the liquid. The parameter P gives the relative magnitude of the viscous forces in the gas and liquid phases, while Re_l indicates the convective conditions under which the droplet is burning. The pure vaporization of the droplet is a particular case of the analysis. The governing equations and boundary conditions in this case become identical to those given by Eqs. (4.20) and (4.21) by defining the nondimensional temperature as $\theta = G_0 + \sigma^2 G_1$, replacing the B number with the Jacob number, $Ja = c_p(T_w - T_\infty)/L$, and using the values of A_i corresponding to $\eta > \eta_f$ with $G_f = 1$. The number of parameters is reduced to five, *i.e.*, Ja, τ, Pr, Re_l, and P.

4.4 Results

The coupled sets of ordinary differential equations (4.20) and (4.21) are integrated simultaneously using a quasilinearization and iteration scheme and a Runge-Kutta-Gill fourth-order method (Wu *et al.*, 1982). An initial guess or the previous iterated value is used for C and its value is compared with the new value calculated with Eq. (4.23). The solution is considered achieved when the difference between the previous and the new value of C differ by less than 0.1 percent.

Because of the large number of parameters involved in the problem and for the sake of clarity , this section has been organized as follows: The basic case of a hexadecane droplet evaporating or burning in air under forced flow conditions at the predetermined Reynolds number and atmospheric conditions is presented in detail. The effect of the liquid motion and mixed-flow intensities on the combustion of the droplet is analyzed by presenting the variation with P and ϕ of the most characteristic values of the droplet-combustion process. Since, as it will be shown later, the internal circulation does not affect substantially the droplet combustion process once the heating period has been completed, the reader is referred to the works of Fernandez-Pello (1982) and (1982) for details about the influences of the fluid properties, ambient oxygen concentration or intensity of the mixed-convection flow on the combustion of the droplet. The numerical values of the parameters corresponding to hexadecane burning in air at T_∞ = 20°C and 1 atm. are: B=11.6, τ=0.91, Λ=9.85, γ=0.0663, Pr=0.72,

Re_l=2500 and P=0.0137; and for the inert evaporation of hexadecane in air at an ambient temperature equal to the flame temperature in the combustion case, T_∞=2725°C and 1 atm they are: Ja=-21.06, τ=-0.813, Pr=0.72, Re_l=2500 and P=0.0137. To analyze the effect of the liquid motion on the characteristics of the combustion process of the droplet under varied flow conditions, calculations are performed for several values of P and ϕ while keeping the other parameters fixed and equal to those corresponding to the basic hexadecane case.

The velocity profiles in the liquid and gaseous boundary layers as functions of the polar angle are presented in Figs. 4.2a and 4.2b respectively for the cases of pure vaporization and combustion under forced flow conditions. Comparison of both velocity fields shows that the predicted liquid velocities are larger in the case of combustion than in the case of evaporation. The stronger internal circulation in the combustion case is caused by a larger shear stress at the droplet surface which results from the presence of larger gas velocities and a thinner boundary layer. The larger velocities are caused by the expansion of the gas in the vicinity of the reaction zone. The separation of the boundary layer occurs at a slightly larger polar angle for the case of evaporation. Although a stronger internal circulation helps to retard the separation of the boundary layer, the larger flow velocities existing in the combustion case seem to counteract the fact that the internal motion is stronger in the case of

evaporation.

Figures 4.3a and 4.3b show respectively, for the cases of pure evaporation and combustion in forced convection, the temperature and species distributions for several polar angles. In both cases, the results show the growth of the boundary layer and the increase, in the combustion case, of the flame stand-off distance with the polar angle. The temperature gradients at the droplet surface are larger in the case of combustion due to the proximity of the flame to the droplet surface. Comparison of the gas-phase velocity and temperature distributions for the case of combustion (Figures 4.2b and 4.3b) with those reported by Fernandez-Pello (1982a) for the combustion of a solid PMMA sphere, indicate that the motion of the liquid does not affect the overall characteristics of the droplet combustion process. As it will be shown below, it does affect the quantitative values of some of the variables involved in the process.

The streamline field for the case of droplet combustion in a forced-convection flow is shown in figure 4.4 for the purpose of flow visualization. The figure is developed by first calculating the streamline pattern in each of the regions I to IV and then by superposition of the different patterns. The matching between the streamlines of the inviscid and viscous flows is performed by approximately joining the corresponding streamlines. The liquid streamline pattern indicates that most of the vaporizing liquid is convectively brought to the surface from the region surrounding the axis of symmetry of the droplet. The liquid contained in the core of the Hill's vortex has no access to the droplet surface except through the

mechanism of regression of the droplet surface. The gas-phase streamline pattern shows the converging streamline moving away from the surface for increasing values of the polar angle and it also indicates that the flame is located near the outer edge of the boundary layer.

The velocity and temperature profiles for the forced-convection combustion of a droplet for different values of the parameter P are presented in Figures 4.5a and 4.5b for a polar angle of 45°. The value of P=0 corresponds to no internal motion and P=1 to a liquid and a gas of comparable densities and viscosities. The results show that the value of P affects considerably the magnitude of the velocity in the internal circulation, increasing with P as expected. With respect to the gas phase, the droplet internal circulation affects primarily the thickness of the boundary layer, decreasing as P increases. A thinner gaseous boundary layer results in a flame closer to the droplet surface and consequently in an increase of the surface heat flux. The maximum gas velocity, however, remains practically constant because as P increases the velocity becomes larger near the droplet surface, counteracting the thinning of the boundary layer and the increase of fuel vapor additions (Figure 4.7).

The variation of the normalized shear stress along the periphery of a droplet burning in forced convection is presented in Figure 4.6a for several values of P. For comparison, the case of pure vaporization of hexadecane is also included in the figure. It is seen that the predicted shear stress for the case of pure vaporization is considerably smaller than for the case of combustion. This results in a

weaker internal motion for the case of pure vaporization as it was shown in the comparison of Figures 4.2a and 4.2b. The variation of the shear stress distribution with P is less significant, decreasing as P increases. Figure 4.6a also shows the variation with P of the value of the polar angle at which the boundary layer separates. It is seen that as the internal circulation increases the location of boundary layer separation is displaced downstream. The displacement, however, is small, indicating that the existence of internal circulation does not vary significantly the location of boundary-layer separation. Figure 4.6b shows the variation of the normalized shear stress along the periphery of a hexadecane droplet for several values of the mixed-convection ratio. The predicted locations of the maximum shear stress and of the separation point occur farther downstream as the flow gradually passes from the forced to the free-convection limit. This is a consequence of the reduction of the adverse pressure gradient as the flow approaches the free-convection limit. The point of separation is slightly displaced downstream when circulation is present.

The predicted variation of the normalized mass burning rate along the periphery of a droplet burning in forced convection is shown in Figure 4.7a for several values of P. Also included in the figure is the vaporization rate for the case of pure vaporization of hexadecane. It is seen that the predicted rate of fuel vaporization is considerably larger for the case of combustion than for pure vaporization at an ambient temperature equal to the flame temperature. The fact that in a burning droplet the boundary layer is thinner and the flame lies within it results in higher vaporization rates than for pure

vaporization. The predicted variations of the mass burning rates with P indicates that the rate of fuel vaporization increases with the internal circulation. This result is due to the thinning of the boundary layer as P increases. Because the flame stand-off distance decreases (Figure 4.5a), the surface heat flux and consequently the rate of fuel vaporization both increase. It should be noted, however that the predicted influence of the liquid motion on the rate of fuel vaporization is not large under normal conditions. The internal circulation must be increased considerable to produce significant variations in the vaporization rate. Figure 4.7b shows the predicted variation of the local mass burning rate along the periphery of a hexadecane droplet for different values of the mixed-convection parameter. The local burning rate decreases with the polar angle as the flame moves away from the surface in the thickening boundary layer. This decrease is more pronounced when forced convection is dominant ($0<\phi<1$) since for these cases the boundary layer grows more rapidly. For the case $\phi=1$ the flame at the front stagnation point is closest to the surface (Fernandez-Pello and Law, 1982) and thus gives the maximum burning rate at that location.

The dependence on P of the temporal variation of the droplet radius squared in the forced-convection combustion of a droplet is presented in Figure 4.8a. The overall rate of fuel vaporization is calculated here by integrating the local burning rate along the droplet periphery up to the point of boundary-layer separation and assuming that the burning rate is zero beyond the separation point (Fernandez-Pello, 1982a). Also

included in the figure is the variation of the vortex constant C with the parameter P. This last information is particularly interesting because it permits the correlation of the results obtained varying P with those that would be obtained varying the droplet Reynolds number (Eq. 4.23), which is the information most probably available in a practical application. In Figure 4.8a it is seen that in spite of the fact that the droplet regression rate is relatively sensitive to variations of P when this parameter is small, the overall effect of the internal motion on the magnitude of the burning rate is not large. For example, for the normalized regression rate to increase 10 percent above the basic case calculated here (P=0.0137, C=0.07), the flow velocity must be increased approximately ten times. The strength of the internal motion is also most sensitive to P when this parameter is small. The circulation increases with P because there is less resistance of the liquid to the imposed motion. Figure 4.8b shows the variation with time of the droplet radius squared for a hexadecane droplet burning under different mixed-flow conditions. The overall mass burning rate is calculated for the cases of zero burning rate and of constant burning rate (equal to that obtained at the point of separation) beyond the separation point. In the former case the calculated droplet regression rate increases with ϕ because separation occurs further downstream as $\phi \rightarrow \infty$. In the latter case the predicted droplet regression rate is fairly independent of ϕ. This result is important because it permits the evaluation of the droplet

burning rate under any flow conditions. The variation of the vortex strength C with the flow intensity is also weakly dependent on ϕ. The maxima observed near $\phi=1$ for the droplet regression rate and the circulation strength are due to the combination of natural and forced-convection effects which reduce the thickness of the boundary layer, increasing the burning rate and the shear stress at the droplet surface.

4.5 Concluding Remarks

An analysis has been performed of the effect of the internal circulation on the mixed-convective combustion of a fuel droplet once the internal transient heating of the liquid has been completed. The use in the analysis of the scaling factor $[(3Re/2)^4 + Gr^2]^{1/8}$ yields a continuous solution between the forced and free-convection limits. The analysis provides explicit expressions for the local vaporization rate and for the variation of the droplet diameter with time as functions of the gas mixed flow and liquid circulation intensities. It is predicted that, for any mixed-flow condition, the existence of liquid motion results primarily in the reduction of the thickness of the gaseous boundary layer, the downstream displacement of the point of boundary-layer separation and the augmentation of the local and overall vaporization rates.

The internal circulation inside the droplet appears in the problem through two interrelated parameters, $P=\sqrt{\mu_\infty\rho_\infty/\mu_l\rho_l}$ and $C=\text{const.}(3Re/2)^{1/2}(1+\phi^2)^{1/8}$. The former parameter represents the

shear-stress characteristics at the droplet surface. The presence in it of the ratio of gas to liquid densities reflects primarily the effects of the expansion of the gas near the flame region on the velocity gradient normal to the droplet surface. The latter parameter reflects the intensity of the convective flow and is directly related to the strength of the internal liquid circulation. Noteworthy is the identification of the strength of the internal circulation for any mixed flow condition as $A=CV_{\infty}[(3Re/2)^4+Gr^2]^{1/4}/R^3$.

The study of the transient heating of the droplet could be performed using the present model by: (1) incorporating to the formulation the transient liquid energy equation; (2) removing the condition that the surface temperature is constant; and (3) adding the heat flux at the liquid side in the interface energy conservation equation, *i.e:* replacing the boundary condition given in Eq.(4.12) by $\lambda\partial T/\partial y = m''L + (\lambda\partial T/\partial y)_l$. Since the liquid momentum and energy equations are uncoupled except for the above boundary condition, the application of the present results to any instant during the droplet lifetime will depend only on the error introduced by using the boundary conditions as given by Eqs.(4.12). With regard to the surface temperature of the droplet, there is experimental evidence that for hydrocarbon droplets burning in the standard atmosphere, the droplets start to evaporate very soon after injection in the hot environment (Faeth, 1977; Law, 1982; Lasheras *et al.*, 1981). Theoretical studies (Law, 1982) also predict that the droplet surface temperature reaches an approximately constant

value very early during its lifetime. Therefore, since the constant surface temperature condition applies to most of the droplet lifetime, the extension of the present results to the transient droplet-burning process depends primarily on the error introduced in the energy conservation condition at the interface. This error depends on the relative magnitude of the heat conducted toward the interior of the droplet and the heat used to evaporate the liquid. In general we can conclude that this analysis is applicable to most of the evaporating droplet lifetime if $(\lambda\partial T/\partial y)_l < m''L$. This is the case for most low boiling point, light hydrocarbons burning under atmospheric pressure. However, whenever the contribution of the liquid heat flux becomes important, the present analysis will predict larger vaporization rates than those actually occurring. The larger gas normal velocity will perturb the characteristics of the boundary layer and an earlier separation of the boundary layer will be predicted. Since the errors introduced in the prediction of the local vaporization rate and boundary-layer separation counteract each other when calculating the total vaporization rate, it is possible that the present analysis will provide reasonable estimates of the droplet lifetime under transient-heating droplet-burning conditions.

It should be pointed out that although internal circulation may not affect significantly the process of steady droplet evaporation or combustion, it is very influential during the initial transient heating of the droplet. From the characteristics of the streamline pattern in the interior of the droplet (Figure 4.4), it can be inferred that droplet

heating by convection should be important, with the slower conductive heating being limited to the vortex core. Prakash and Sirignano (1978) estimate that the droplet heating time could be reduced by an order of magnitude due to the presence of the internal circulation.

Chapter 5

Conclusions

Analytical and numerical methods have been employed to model the behavior of three relevant reacting flows in the presence of mixed (forced and free) convective conditions. One group of problems involves the initiation of a gas-phase reaction by a hot cylindrical surface inmersed in a premixed combustible mixture. The treatment of this type of combustion problems has been limited so far to the simpler geometries of ignition by a flat plate and ignition in the stagnation-point boundary layer. In the analysis presented in Chapter 2, the method of matched asymptotic expansions has been used to divide the flow region into a frozen-flow zone and a weakly-reactive zone. Some assumptions of previous investigations, such as the existence of a laminar boundary layer and of a constant and uniform surface temperature have been retained. However, in the present study, the analysis of ignition by a hot cylindrical surface has been extended beyond the front stagnation point, and in fact has included the portion of the flow up to the point of boundary-layer separation. It is worth mentioning that in the case of a free-convective flow, separation does not occur until very near the rear stagnation point, and therefore, the analysis is valid along most of the cylinder surface. An important result of the present investigation has been the ability to predict and understand the role of the flow chemical and residence times in

determining the region of the flow field which has reached critical ignition conditions and that consequently will become the ignition zone. The critical ignition condition is given by a particular value of the Damköhler number, which is the ratio of the residence and chemical times. The analysis has shown that ignition should begin near the rear stagnation point in the case of an inert surface, and near the point of boundary-layer separation in the case of a catalytic surface. The fact that ignition always occurs very close to the hot surface has resulted in an equation governing the energy transport in the ignition zone which is only diffusive-reactive in nature with negligible convective effects. This behavior is the same independently of the type of surface promoting the gas-phase ignition, but in the case of a catalytic surface supporting a catalytic reaction, ignition is more readily accomplished due to the more elevated surface temperature.

The method of matched asypmtotic expansions has also been employed in Chapter 3 to study the gas-phase thermal ignition of a fuel droplet vaporizing in a convective oxidizing environment. The qualitative description of the ignition process is similar to that observed in the case of ignition of a premixed gas, but, in the case of an evaporating droplet, the thin ignition zone is located at the edge of the gaseous boundary layer surrounding the droplet, where the temperature approaches the ambient conditions. Critical assumptions have been made in order to concentrate efforts on the effect of the flow conditions on the location of the critical ignition point. Previous studies of droplet ignition have assumed spherically-symmetric conditions and therefore have

assumed the existence of a stagnant ambient. Such an assumption has been removed in the present study, but some other fundamental assumptions have been retained such as the existence of a state of equilibrium vaporization with all the heat arriving at the droplet surface being used to evaporate the liquid, with no heat transfer to the interior of the droplet. The existence of a laminar flow around the droplet, the neglect of internal circulation, and the existence of a perfectly spherical droplet are other limiting assumptions made in the analysis. Since the ignition process occurs toward the outer edge of the boundary layer, it has been shown that the form of the equation governing the transport of energy in the reaction zone is different for different types of flow conditions. In the case of a free-convective flow, the velocity in the reaction zone approaches the value of zero prevailing at infinity. Therefore in this case, the resulting equation is diffusive-reactive in nature with convection effects being negligible. On the other hand, in the case of a forced or mixed-convective flow, the gas velocity approaches the non-zero value existing in the outer flow, and consequently the energy-transport equation in the ignition zone contains diffusive, convective, and reactive terms, and the solution becomes more involved. As in the case of ignition of a premixed gas, the ignition of the gas around a droplet is more likely to begin near the rear portion of it, although in some cases an ignition reaction may completely surround the droplet.

The study of gas-phase reactions around a vaporizing droplet has been carried out one step further in Chapter 4 by investigating the regime of quasi-steady combustion of a droplet

in mixed-convective conditions. The analysis has assumed that the droplet has reached thermal equilibrium and that the gas-phase reaction can be well represented by the flame-sheet approximation. Under these conditions, it has been shown that the internal motion of the droplet has only a minor influence on the combustion characteristics of the droplet. The influence of the convective conditions on the mass burning rate of the droplet has also been studied in this work, and it was found that the largest global burning rate corresponds to the case of a mixed-convection ratio of approximately one when a constant value of the local burning rate is assumed beyond the point of boundary layer separation (Fig.4.8).

Acknowledgements

This work was partially supported by the U.S. Army Tank-Automotive Command under contract No. DAAE07-85-R025 and by the National Science Foundation under Grants CPE-8502114 and INT. 8115965.

REFERENCES

Ablow, C. M., Schechter, S. and Wise, H. (1980). Catalytic Combustion in a Stagnation Point Boundary Layer. *Comb. Sci. Tech.* **22**, 107-117.

Adomeit, G. (1965). Ignition of Gases at Hot Surfaces under Nonsteady-State Conditions. *Tenth Symp. (Intnl.) on Comb.*, 237-243.

Alkidas, A. and Durbetaki, P. (1971). Ignition Characteristics of a Stagnation Point Combustible Mixture. *Comb. Sci. Tech.*,**3**, 187-194.

Alkidas, A. and Durbetaki, P. (1973). Ignition of a Gaseous Mixture by a Heated Surface. *Comb. Sci. Tech.*,**7**, 135-140.

Berman, V. S. and Ryazantsev, Yu. S. (1978). Ignition of a Gas in a Boundary Layer at a Heated Plate. *Fluid Dyn.*, **12**, 758-763.

Blazowski, W. S. and Walsh, D. E. (1975). Catalytic Combustion: An Important Consideration for Future Applications. *Comb. Sci. Tech.*, **10**, 233-244.

Blazowski, W. S. (1978). Future Jet Fuel Combustion Problems and Requirements, *Prog. Energy Combust. Sci.* **4**,177-199.

Buckmaster, J. D. and Ludford, G. S. (1982). *Theory of Laminar Flames,* Cambridge University Press.

Cairnie, L. R., Harrison, A. J. and Morgan, P. A. (1981). Autoignition in a Free Convection Boundary Layer. *Eighteenth Symp. (Intnl.) on Comb.*, 1799-1806.

Chiang, T., Ossin, A. and Tien, C. L. (1964). Laminar Free Convection from a Sphere. *Journal of Heat Transfer.*

Chigier, N. A. (1976). The Atomization and Burning of Liquid Fuel Sprays, *Prog. Energy Combust. Sci.* **2**, 97-114.

El-Wakil, M. M. and Abdou, M. I. (1966). The Self-ignition of Fuel Drops in Heated Air Streams. *Fuel,* **45**, 177-205.

Faeth, G. M. (1977). Current Status of Droplet and Liquid Comustion. *Prog. Energy Comb. Sci.,* **3**, 191-224.

Fakhery, A. and Buckius, R. O. (1983). Transient Catalytic Combustion on a Flat Plate. *Comb. Flame,* **52**, 169-184.

Fendell, F. E. (1965). Ignition and Extintion in Combustion of Initially Unmixed Reactants. *J. Fluid Mech.,* **21**, 281-303.

Fernandez-Pello, A. C. (1982a). An Analysis of the Forced Convective Burning of a Combustible Particle. *Comb. Sci. Tech.,***28**, 305-313.

Fernandez-Pello, A. C. (1982b). Theory of the Mixed Convective Burning of a Combustible Particle. *Comb. Flame.,***53**, 23-

Fernandez-Pello, A. C. and Law, C. K. (1982a). On the Mixed-Convective Flame Structure in the Stagnation Point of a Fuel Particle. *Nineteenth Symp. (Intnl.) on Comb.,* 1037-1044.

Fernandez-Pello, A. C. and Law, C. K. (1982b). A Theory for the Free-Convective Burning of a Condensed Fuel Particle. *Comb. Flame,* **44**, 97-112.

Glassman, I. (1977). *Combustion,* Academic Press, New York.

Harper, J. F. and Moore, D. W. (1968). The Motion of a Spherical Liquid Drop at High Reynolds Number. *J. Fluid*

Mech.,**32**,367-391.

Hottel, H. C., Williams, G. C. and Simpson, H. C. (1954). Combustion of Droplets of Heavy Liquid Fuels. *Fifth Symp. (Int.) on Comb.*,101-128.

Kanury, A. M. (1975). *Introduction to Combustion Phenomena,* Gordon and Breach, New York.

Knight, B. and Williams, F.A. Observations on the Burning of Droplets in the Absence of Buoyancy. *Comb. Flame,* **38**, 111-119.

Krishnamurthy, L. (1976). On Gas-Phase Ignition of Diffusion Flame in the Stagnation-Point Boundary Layer. *Acta Astro.,* **3**, 935-942.

Lasheras, J. C., Fernandez-Pello, A. C., and Dryer, F. L. (1981). On the Disruptive Burning of Free Droplets of Alcohol/n-paraffin Solutions and Emulsions. *Eighteenth Symp. (Int.) on Comb.,* 293-305.

Laurendeau, N. M. (1982). Thermal Ignition of Methane-Air Mixtures by Hot Surfaces: A Critical Examination. *Comb. Flame,* **46**, 29-49.

Law, C. K. (1975). Asymptotic Theory for Ignition and Extinction in Droplet Burning. *Comb. Flame,* **24**, 89-98.

Law, C. K. (1978a). Ignition of a Combustible Mixture by a Hot Particle. *AIAA J.,* **16**, 628-630.

Law, C. K. (1978b). On the Stagnation Point Ignition of a Premixed Combustible. *Intnl. J. Heat Mass Transfer,* **21**, 1363-1368.

Law, C. K. (1978b). Theory of Thermal Ignition in Fuel Droplet Burning. *Comb. Flame,* **31**, 285-296.

Law, C. K. (1979). Transient Ignition of a Combustible by Stationary Isothermal Bodies. *Comb. Sci. Tech.*, **19**, 237-242.

Law, C. K. (1982a). Recent Advances in Droplet Vaporization and Combustion. *Prog. Energy Combust. Sci.*, **8**, 169-199.

Law, C. K. (1982b). Mechanisms of Droplet Combustion. *Second Int. Colloq. on Drops and Bubbles*. Publication 82-7.

Law, C. K. and Chung, S. H. (1983). Thermal and Catalytic Inhibition of Ignition through Reactant Depletion. *Comb. Sci. Tech.*, **32**, 307-312.

Law, C. K., Chung, S. H. and Srinivasan, N. (1979). Experimental and Theoretical Re-examination of the Classical d^2-Law of Droplet Combustion. WSS Meeting. *Combust. Inst.* Provo, Utah.

Law, C. K. and Law, H. K. (1979). Thermal Ignition Analysis in Boundary-Layer Flows. *J. Fluid Mech.*, **92**, 97-108.

Law, C. K. and Law, H. K. (1981). Flat Plate Ignition with Reactant Consumption. *Comb. Sci. Tech.*, **25**, 1-8.

Liñan, A. (1974). The Asymptotic Structure of Counterflow Diffusion Flames for Large Activation Energy. *Acta Astronautica*, **1**, 1007-1039.

Merzhanov, A. G. and Averson, A. E. (1971). The Present State of the Thermal Ignition Theory: An Invited Review. *Combustion and Flame*, **16**, 89-124.

Mory, Y., Miyauchi, T. and Hirano, M. (1977). Catalytic Combustion of Premixed Hydrogen-Air. *Comb. Flame*, **30**, 193-205.

Mullen, J. W., Fenn, J. B. and Moreland, R. I. (1949). The

Ignition of High Velocity Streams of Combustible Gases by Heated Cylindrical Rods. *Third Symp. on Comb. Flame and Explo. Pheno.,* 317-329.

Nuruzzaman, A. S. and Beér, J. M. (1971). On the Non-Steady Nature of Droplet Combustion. *Comb. Sci. Tech.,***3**, 17-24.

Pagni, P. J. (1980/81). Diffusion Flame Analyses. *Fire Safety J.,***3**, 273-285.

Pfefferle, W. C. (1978). The Catalytic Combustor: An Approach to Cleaner Combustion. *J. Energy,* **2**, 3, 142-146.

Pindera, M-Z. and Brzustowski, T. A. (1984). A model for the Ignition and Extinction of Liquid Fuel Droplets. *Comb. Flame,* **55**, 79-91.

Polymeropoulos, C. E. (1973). Steady State Vaporization and Ignition of Liquid Spheres. *Comb. Sci. Tech.,* **8**, 111-120.

Potter, J. M. and Riley, N. (1980). Free Convection over a Burning Sphere. *Comb. Flame,* **39**, 83-96.

Prakash, S. and Sirignano, W. A. (1978). Liquid Fuel Droplet Heating with Internal Circulation. *Int. J. Heat Mass Transfer,* **21**, 885-895.

Prakash, S. and Sirignano, W. A. (1980). Theory of Convective Droplet Vaporization with Unsteady Heat Transfer in the Circulating Liquid Phase. *Int. J. Heat Mass Transfer,* **23**, 253-268.

Saitoh, T., Ishiguro, S. and Niioka, T. (1982). An Experimental Study of Droplet Ignition Characteristics Near the Ignitable Limit. *Comb. Flame,* **48**, 27-32.

Sanchez Tarifa, C., Perez del Notario, P. and Garcia Moreno, F. (1960). Combustion of Liquid Monopropellants and bipropellants in droplets. *Eighth Symp. (Int.) on Comb.*,1035-1056.

Sangiovanni, J. J. and Kesten, A. S. (1975). A Theoretical and Experimental Investigation of the Ignition of Fuel Droplets. CSS/WSS Joint Meeting. Paper No 16. *Comb. Inst.* San Antonio, Texas.

Schefer, R. W. (1982). Catalyzed Combustion of H_2/Air Mixtures in a Flat Plate Boundary Layer: II. Numerical Model. *Comb. Flame*, **45**, 171-190.

Schefer, R., Robben, F. and Cheng, R. (1980). Catalyzed Combustion of H_2/Air Mixtures in a Flat Plate Boundary Layer: I. Experimental Results. *Comb. Flame*, **38**, 51-63.

Sharma, O. P. and Sirignano, W. A. (1969). Ignition of Stagnation Point Flow by a Hot Body. *Comb. Sci. Tech.*, **1**, 95-104.

Sharma, O. P. and Sirignano, W. A. (1970). On the Ignition of a Premixed Fuel by a Hot Projectile. *Comb. Sci. Tech.*, **1**, 481-494.

Sirignano, W. A. (1983). Fuel Droplet Vaporization and Spray Combustion Theory. *Prog. Energy Combust. Sci.*, **9**, 291-322.

Stout, H. P. and Jones, E. (1949). The Ignition of Gaseous Explosive Media by Hot Wires. *Third Symp. on Comb. Flame and Explo. Pheno.*, 329-336.

Su, Y. P., Homan, H.S. and Sirignano, W. A. (1979). Numerical

Predictions of Conditions for Ignition of a Combustible Gas by a Hot Particle. *Comb. Sci. Tech.*, **21**, 65-74.

Su, Y. P. and Sirignano, W. A. (1981). Ignition of a Combustible Mixture by an Inert Hot Particle. *Eightteenth Symp. (Intnl.) on Comb.*, 1719-1728.

Tong, A. Y. and Sirignano, W. A. (1982a). Analytical Solution for Diffusion and Circulation in a Vaporizing Droplet. *Nineteenth Symp. (Intnl.) on Comb.*, 1007-1020.

Tong, A. Y. and Sirignano, W. A. (1982b). Transient Thermal Boundary Layer in Heating of Droplet with Internal Circulation: Evaluation of Assumptions. *Comb. Sci. Tech.*, **29**, 87-94.

Tong, A. Y. and Sirignano, W. A. (1983). Analysis of Vaporizing Droplet with Slip, Internal Circulation, and Unsteady Liquid-Phase and Quasi-Steady Gas-Phase Heat Transfer. ASME-JSME *Thermal Engng. Joint Conf.* Honolulu, Hawaii.

Treviño, C. (1983). Gas-Phase Ignition of Premixed Fuel by Catalytic Bodies in Stagnation Flow. *Comb. Sci. Tech.* **30**, 213-229.

Treviño, C. and Fernandez-Pello, A. C. (1981). Catalytic Flat Plate Boundary Layer Ignition. *Comb. Sci. Tech.*, **26**, 245-251.

Treviño, C. and Fernandez-Pello, A. C. (1983). On the Influence of the Plate Thickness on the Boundary Layer Ignition for Large Activation Energies. *Comb. Flame*, **49**, 91-100

Treviño, C. and Sen, M. (1980). Transient Ignition in a Flat Plate Boundary Layer. *Proc. of the 1980 Heat*

Transfer and Fluid Mech. Inst., 92-107.

Treviño, C. and Sen, M. (1981a). Transient Phenomena in Boundary Layer Ignition with Finite Plate Thermal Resistance. *Eighteenth Symp. (Intnl.) on Comb.*,1781-1789.

Treviño, C. and Sen, M. (1981b). Effect of Plate Thermal Resistance on Boundary Layer Ignition. *Comb. Flame*, **43**, 121-129.

Treviño, C. and Sen, M. (1982). Effect of Prandtl Number on Boundary Layer Ignition. *Comb. Flame*, **46**, 211-212.

Waldman, C. H. (1974). Theory of Non-Steady Droplet Combustion. *Fifteenth Symp. (Int.) on Comb.*, 429-442.

Williams, A. (1973). Combustion of Droplets of Liquid Fuels: A Review. *Comb. Flame*, **21**, 1-31.

Williams, F. A. (1965). *Combustion Theory*, Addison Wesley, Reading, Massachusetts.

Wise, H., Lorell, J. and Wood, B. (1954). The Effects of Chemical and Physical Parameters on the Burning Rate of a Liquid Droplet. *Fifth Symp. (Int.) on Comb.*, 132-141.

Wu, X., Law, C, K., and Fernandez-Pello, A. C. (1982). A Unified Criterion for the Convective Extinction of Fuel Particles. *Comb. Flame* **44**, 113-124.

Yuen, M. C. and Chen, L. W. (1976). On Drag of Evaporating Droplets. *Comb. Sci. Tech.*, **14**, 147-154.

Appendix A

The transformation of Equations (2.3)-(2.5) starts by the introduction of the new independent variables:

$$z = \int_0^y \frac{\rho}{\rho_\infty}\frac{dy}{R} \quad , \quad \sigma = \frac{x}{R} \tag{A.1}$$

and the dependent variables:

$$\tilde{T} = \frac{c_p T}{Q} \quad , \quad \tilde{Y}_i = \frac{\nu_F W_F}{\nu_i W_i} Y_i \tag{A.2}$$

Upon transforming Equations (2.3)-(2.5), terms containing x-derivatives of the density cancel out, so that the effect of the transformation, after assuming that the quantities ρT, $\rho\lambda$, $\rho\mu$, ρD^2, and c_p are constant, is to obtain a set of equations equivalent to that for a constant-property formulation:

$$\frac{\partial\psi}{\partial z}\frac{\partial^2\psi}{\partial\sigma\partial z} - \frac{\partial\psi}{\partial\sigma}\frac{\partial^2\psi}{\partial z^2} = Re^2\frac{\sin(2\sigma)}{2} + \frac{\tilde{T}-\tilde{T}_\infty}{\tilde{T}_w-\tilde{T}_\infty} Gr \sin\sigma + \frac{\partial^3\psi}{\partial z^3} \tag{A.3}$$

$$\frac{\partial\psi}{\partial z}\frac{\partial\tilde{T}}{\partial\sigma} - \frac{\partial\psi}{\partial\sigma}\frac{\partial\tilde{T}}{\partial z} = \frac{1}{Pr}\frac{\partial^2\tilde{T}}{\partial z^2} + \frac{A W_0 \nu_0 \rho_\infty^2 T_\infty R^2}{\mu_\infty}\tilde{Y}_F \tilde{Y}_0 \exp(-\tilde{T}a/\tilde{T}) \tag{A.4}$$

$$\frac{\partial\psi}{\partial z}\frac{\partial\tilde{Y}_i}{\partial\sigma} - \frac{\partial\psi}{\partial\sigma}\frac{\partial\tilde{Y}_i}{\partial z} = \frac{1}{Sc}\frac{\partial^2\tilde{Y}_i}{\partial z^2} - \frac{A W_0 \nu_0 \rho_\infty^2 T_\infty R^2}{\mu_\infty}\tilde{Y}_F \tilde{Y}_0 \exp(-\tilde{T}a/\tilde{T}) \tag{A.5}$$

where the nondimensional parameters are defined in Chapter 2.

The boundary conditions [Eqs.(2.7) and (2.8)] are correspondingly transformed, and become:

At $z=0$:

$\partial\psi/\partial z=0$, $\partial\psi/\partial\sigma=0$, $T=T_w$,

catalytic surface: $Y_F=0$, $Y_O=Y_{O\infty}-(\gamma_{os}/\gamma_o)Y_{F\infty}$,

inert surface: $Y_F=Y_{F\infty}$, $Y_O=Y_{O\infty}$. (A.5a)

At $z\rightarrow\infty$:

$\partial\psi/\partial z=Re\ \sin\sigma$, $T=T_\infty$, $Y_F=Y_{F\infty}$, $Y_O=Y_{O\infty}$. (A.5b)

The next step is to transform the transverse coordinate z and the stream function ψ into more convenient scaled variables according to the assumption of the existence of a boundary layer. The new variables are defined as:

$$\eta = (Re^4 + Gr^2)^{1/8}\, z \quad , \quad \bar{\psi} = \frac{\psi}{(Re^4 + Gr^2)^{1/8}} \qquad (A.6)$$

and Equations (A.3)-(A.5) become:

$$\frac{\partial\bar{\psi}}{\partial\eta}\frac{\partial^2\bar{\psi}}{\partial\sigma\partial\eta} - \frac{\partial\bar{\psi}}{\partial\sigma}\frac{\partial^2\bar{\psi}}{\partial\eta^2} = \frac{\sin(2\sigma)}{2(1+\psi^2)^{1/2}} + \frac{\tilde{T}-\tilde{T}_\infty}{\tilde{T}_w-\tilde{T}_\infty}\frac{\psi\sin\sigma}{(1+\psi^2)^{1/2}} + \frac{\partial^3\bar{\psi}}{\partial\eta^3} \qquad (A.7)$$

$$\frac{\partial\bar{\psi}}{\partial\eta}\frac{\partial\tilde{T}}{\partial\sigma} - \frac{\partial\bar{\psi}}{\partial\sigma}\frac{\partial\tilde{T}}{\partial\eta} = \frac{1}{Pr}\frac{\partial^2\tilde{T}}{\partial\eta^2} + D_a\tilde{Y}_F\tilde{Y}_O\exp(-\tilde{T}a/\tilde{T}) \qquad (A.8)$$

$$\frac{\partial\bar{\psi}}{\partial\eta}\frac{\partial\tilde{Y}_i}{\partial\sigma} - \frac{\partial\bar{\psi}}{\partial\sigma}\frac{\partial\tilde{Y}_i}{\partial\eta} = \frac{1}{Sc}\frac{\partial^2\tilde{Y}_i}{\partial\eta^2} - D_a\tilde{Y}_F\tilde{Y}_O\exp(-\tilde{T}a/\tilde{T}) \qquad (A.9)$$

while the boundary conditions [Eqs.(A.5a-b)] are transformed to:

At $\eta=0$:

$\partial\psi/\partial\eta=0$, $\partial\psi/\partial\sigma=0$, $T=T_w$,

catalytic surface: $Y_F=0$, $Y_O=Y_{O\infty}-(\gamma_{os}/\gamma_{os})Y_{F\infty}$,

inert surface: $Y_F=Y_{F\infty}$, $Y_O=Y_{O\infty}$. (A.10a)

At $\eta\rightarrow\infty$:

$\partial\psi/\partial\eta=\sin\sigma/(1+\phi^2)^{1/4}$, $T=T_\infty$, $Y_F=Y_{F\infty}$, $Y_O=Y_{O\infty}$. (A.10b)

Finally, recognizing that the stream function ψ must contain a factor of σ, the new stream function is defined as:

$$f = \psi/\sigma \tag{A.11}$$

and when this is used in Equations (A.7)-(A.9) the result is Equations (2.12)-(2.14).

Appendix B

Equations (2.28) and (2.30) for the perturbed temperatures in the catalytic and inert case respectively are obtained in the following manner. The stretched variable χ defined by Eq.(2.26) is introduced in the energy and species equations [Eqs.(2.19) and (2.20)] together with Equations (2.25) for the temperature and concentrations in the inner zone. Terms containing the stream function f as well as the frozen-flow temperature and species concentrations are represented by their Taylor-series expansions near the cylinder surface (η=0), i.e.:

$$\frac{\partial f}{\partial \sigma} = \frac{1}{2}\frac{\partial^3 f}{\partial \sigma \partial \eta^2}\bigg|_w \eta^2 + \cdots \tag{B.1}$$

$$\frac{\partial f}{\partial \eta} = \frac{\partial^2 f}{\partial \eta^2}\bigg|_w \eta + \cdots \tag{B.2}$$

$$\tilde{T}_f = \tilde{T}_w + \frac{\partial \tilde{T}_f}{\partial \eta}\bigg|_w \eta + \cdots \tag{B.3}$$

$$\tilde{Y}_{if} = \tilde{Y}_i + \frac{\partial \tilde{Y}_{if}}{\partial \eta}\bigg|_w \eta + \cdots \tag{B.4}$$

where the boundary conditions at the surface for the stream function [Eqs.(2.16)] have been taken into account in (B.1) and (B.2). The temperature exponential in the reaction term is treated as follows:

$$\exp(-\tilde{T}_a/\tilde{T}) = \exp\left[\frac{-\tilde{T}_a}{\tilde{T}_w + \left.\frac{\partial \tilde{T}_f}{\partial \eta}\right|_w \eta + \epsilon\theta}\right] =$$

$$\exp\left[\frac{-\tilde{T}_a}{\tilde{T}_w}\left[1 - \frac{\epsilon}{\tilde{T}_w}(\theta-\chi)\right]\right] = \exp(-T_a/T_w)\exp(\theta-\chi) \qquad \text{(B.5)}$$

where higher-order terms have been neglected in the Taylor-series expansion for the frozen temperature and the small parameter has been selected as $\varepsilon = T_w^2/Ta$ in the last step of (B.5). The energy and species equations [Eqs.(2.19) and (2.20)] become:

Catalytic cylinder:

$$\frac{1}{Pr}\left[\left.\frac{\partial \tilde{T}_f}{\partial \eta}\right|_w\right]^2 \frac{\partial^2\theta}{\partial\chi^2} +$$
$$\sigma\epsilon^3\left[\left.\frac{\partial \tilde{T}_f}{\partial \eta}\right|_w\right]^{-1}\left(\frac{1}{2}\left.\frac{\partial^3 f}{\partial\sigma\partial\eta^2}\right|_w \frac{\partial\theta}{\partial\chi}\chi^2 - \left.\frac{\partial^2 f}{\partial\eta^2}\right|_w \frac{\partial\theta}{\partial\sigma}\chi\right) + \qquad \text{(B.6)}$$
$$\exp(-Ta/T_w)\,Da\,\epsilon^2(-r_F\chi - \beta_F\theta)(\tilde{Y}_{0w} - \epsilon r_0\chi - \epsilon\beta_0\theta)\exp(\theta-\chi) = 0.$$

$$\frac{\beta_i}{Sc}\left[\left.\frac{\partial \tilde{T}_f}{\partial \eta}\right|_w\right]^2 \frac{\partial^2\theta}{\partial\chi^2} +$$
$$\sigma\epsilon^3\beta_i\left[\left.\frac{\partial \tilde{T}_f}{\partial \eta}\right|_w\right]^{-1}\left(\frac{1}{2}\left.\frac{\partial^3 f}{\partial\sigma\partial\eta^2}\right|_w \frac{\partial\theta}{\partial\chi}\chi^2 - \left.\frac{\partial^2 f}{\partial\eta^2}\right|_w \frac{\partial\theta}{\partial\sigma}\chi\right) + \qquad \text{(B.7)}$$
$$\exp(-Ta/T_w)\,Da\,\epsilon^2(-r_F\chi - \beta_F\theta)(\tilde{Y}_{0w} - \epsilon r_0\chi - \epsilon\beta_0\theta)\exp(\theta-\chi) = 0.$$

Inert Cylinder:

$$\frac{1}{Pr}\left[\frac{\partial \tilde{T}_f}{\partial \eta}\bigg|_w\right]^2 \frac{\partial^2 \theta}{\partial \chi^2} +$$

$$\sigma\epsilon^3\left[\frac{\partial \tilde{T}_f}{\partial \eta}\bigg|_w\right]^{-1}\left(\frac{1}{2}\frac{\partial^3 f}{\partial\sigma\partial\eta^2}\bigg|_w \frac{\partial\theta}{\partial\chi}\chi^2 - \frac{\partial^2 f}{\partial\eta^2}\bigg|_w \frac{\partial\theta}{\partial\sigma}\chi\right) + \tag{B.8}$$

$$\exp(-Ta/T_w)\, Da\, \epsilon\, (\tilde{Y}_{F\infty} - \epsilon\, \beta_F\theta)(\tilde{Y}_{O\infty} - \epsilon\beta_O\theta)\exp(\theta-\chi) = 0.$$

$$\frac{\beta_i}{Sc}\left[\frac{\partial \tilde{T}_f}{\partial \eta}\bigg|_w\right]^2 \frac{\partial^2 \theta}{\partial \chi^2} +$$

$$\sigma\epsilon^3\beta_i\left[\frac{\partial \tilde{T}_f}{\partial \eta}\bigg|_w\right]^{-1}\left(\frac{1}{2}\frac{\partial^3 f}{\partial\sigma\partial\eta^2}\bigg|_w \frac{\partial\theta}{\partial\chi}\chi^2 - \frac{\partial^2 f}{\partial\eta^2}\bigg|_w \frac{\partial\theta}{\partial\sigma}\chi\right) + \tag{B.9}$$

$$\exp(-Ta/T_w)\, Da\, \epsilon\, (\tilde{Y}_{F\infty} - \epsilon\, \beta_F\theta)(\tilde{Y}_{O\infty} - \epsilon\beta_O\theta)\exp(\theta-\chi) = 0.$$

where:

$$r_F = \frac{\partial \tilde{Y}_{Ff}}{\partial \eta}\bigg|_w \Big/ \frac{\partial \tilde{T}_f}{\partial \eta}\bigg|_w \quad , \quad r_O = \frac{\partial \tilde{Y}_{Of}}{\partial \eta}\bigg|_w \Big/ \frac{\partial \tilde{T}_f}{\partial \eta}\bigg|_w \tag{B.10}$$

The relative size of the convective and reactive terms can be seen in Equations (B.6)-(B.9). As it is established in the discussion following Equations (2.27), the convective terms are always smaller than the reactive terms and may therefore be neglected.

Appendix C

Introducing the coordinate transformation defined by Equations (3.11) together with the nondimensional variables defined by Equations (3.10) and the stream function defined by Equations (3.9) into the boundary-layer equations for conservation of mass, momentum, energy and species [Eqs.(3.3)-(3.5)] reduces the problem to the following three differential equations:

$$\frac{\partial\psi}{\partial z}\frac{\partial^2\psi}{\partial\sigma\partial z} - \left(\frac{\partial\psi}{\partial\sigma} + n\psi\cot\sigma\right)\frac{\partial^2\psi}{\partial z^2} = Re^2\frac{\sin(2\sigma)}{2} + Gr\frac{\tilde{T}-\tilde{T}_\infty}{\tilde{T}_w-\tilde{T}_\infty}\sin\sigma + \frac{\partial^3\psi}{\partial z^3} \qquad (C.1)$$

$$\frac{\partial\psi}{\partial z}\frac{\partial\tilde{T}}{\partial\sigma} - \left(\frac{\partial\psi}{\partial\sigma} + n\psi\cot\sigma\right)\frac{\partial\tilde{T}}{\partial z} = \frac{1}{Pr}\frac{\partial^2\tilde{T}}{\partial z^2} + \frac{AW_0\nu_0\rho_\infty^2 T_\infty R^2}{\mu_\infty}\tilde{Y}_F\tilde{Y}_0\exp(-\tilde{T}a/\tilde{T}) \qquad (C.2)$$

$$\frac{\partial\psi}{\partial z}\frac{\partial\tilde{Y}_i}{\partial\sigma} - \left(\frac{\partial\psi}{\partial\sigma} + n\psi\cot\sigma\right)\frac{\partial\tilde{Y}_i}{\partial z} = \frac{1}{Sc}\frac{\partial^2\tilde{Y}_i}{\partial z^2} - \frac{AW_0\nu_0\rho_\infty^2 T_\infty R^2}{\mu_\infty}\tilde{Y}_F\tilde{Y}_0\exp(-\tilde{T}a/\tilde{T}) \qquad (C.3)$$

Use of the same variable transformations in the boundary conditions [Eqs.(3.7) and (3.8)], reduces these to:

At $z = 0$:

$$\frac{\partial\psi}{\partial z} = 0 \quad , \quad -\left(\frac{\partial\psi}{\partial\sigma} + n\psi\cot\sigma\right) = \frac{Q}{Pr\, h_{fg}}\frac{\partial\tilde{T}}{\partial z} \quad , \quad \tilde{T} = \tilde{T}_w \quad ,$$

$$\left(\frac{\partial\psi}{\partial\sigma} + n\psi\cot\sigma\right)(1-\tilde{Y}_F) = \frac{1}{Sc}\frac{\partial\tilde{Y}_F}{\partial z} \quad , \qquad (C.4)$$

$$\left(\frac{\partial\psi}{\partial\sigma} + n\psi\cot\sigma\right)\tilde{Y}_i = -\frac{1}{Sc}\frac{\partial\tilde{Y}_i}{\partial z} \qquad i \neq F \quad .$$

At $z \rightarrow \infty$:

$$\partial\psi/\partial z = Re\,\sin\sigma \quad , \quad T = T_\infty \quad , \quad Y_F = 0 \quad , \quad Y_O = Y_{O\infty} . \qquad (C.5)$$

Appropriate boundary-layer scaling is now introduced by defining the transverse independent variable and the new stream function as:

$$\eta = (Re^4 + Gr^2)^{1/8}\, z \quad , \quad \overline{\psi} = \frac{\psi}{(Re^4 + Gr^2)^{1/8}} \qquad (A.6)$$

so that Equations (C.3)-(C.5) become:

$$\frac{\partial\overline{\psi}}{\partial\eta}\frac{\partial^2\overline{\psi}}{\partial\sigma\partial\eta} - \left(\frac{\partial\overline{\psi}}{\partial\sigma} + n\overline{\psi}\cot\sigma\right)\frac{\partial^2\overline{\psi}}{\partial\eta^2} =$$

$$\frac{\sin(2\sigma)}{2(1+\psi^2)^{1/2}} + \frac{\tilde{T}-\tilde{T}_\infty}{\tilde{T}_w-\tilde{T}_\infty}\frac{\psi\sin\sigma}{(1+\psi^2)^{1/2}} + \frac{\partial^3\overline{\psi}}{\partial\eta^3} \qquad (C.7)$$

$$\frac{\partial\overline{\psi}}{\partial\eta}\frac{\partial\tilde{T}}{\partial\sigma} - \left(\frac{\partial\overline{\psi}}{\partial\sigma} + n\overline{\psi}\cot\sigma\right)\frac{\partial\tilde{T}}{\partial\eta} = \frac{1}{Pr}\frac{\partial^2\tilde{T}}{\partial\eta^2} + D_a\tilde{Y}_F\tilde{Y}_0\exp(-\tilde{T}a/\tilde{T}) \qquad (C.8)$$

$$\frac{\partial\overline{\psi}}{\partial\eta}\frac{\partial\tilde{Y}_i}{\partial\sigma} - \left(\frac{\partial\overline{\psi}}{\partial\sigma} + n\overline{\psi}\cot\sigma\right)\frac{\partial\tilde{Y}_i}{\partial\eta} = \frac{1}{Sc}\frac{\partial^2\tilde{Y}_i}{\partial\eta^2} - D_a\tilde{Y}_F\tilde{Y}_0\exp(-\tilde{T}a/\tilde{T}) \qquad (C.9)$$

while the boundary conditions become:

At $\eta = 0$:

$$\frac{\partial\bar{\psi}}{\partial\eta} = 0 \quad , \quad -\left(\frac{\partial\bar{\psi}}{\partial\sigma} + n\bar{\psi}\cot\sigma\right) = \frac{Q}{Pr\, h_{fg}}\frac{\partial\tilde{T}}{\partial\eta} \quad , \quad \tilde{T} = \tilde{T}_w \, ,$$

$$\left(\frac{\partial\bar{\psi}}{\partial\sigma} + n\bar{\psi}\cot\sigma\right)(1-\tilde{Y}_F) = \frac{1}{Sc}\frac{\partial\tilde{Y}_F}{\partial\eta} \quad , \qquad \text{(C.10)}$$

$$\left(\frac{\partial\bar{\psi}}{\partial\sigma} + n\bar{\psi}\cot\sigma\right)\tilde{Y}_i = -\frac{1}{Sc}\frac{\partial\tilde{Y}_i}{\partial\eta} \quad , \quad i \neq F$$

At $\eta \rightarrow \infty$:

$$\frac{\partial\bar{\psi}}{\partial\eta} = \frac{\sin\sigma}{(1+\psi^2)^{1/4}} \quad , \quad \tilde{T} = \tilde{T}_\infty \quad , \quad \tilde{Y}_F = 0 \quad , \quad \tilde{Y}_0 = \tilde{Y}_{0\infty} \qquad \text{(C.11)}$$

The final step, noting that the expansion of the sine function contains a factor of σ, is the introduction of the function f, defined as:

$$f = \psi/\sigma \qquad \text{(C.12)}$$

which permits writing Equations (C.7)-(C.11) in their final form given by Equations (3.13)-(3.15) and (3.19)-(3.20). Other dimensionless parameters have been defined in Chapter 3.

LIST OF FIGURES

2.1. Schematic of the problem and coordinate system for the thermal ignition of a premixed gas by a catalytic or inert hot cylinder.

2.2. Variation with β of the frozen-flow Nusselt number for forced convection (ϕ=0), mixed convection (ϕ=1), and free convection ($\phi=\infty$).

2.3. The lower portions of the ignition-extinction curves for the case of a catalytic surface and for different values of the parameter α.

2.4. Dependence on the parameter α of the critical Damköhler number Δ^c for the case of a catalytic surface.

2.5. The lower portion of the ignition-extinction curve for the case of an inert surface.

2.6. The lower portions of the ignition-exctinction curves at several locations along the catalytic surface for α=0.1 and ϕ=0.

2.7. Variation with the angular coordinate σ, of the critical Damköhler numbers $\Delta^c{}_{1\sigma}$ (catalytic surface) and $\Delta^c{}_{2\sigma}$ (inert surface) for the case of forced convection (ϕ=0).

2.8. Variation with the angular coordinate σ, of the critical

Damköhler numbers $\Delta^c{}_{1\sigma}$ (catalytic surface) and $\Delta^c{}_{2\sigma}$ (inert surface) for the case of mixed convection (ϕ=1).

2.9. Variation with the angular coordinate σ, of the critical Damköhler numbers $\Delta^c{}_{1\sigma}$ (catalytic surface) and $\Delta^c{}_{2\sigma}$ (inert surface) for the case of free convection ($\phi=\infty$).

3.1. Schematic of the problem and coordinate system for the thermal ignition of a vaporizing droplet or other condensed fuel.

3.2. The lower portions of the ignition-extinction curves for several values of the parameter α.

3.3. The frozen-flow entrainment velocity v_∞, as a function on the angular location σ, for a fuel droplet vaporizing in air (Ja=0.1, Pr=0.7).

3.4. The critical ignition distance σ_c, as a function of the critical Damköhler number $\Delta_\sigma{}^c$, for several values of the parameter α.

4.1. Schematic diagram and coordinate system for the mixed-convection combustion of a fuel droplet.

4.2a. Liquid and gas velocity profiles at several angular locations for a hexadecane droplet in forced-convective vaporization.

4.2b. Liquid and gas velocity profiles at several angular

locations for a hexadecane droplet in forced-convective combustion.

4.3. Dimensionless temperature and concentration profiles at several angular locations for a hexadecane droplet in forced-convective vaporization.

4.3b. Dimensionless temperature and concentration profiles at several angular locations for a hexadecane droplet in forced-convective combustion.

4.4. Gas and liquid-phase streamline field for the forced convective combustion of a hexadecane droplet.

4.5a. Influence of the property ratio P, on the nondimensional velocity profile at $\sigma=45^{\circ}$ for a hexadecane droplet burning in forced convection.

4.5b. The influence of the property ratio P, on the nondimensional temperature profile at $\sigma=45^{\circ}$ for a hexadecane droplet burning in forced convection.

4.6a. The variation of the normalized shear stress along the droplet periphery for $\phi=0$ and for several values of the property ratio P.

4.6b. The variation of the normalized shear stress along the droplet periphery for P=0.0137 and for several values of the mixed-convection ratio ϕ.

4.7a. The variation of the normalized mass burning rate along the droplet periphery for $\phi=0$ and for several values of the property ratio P.

4.7b. The variation of the normalized mass burning rate along

the droplet periphery for P=0.0137 and for several values of the mixed-convection ratio ϕ.

4.8a. The time derivative of the droplet-radius squared, and the vortex constant C as functions of the property ratio P, for the case ϕ=0.

4.8b. The time derivative of the droplet-radius squared, and the vortex constant C as functions of the mixed-convection ratio ϕ, for the case P=0.0137.

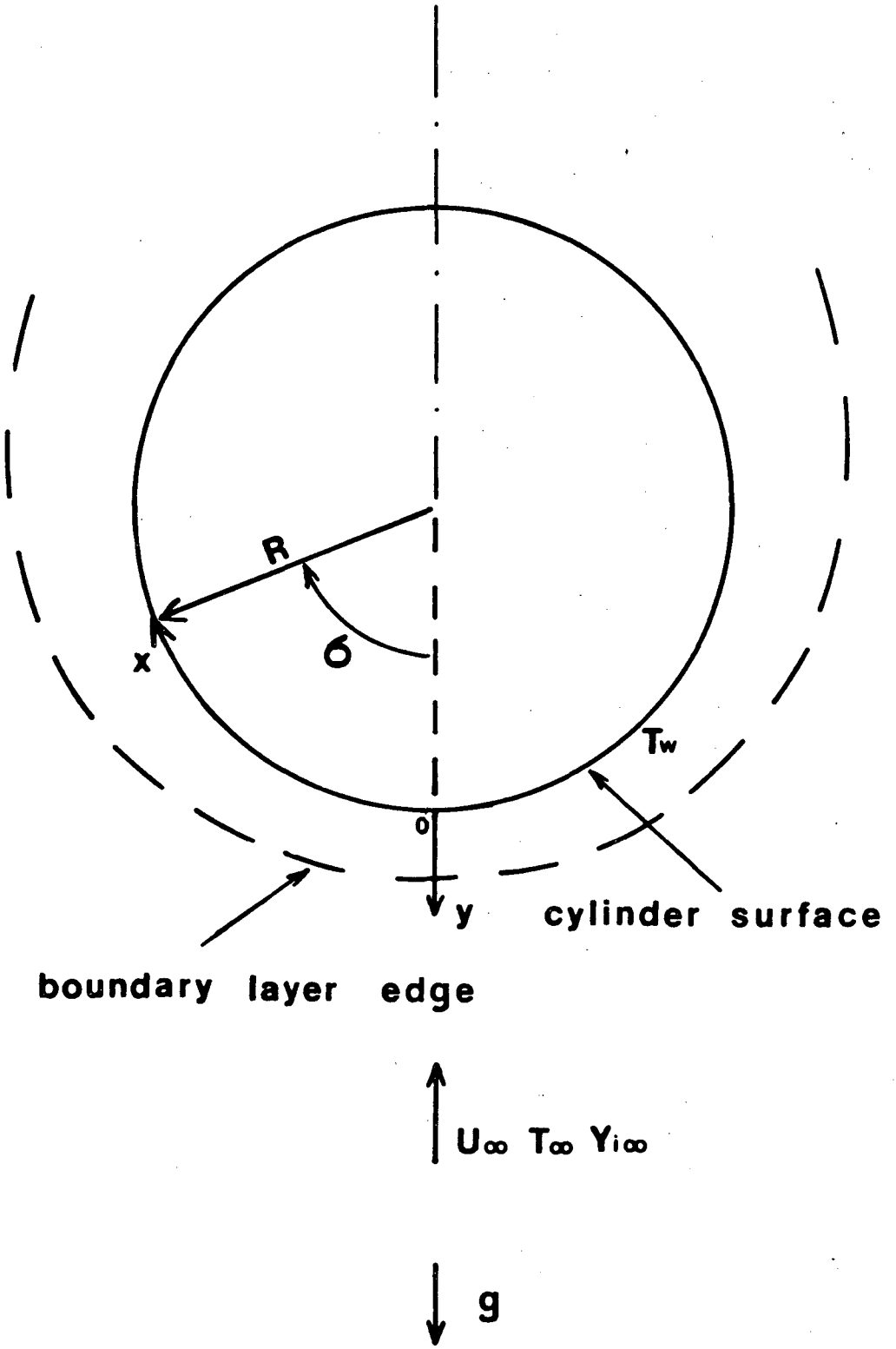

Fig 2.1

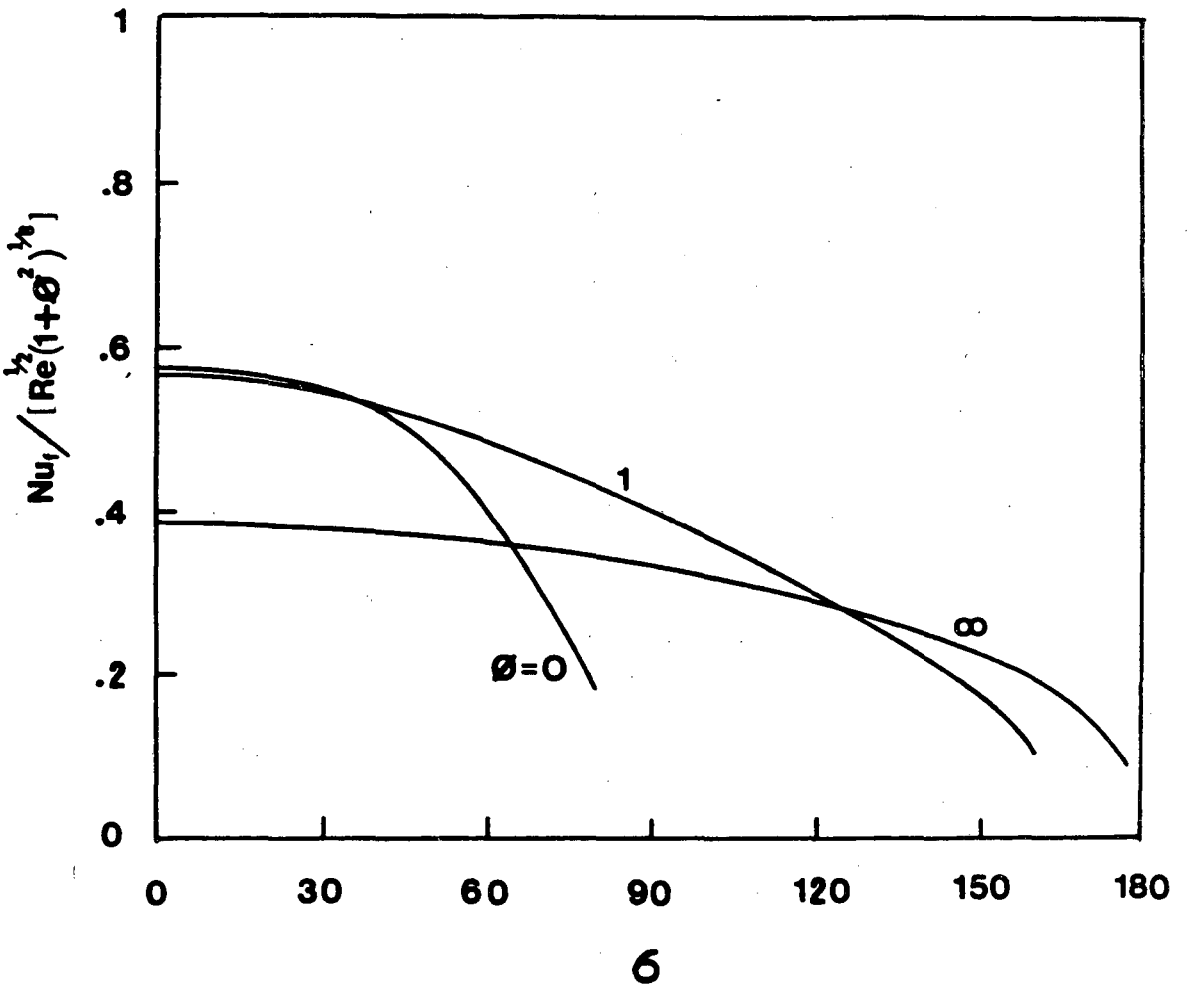

Fig 2.2

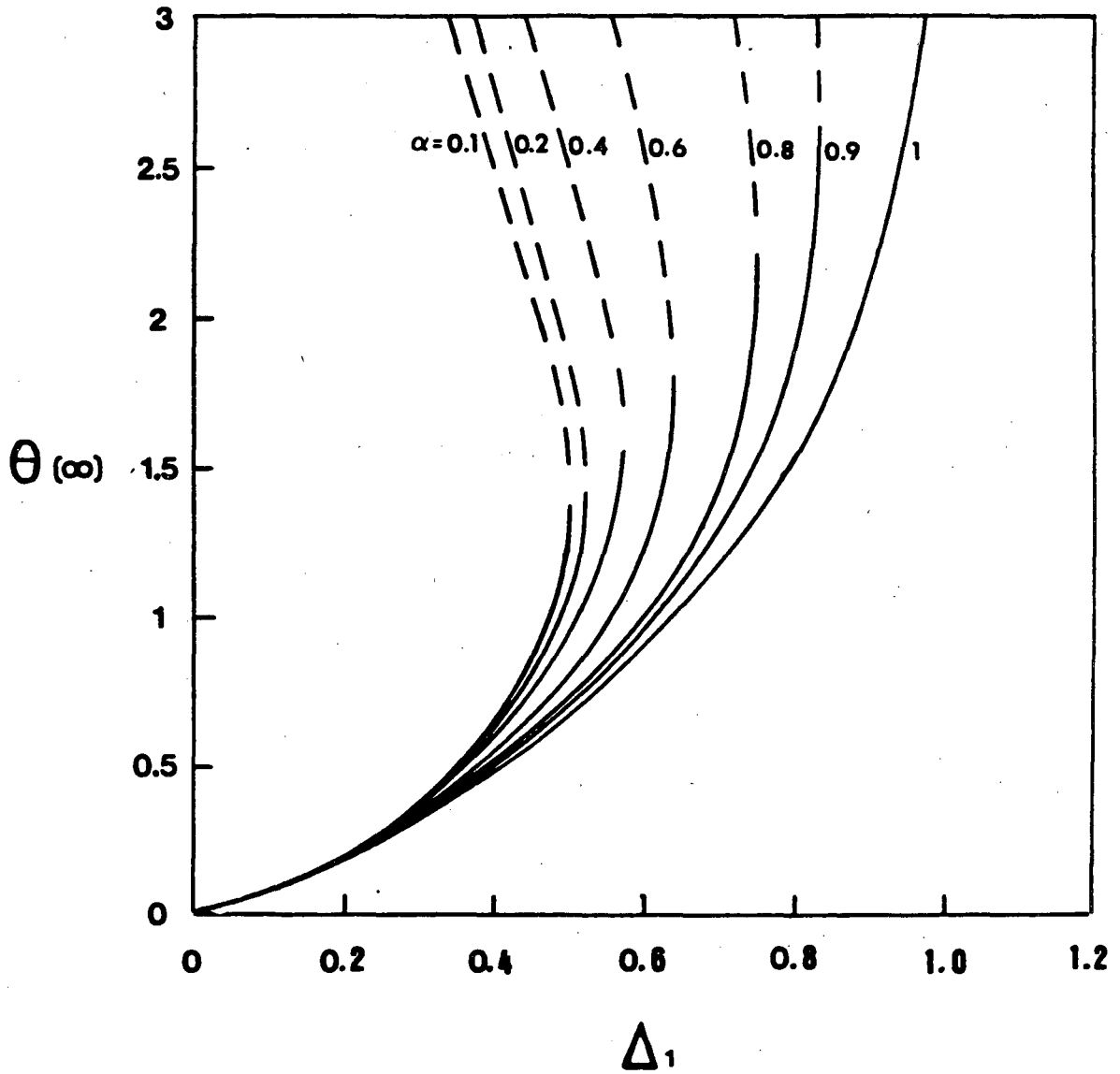

Fig 2.3

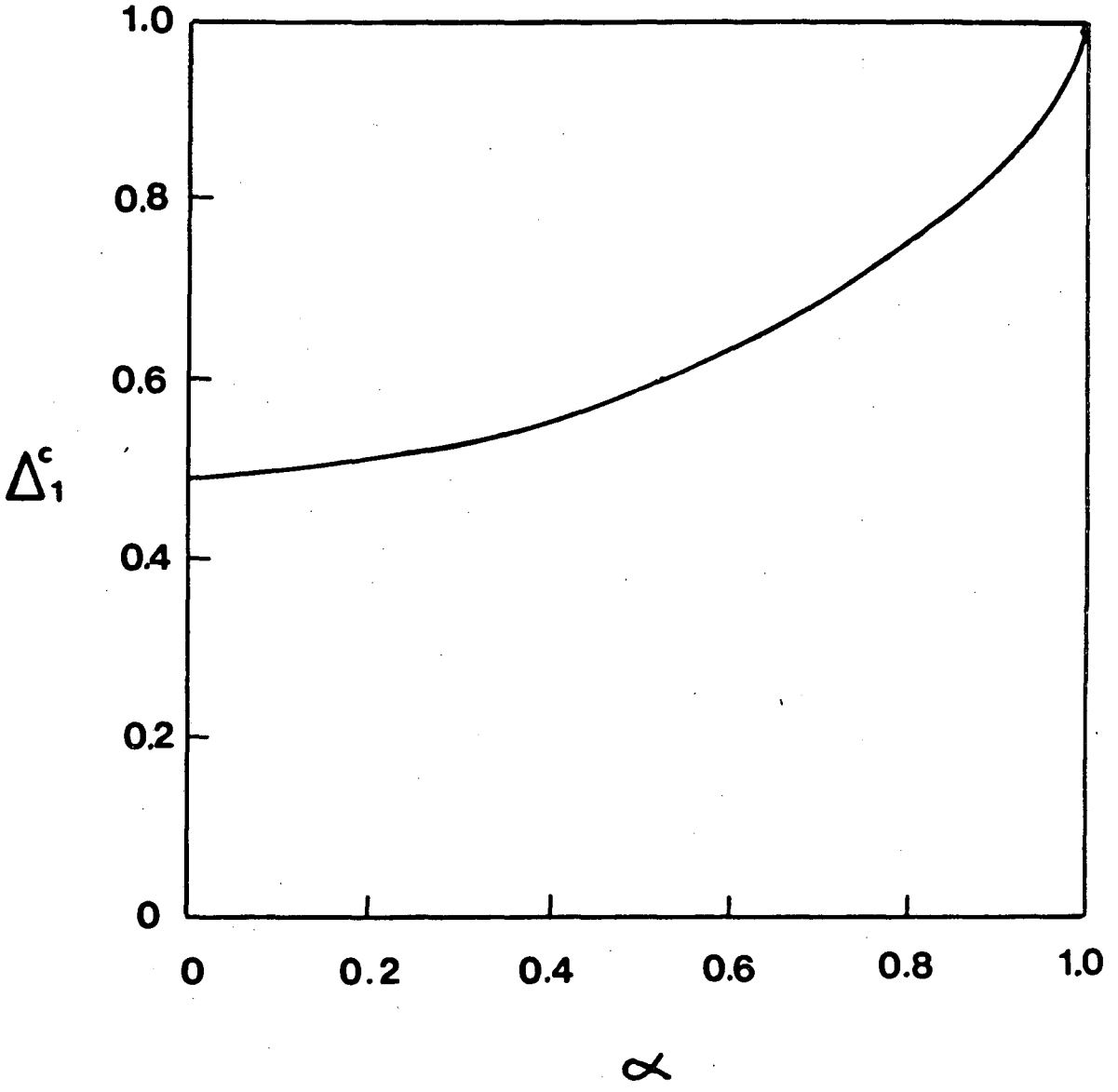

Fig 2.4

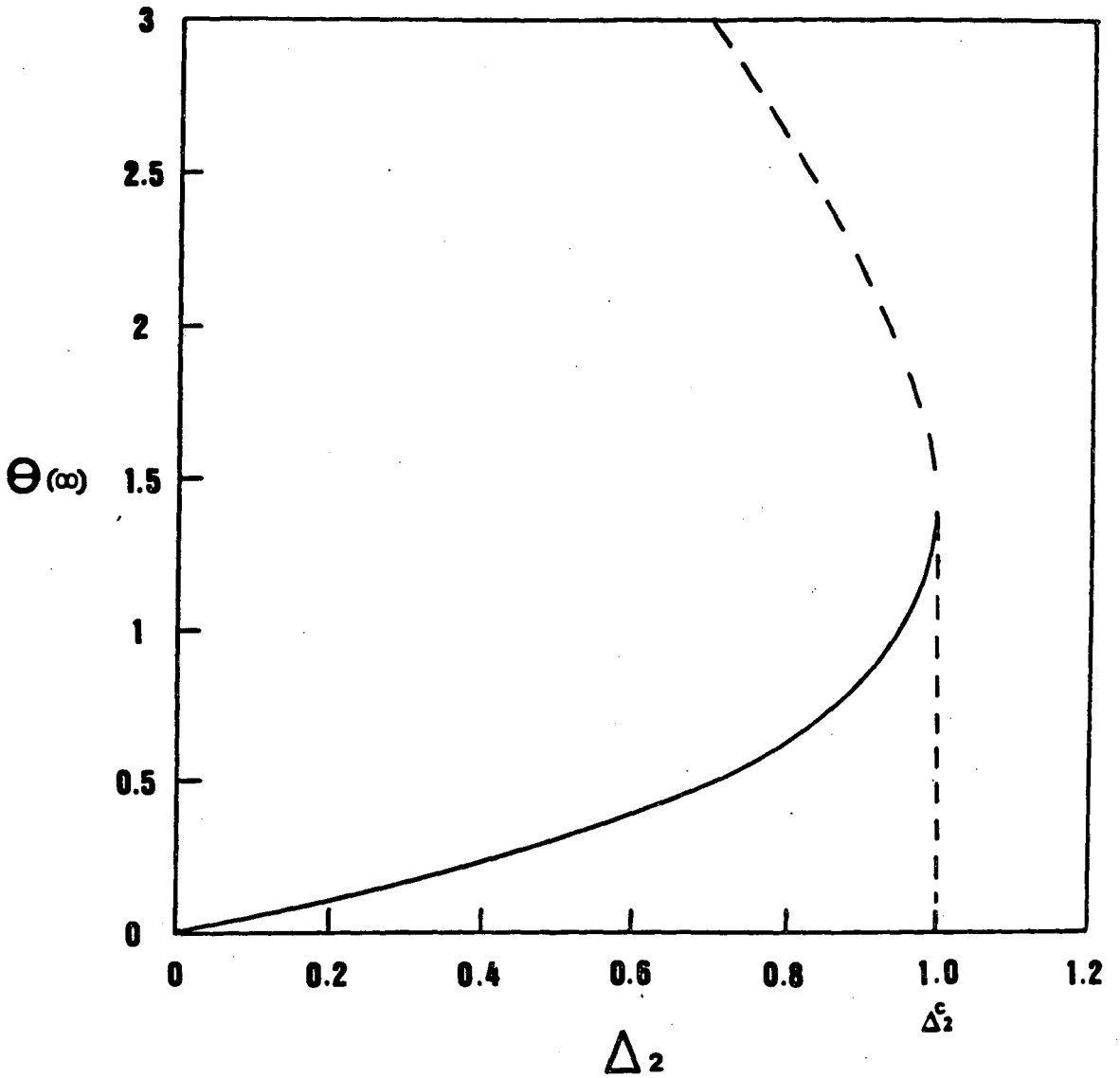

Fig 2.5

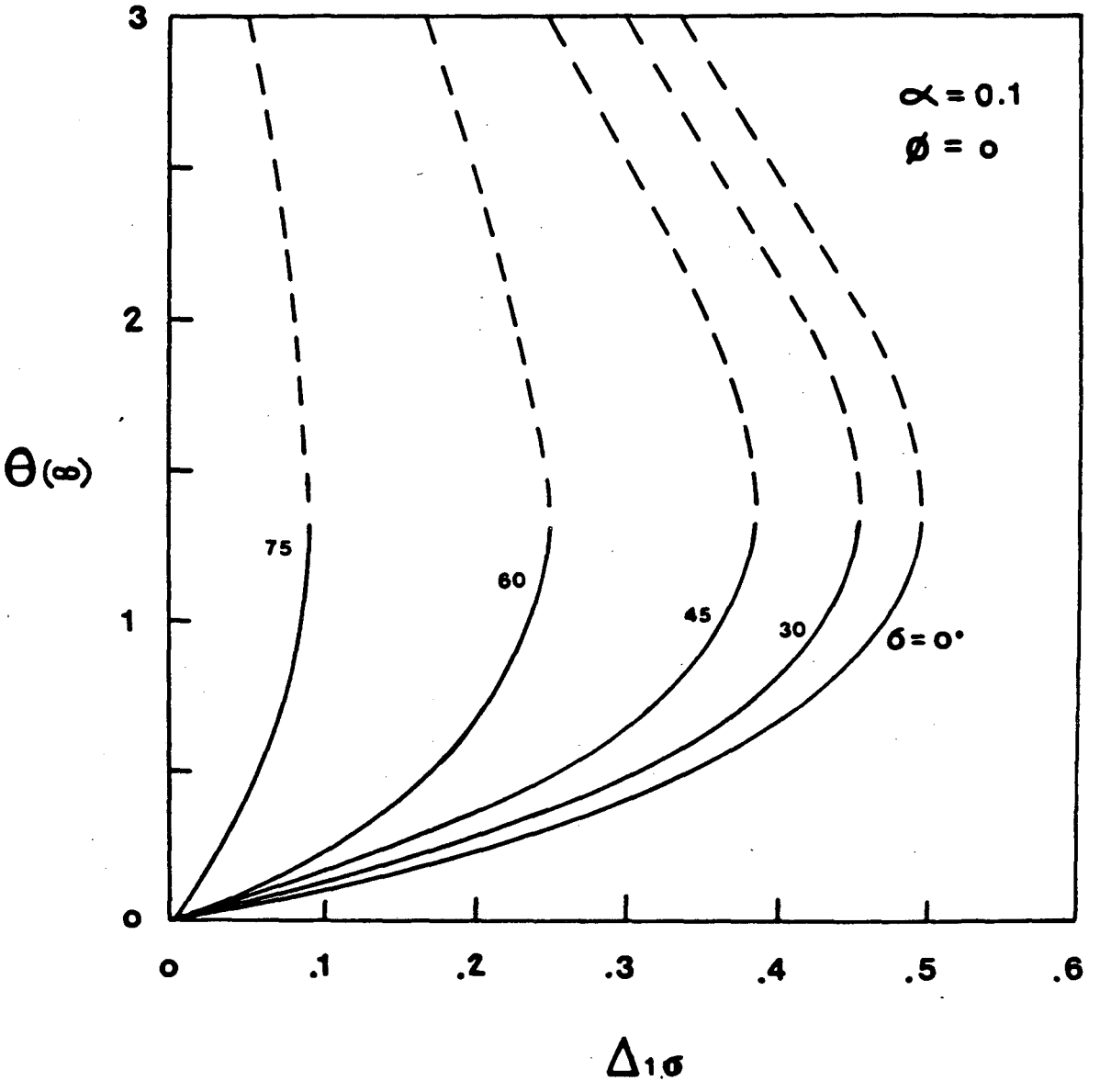

Fig 2.6

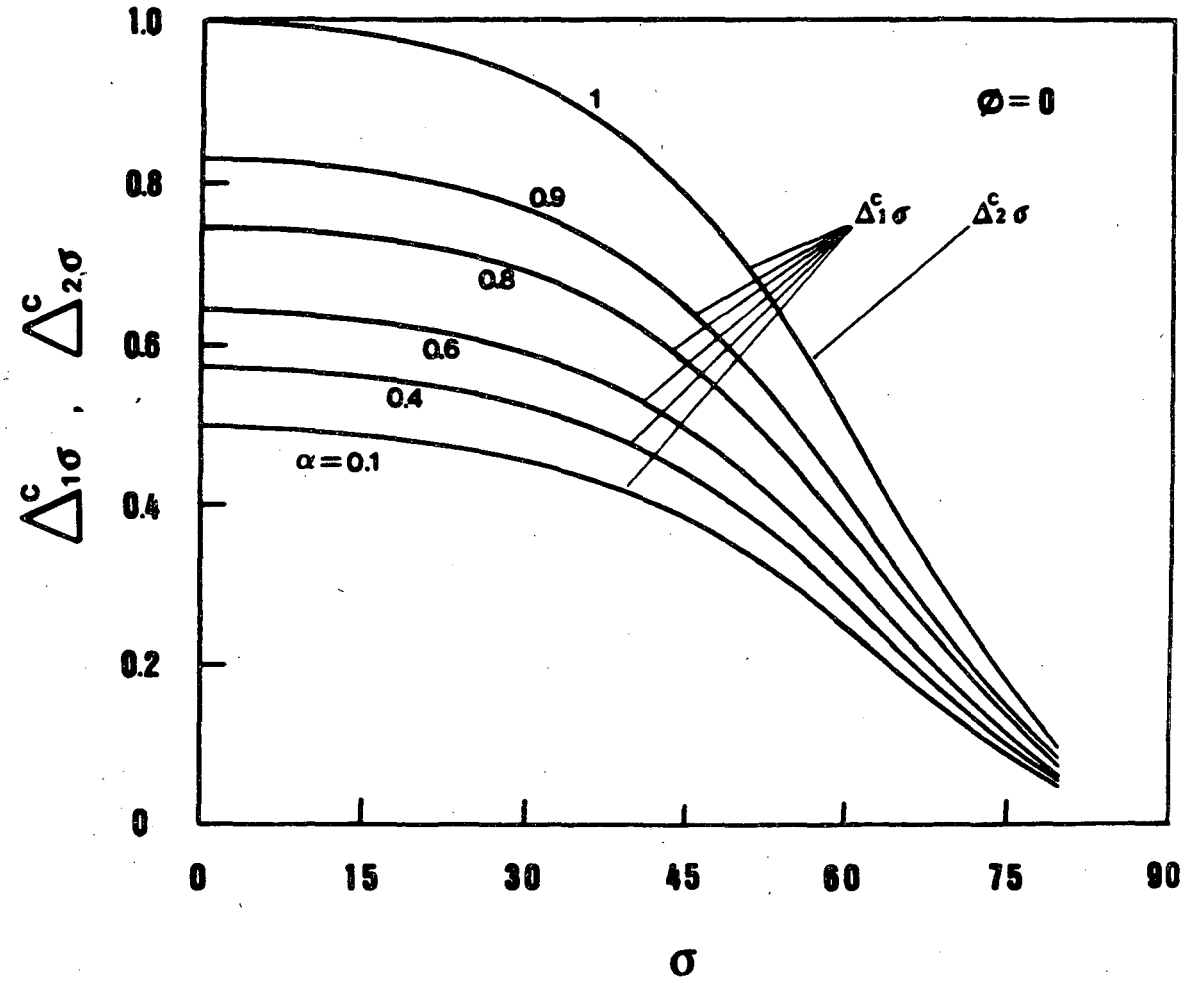
1.0
0.8
0.6
0.4
0.2
0
0
15
30
45
60
75
90
σ
$\Delta^c_{1\sigma}$, $\Delta^c_{2\sigma}$
1
0.9
0.8
0.6
0.4
α = 0.1
Ø = 0
$\Delta^c_{1\sigma}$
$\Delta^c_{2\sigma}$

Fig 2.7

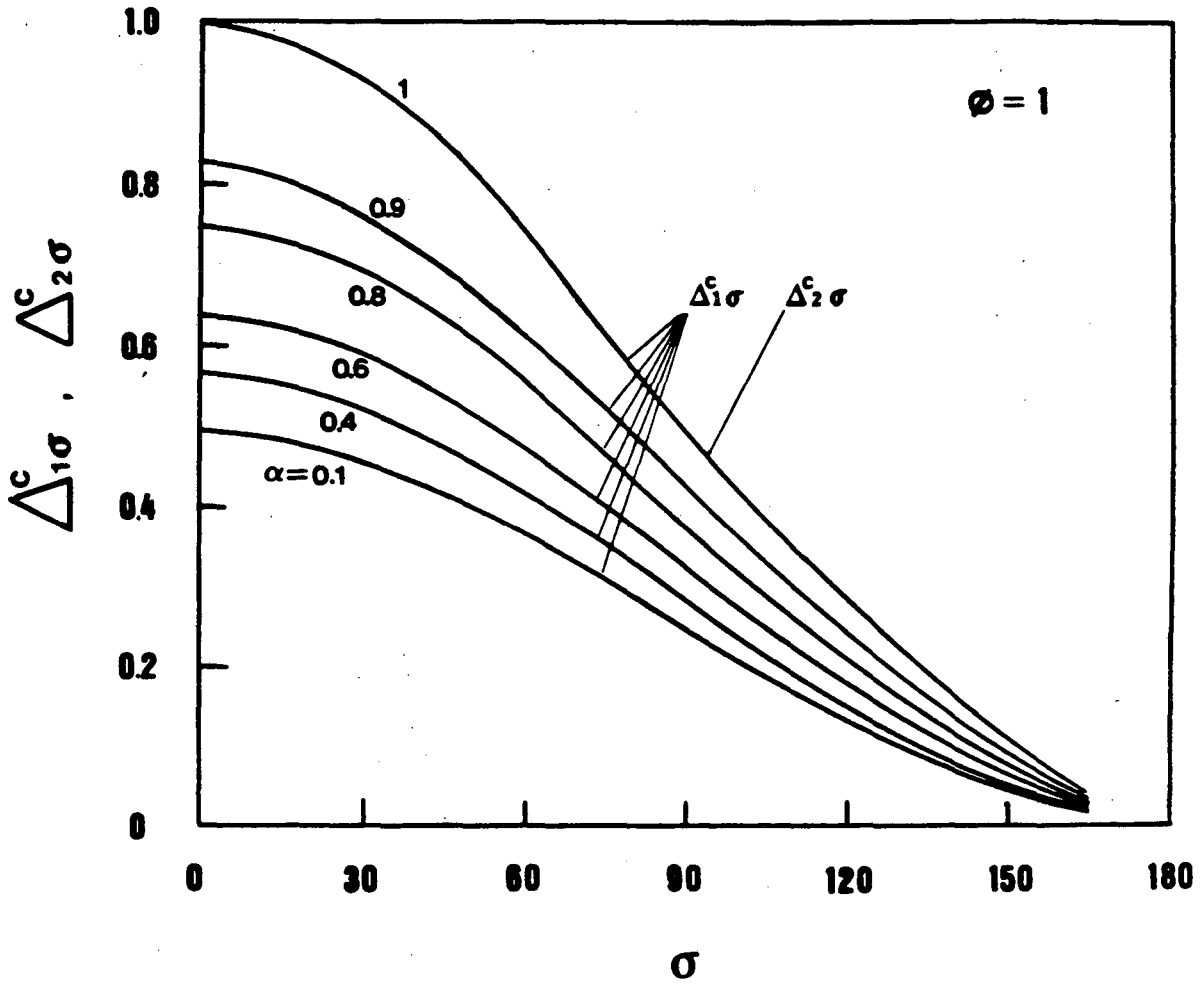
1.0
0.8
0.6
0.4
0.2
0
0
30
60
90
120
150
180
σ
$\Delta^c_{1\sigma}$, $\Delta^c_{2\sigma}$
Ø = 1
1
0.9
0.8
0.6
0.4
α=0.1
$\Delta^c_{1\sigma}$
$\Delta^c_{2\sigma}$

Fig 2.8

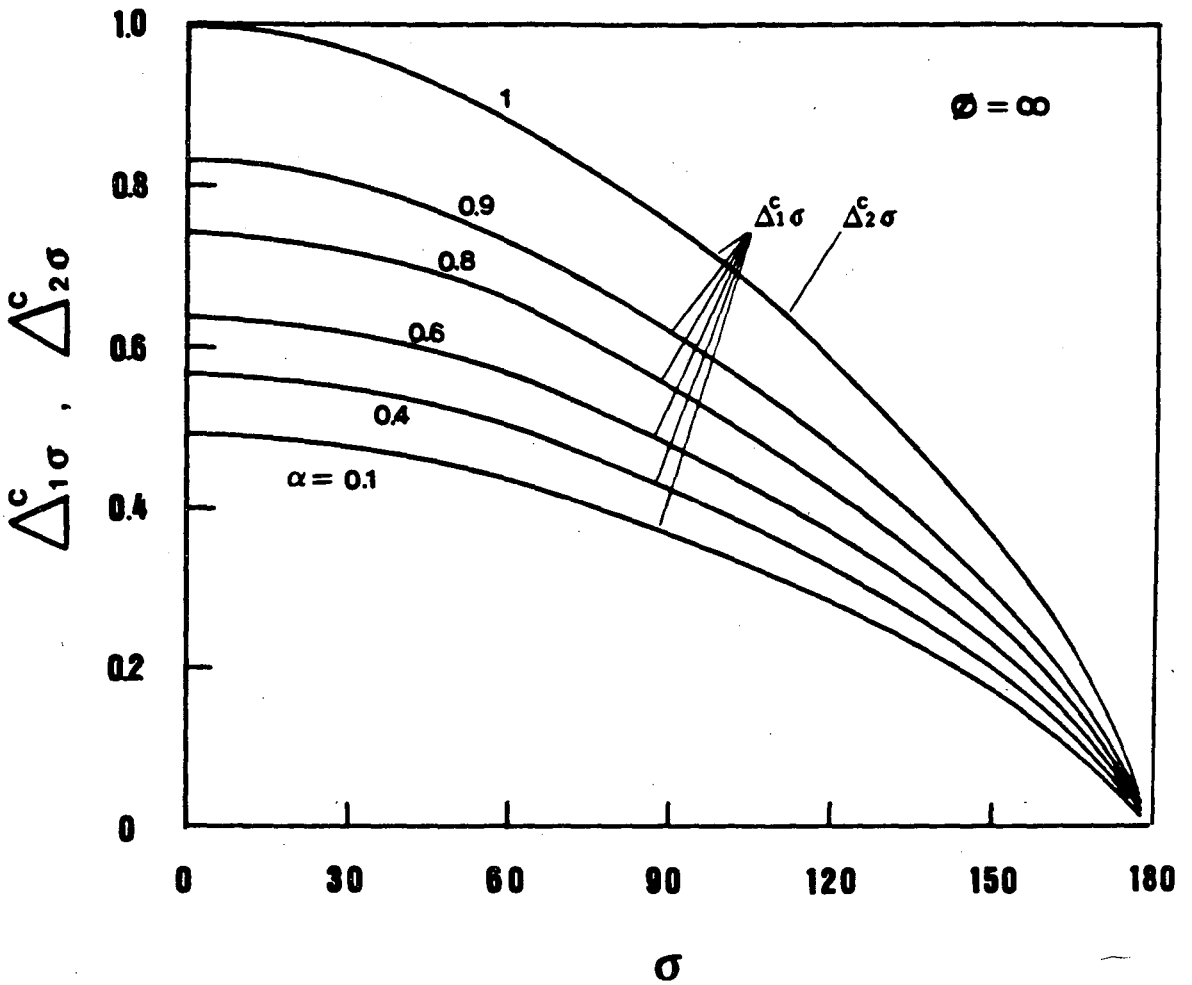
1.0
0.8
0.6
0.4
0.2
0
0
30
60
90
120
150
180
σ
$\Delta^c_{1\sigma}$, $\Delta^c_{2\sigma}$
Ø = ∞
1
0.9
0.8
0.6
0.4
α = 0.1
$\Delta^c_{1\sigma}$
$\Delta^c_{2\sigma}$

Fig 2.9

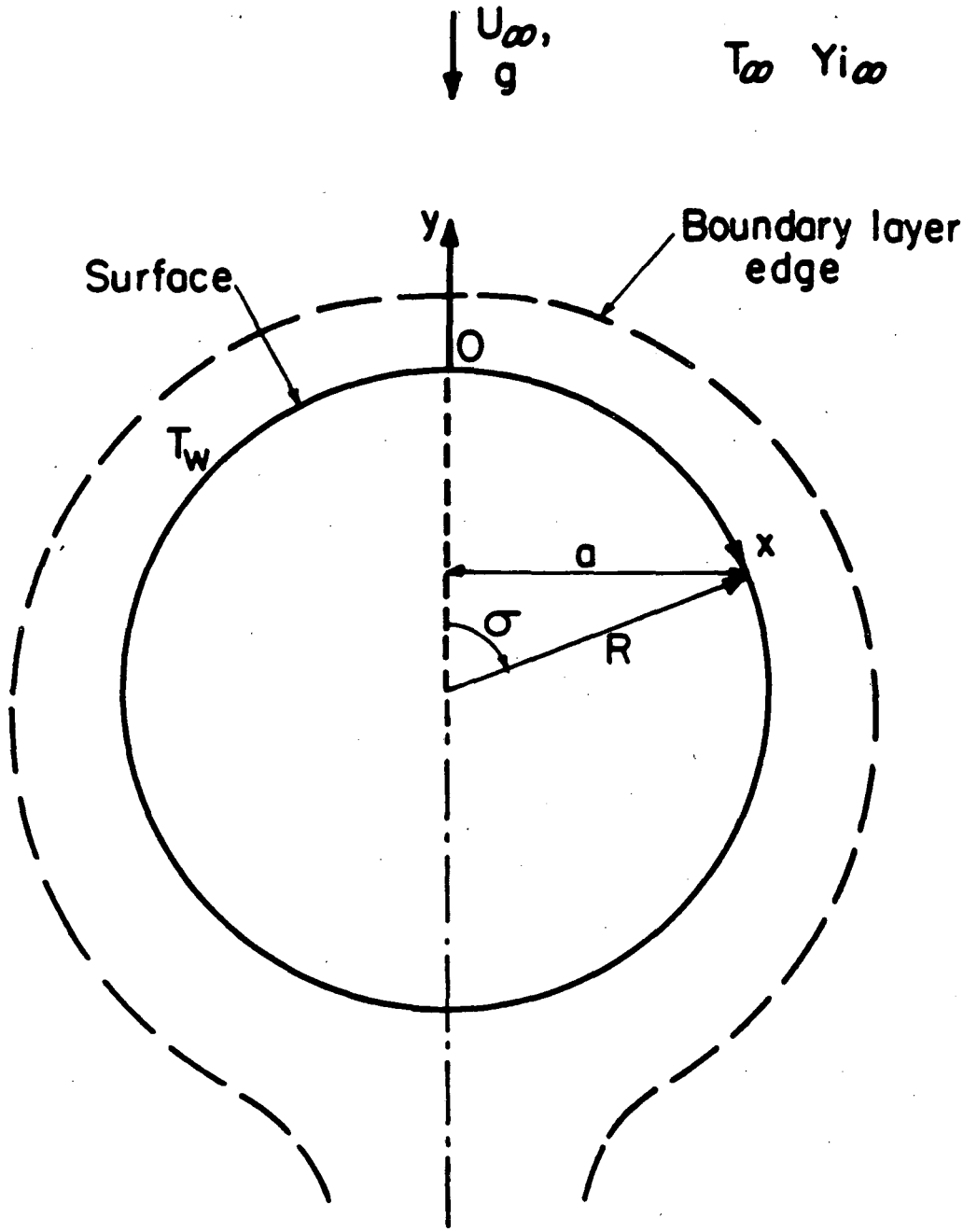
U_∞, g
T_∞ Yi_∞
y
Boundary layer edge
Surface
O
T_w
a
x
σ
R

Fig 3.1

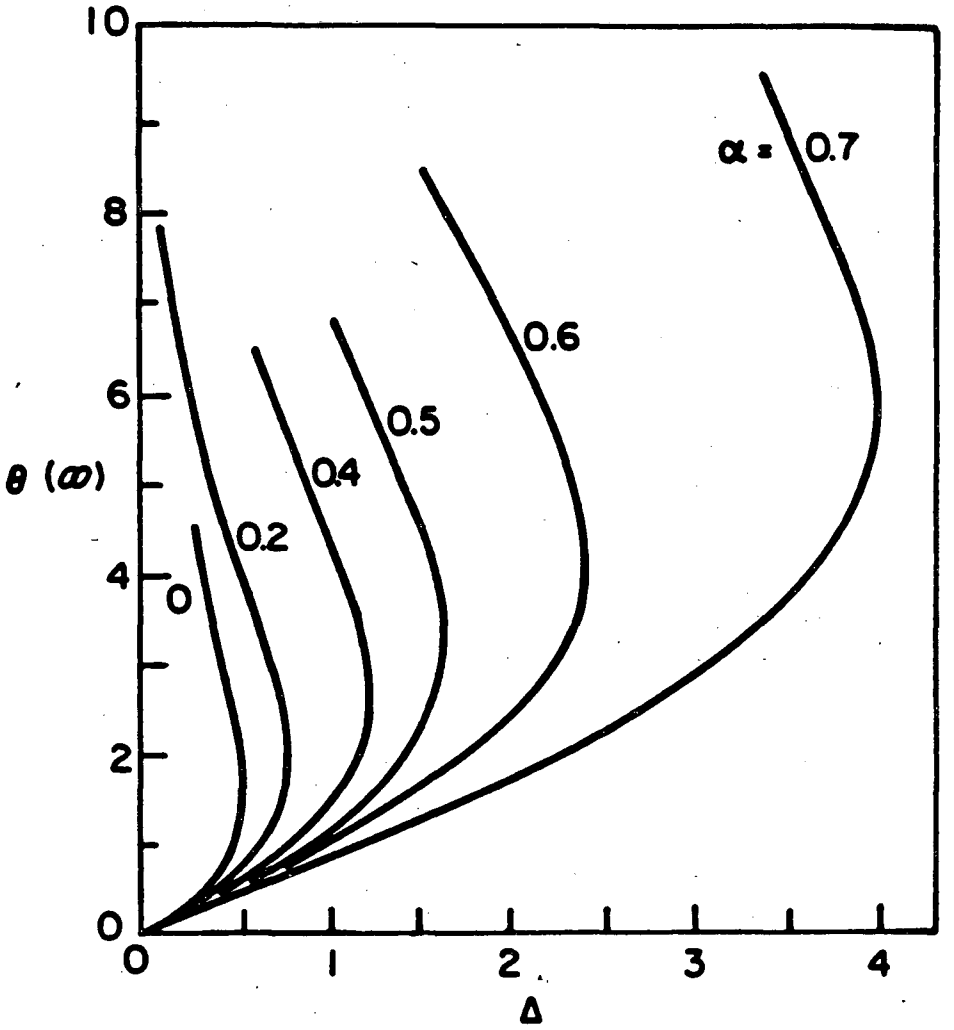

Fig 3.2

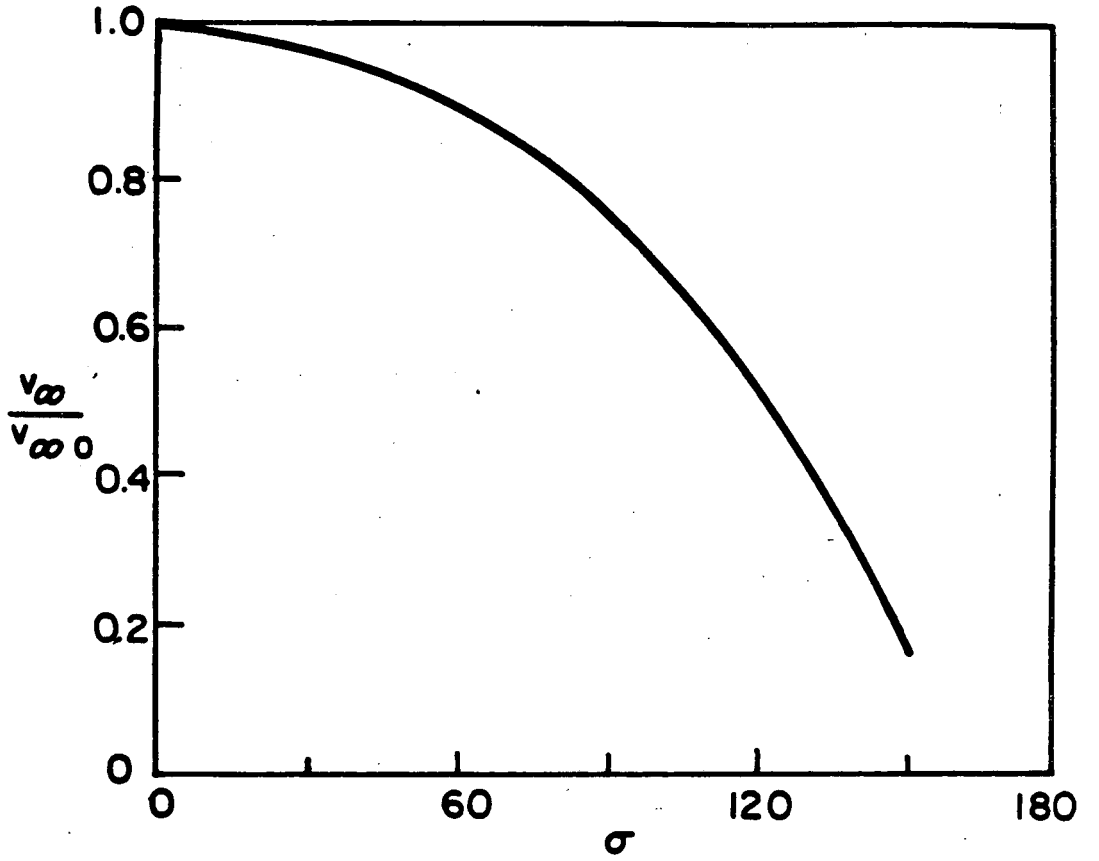

Fig 3.3

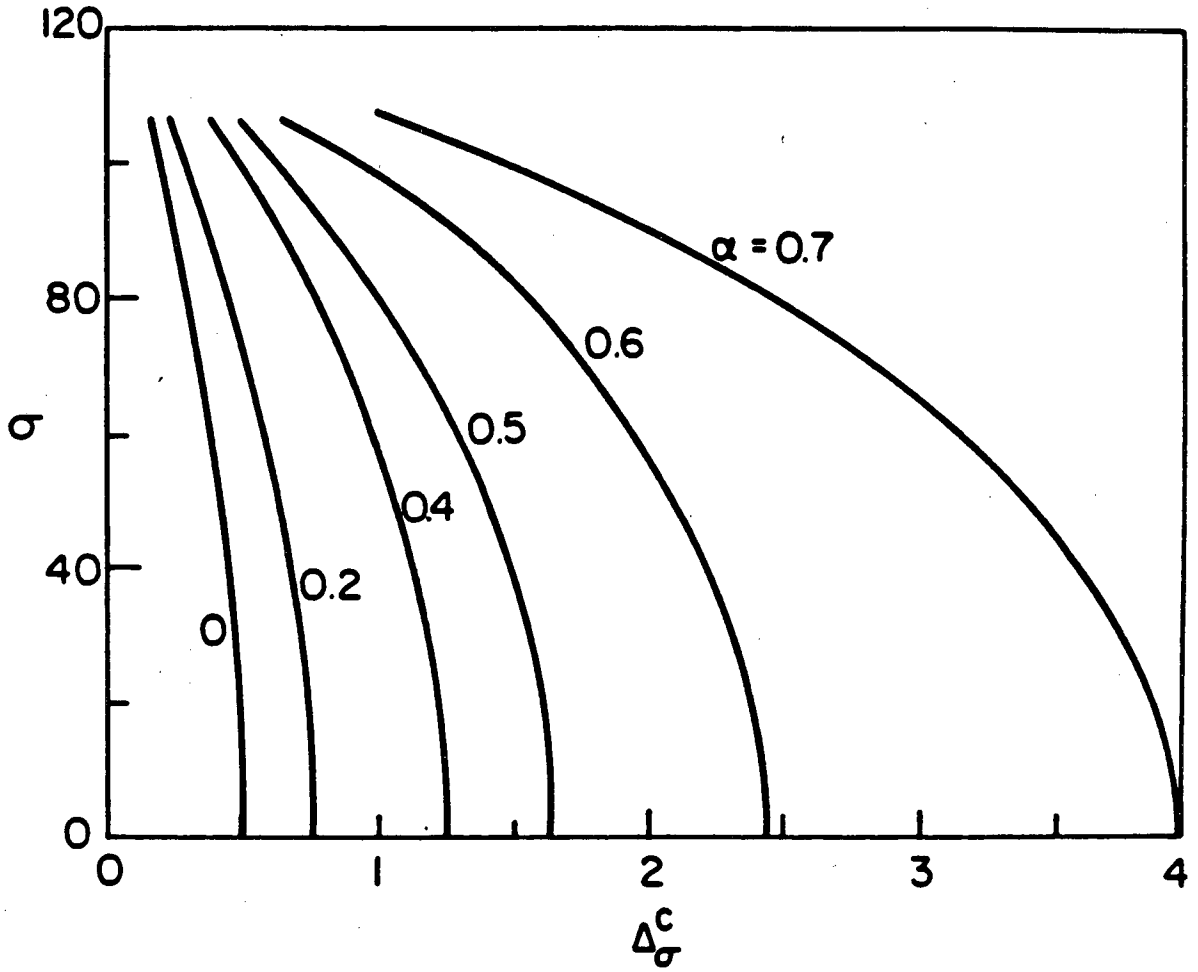

Fig 3.4

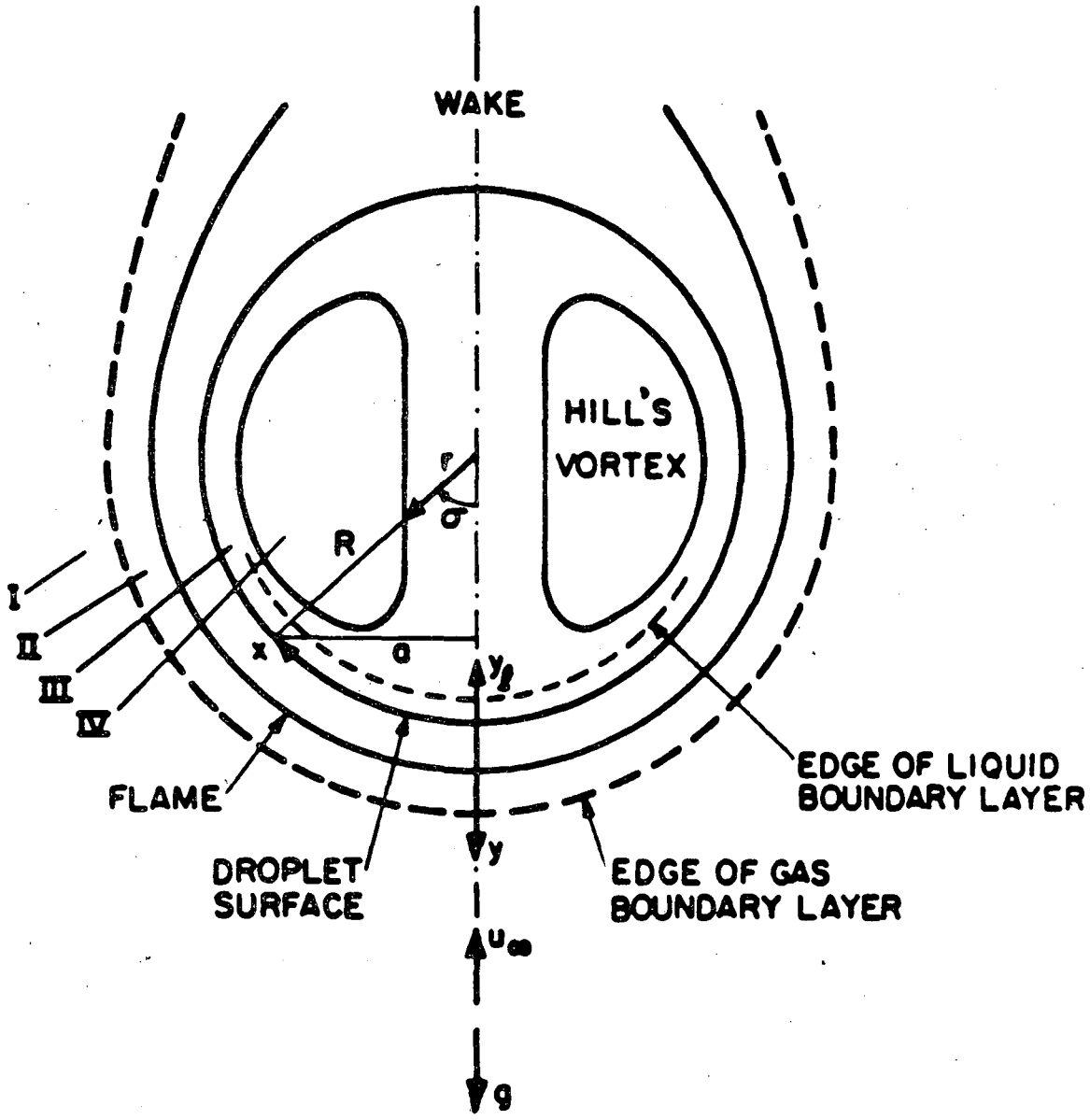
WAKE
HILL'S
VORTEX
r
σ
R
I
II
III
IV
x
a
y_ℓ
FLAME
DROPLET
SURFACE
y
EDGE OF LIQUID
BOUNDARY LAYER
EDGE OF GAS
BOUNDARY LAYER
u_∞
g

Fig 4.1

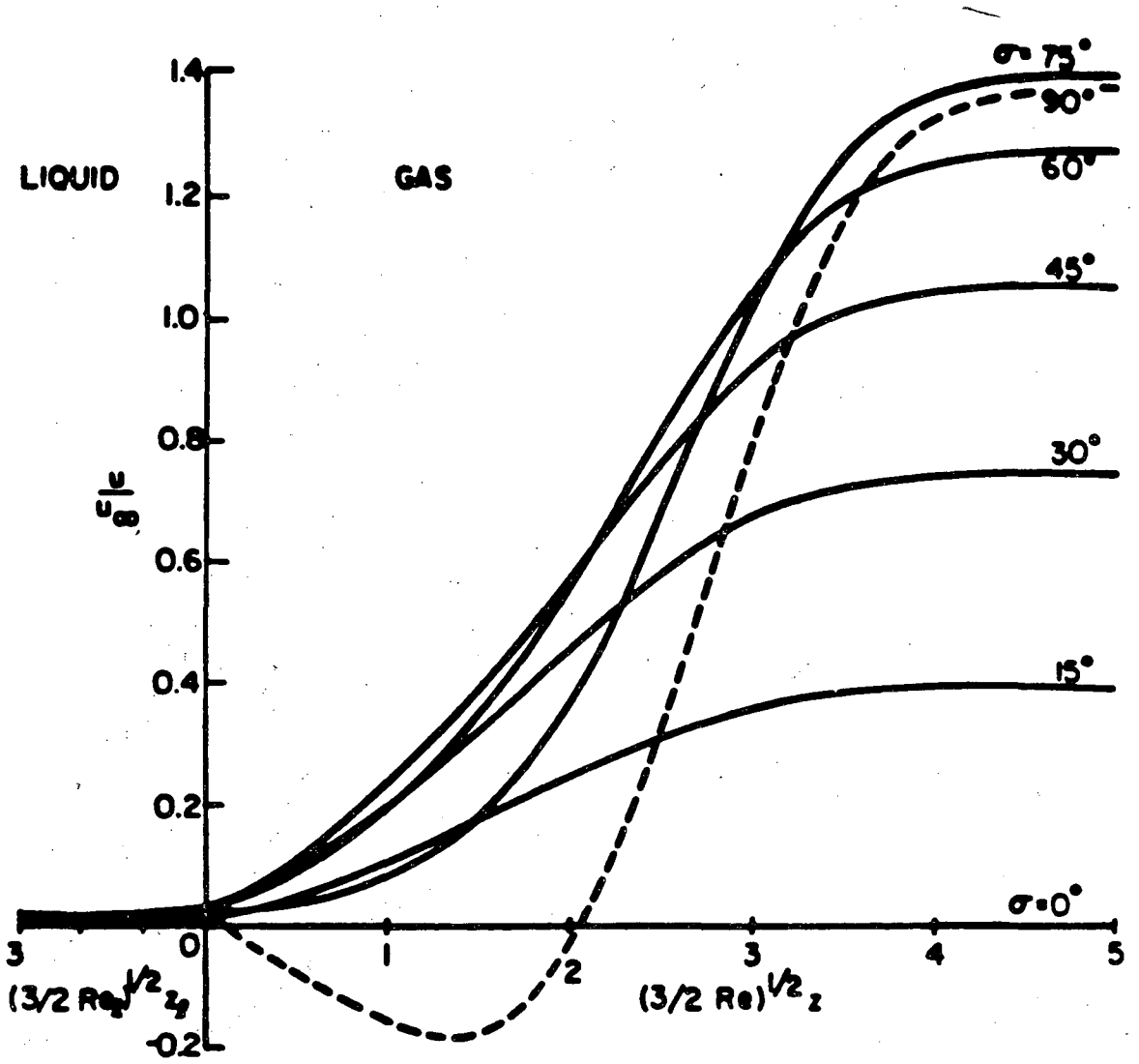
LIQUID
GAS
1.4
1.2
1.0
0.8
0.6
0.4
0.2
-0.2
$\frac{u}{u_\infty}$
σ = 75°
90°
60°
45°
30°
15°
σ = 0°
3
0
1
2
3
4
5
$(3/2\ Re_g)^{1/2} z_g$
$(3/2\ Re)^{1/2} z$

Fig 4.2a

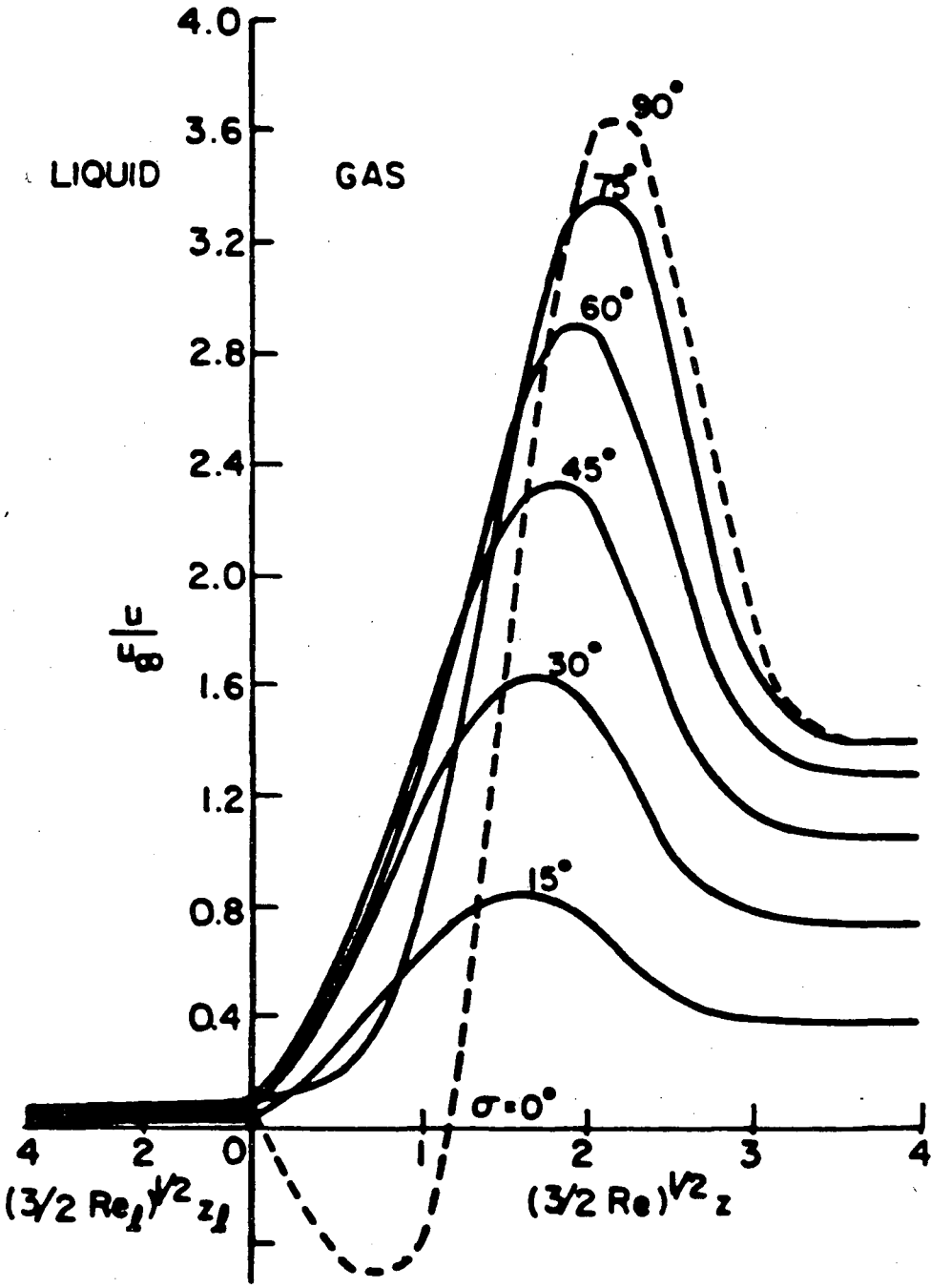
4.0
3.6
3.2
2.8
2.4
2.0
1.6
1.2
0.8
0.4
LIQUID
GAS
90°
75°
60°
45°
30°
15°
σ=0°
$\frac{u}{u_\infty}$
4
2
0
1
2
3
4
$(3/2\ Re_l)^{1/2} z_l$
$(3/2\ Re)^{1/2} z$

Fig 4.2b

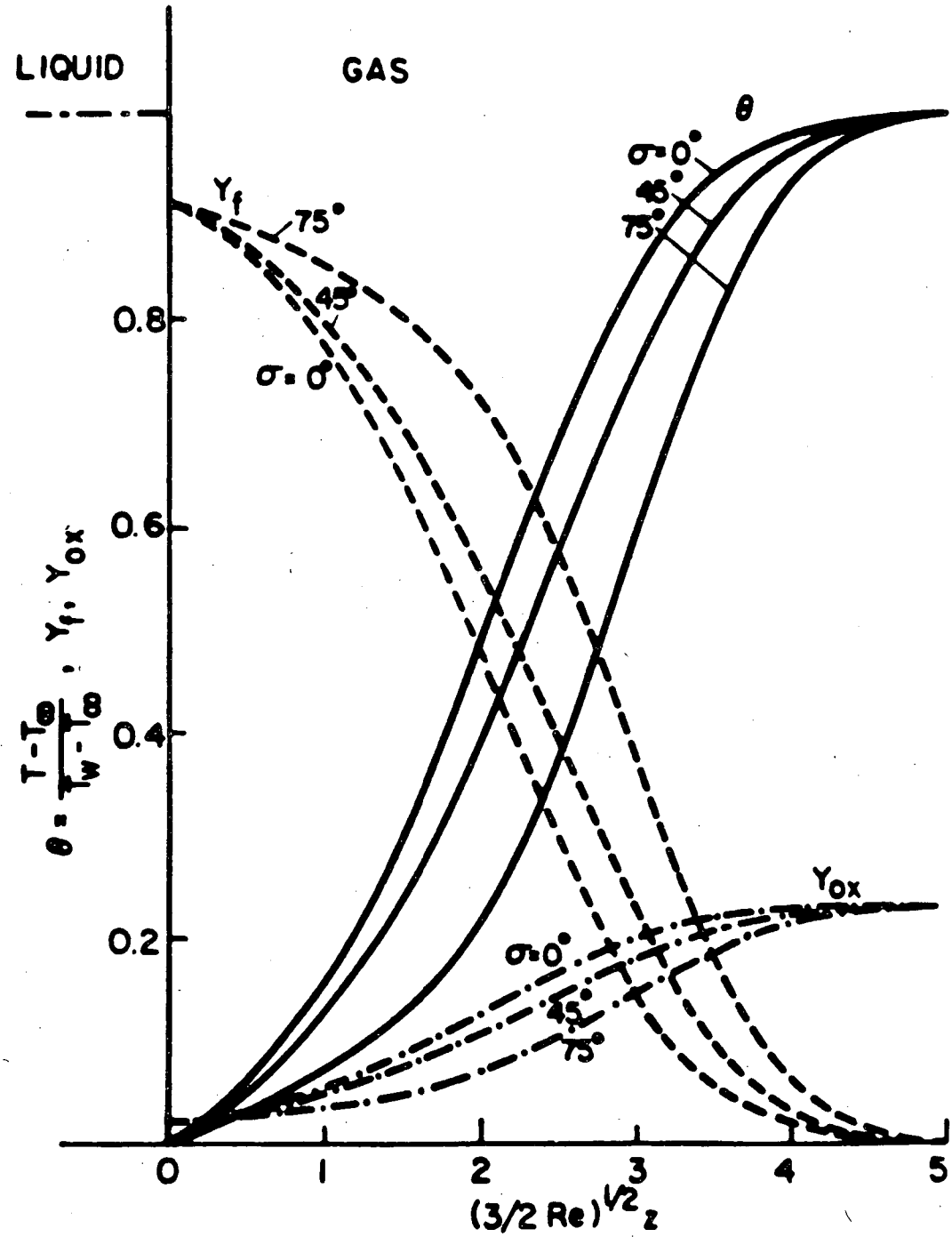
LIQUID
GAS
θ
σ=0°
45°
75°
Yf
75°
45°
σ=0°
0.8
0.6
0.4
0.2
θ = (T-T∞)/(Tw-T∞) , Yf, Yox
Yox
σ=0°
45°
75°
0
1
2
3
4
5
(3/2 Re)^1/2 z

Fig 4.3a

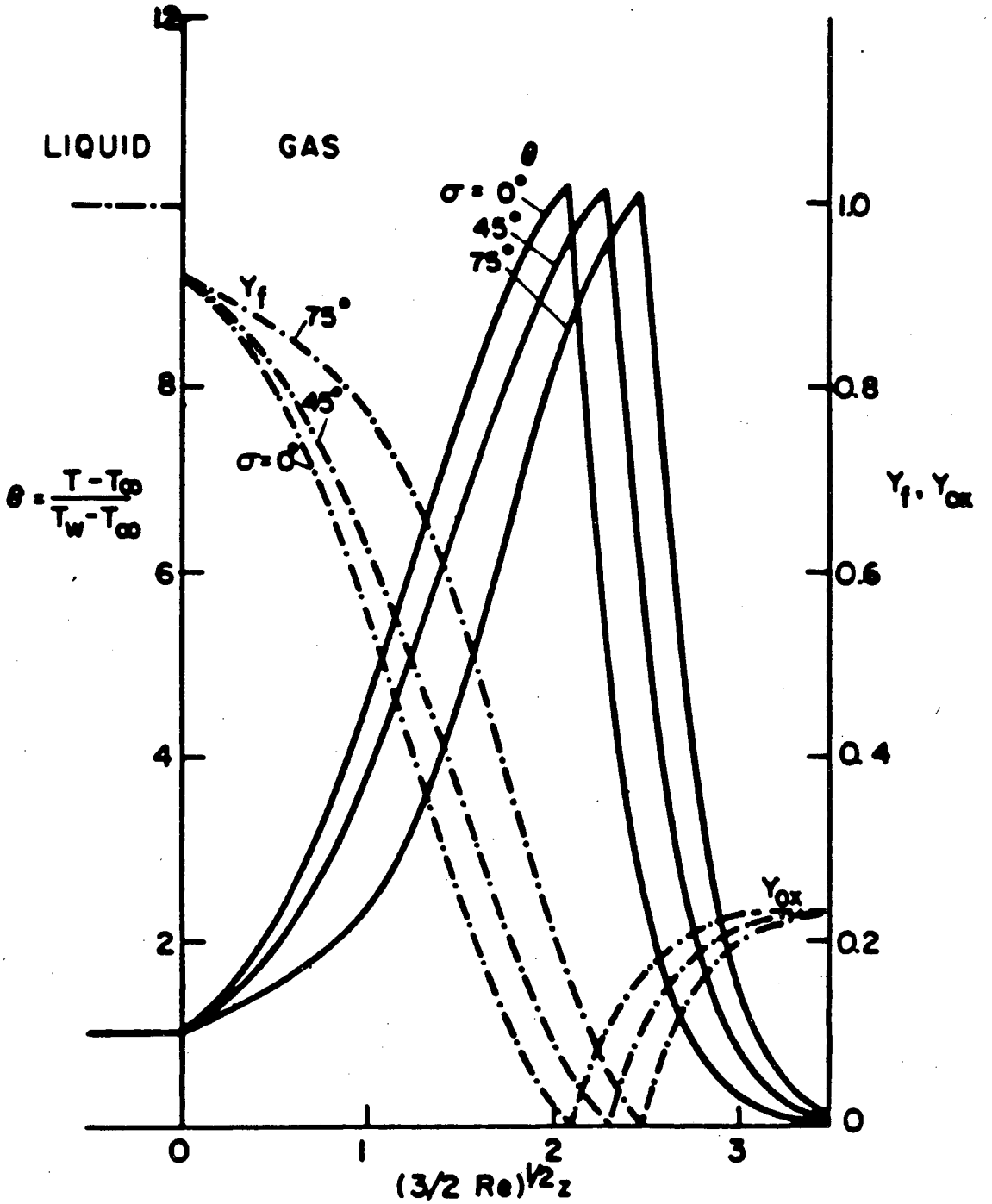
LIQUID
GAS
θ
σ = 0°
45°
75°
Yf
75°
45°
σ = 0°
θ = (T - T∞)/(Tw - T∞)
Yf, Yox
Yox
12
8
6
4
2
1.0
0.8
0.6
0.4
0.2
0
0
1
2
3
(3/2 Re)^1/2 z

Fig 4.3b

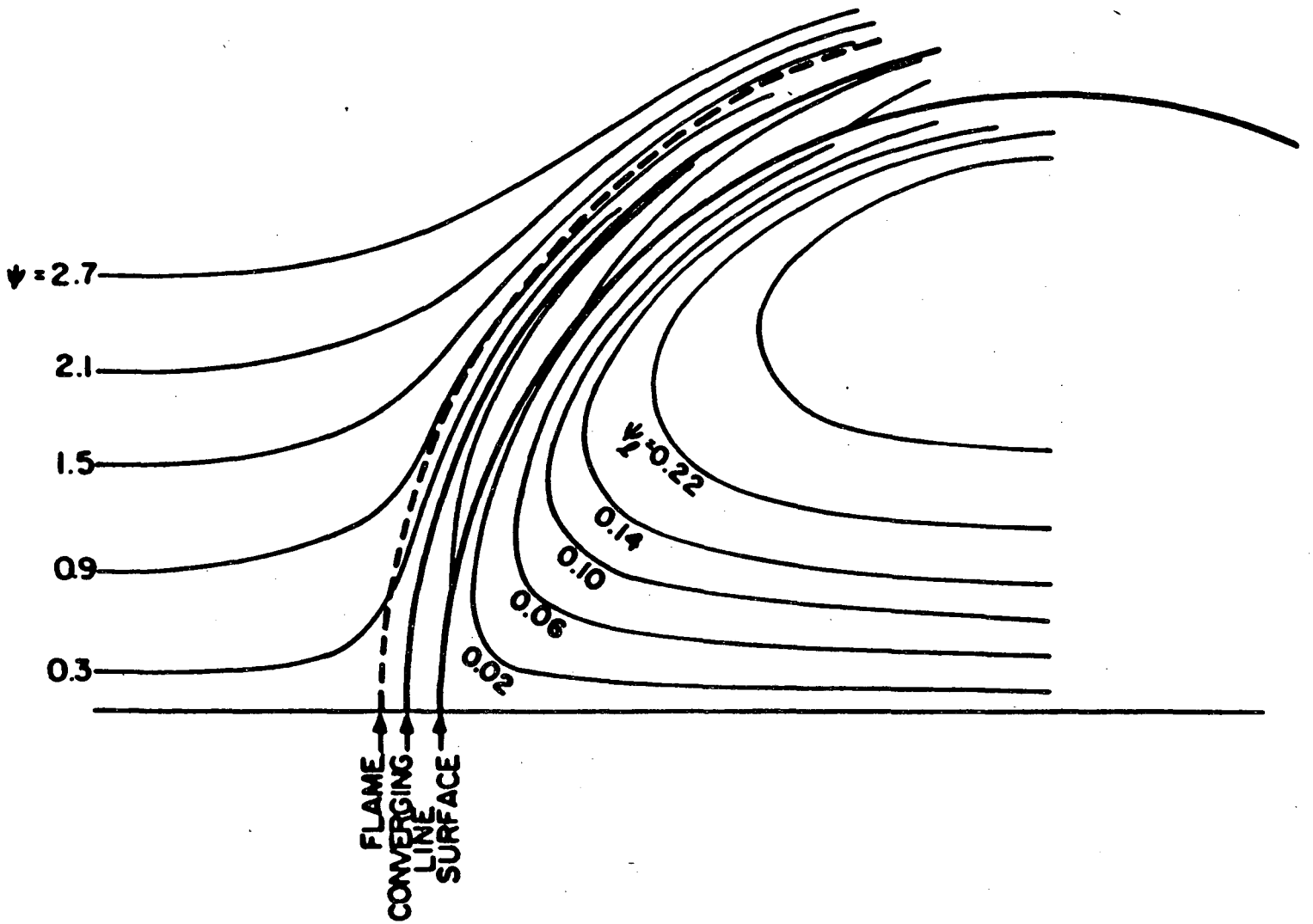
ψ = 2.7
2.1
1.5
0.9
0.3
ψ = 0.22
0.14
0.10
0.06
0.02
FLAME
CONVERGING
LINE
SURFACE

Fig 4.4

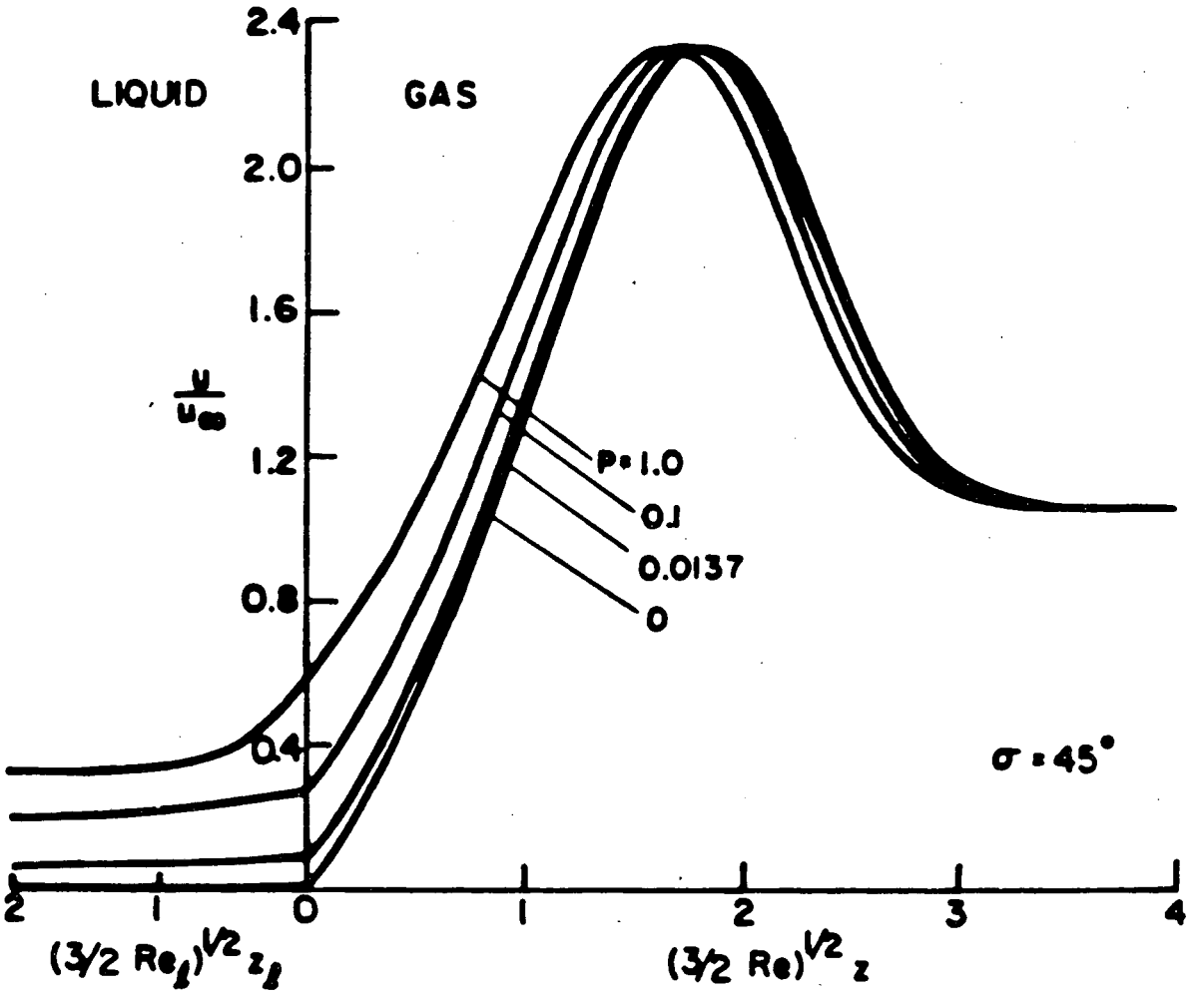
LIQUID
GAS
2.4
2.0
1.6
1.2
0.8
0.4
u/u∞
P = 1.0
0.1
0.0137
0
σ = 45°
2
1
0
1
2
3
4
(3/2 Re_l)^1/2 z_l
(3/2 Re)^1/2 z

Fig 4.5a

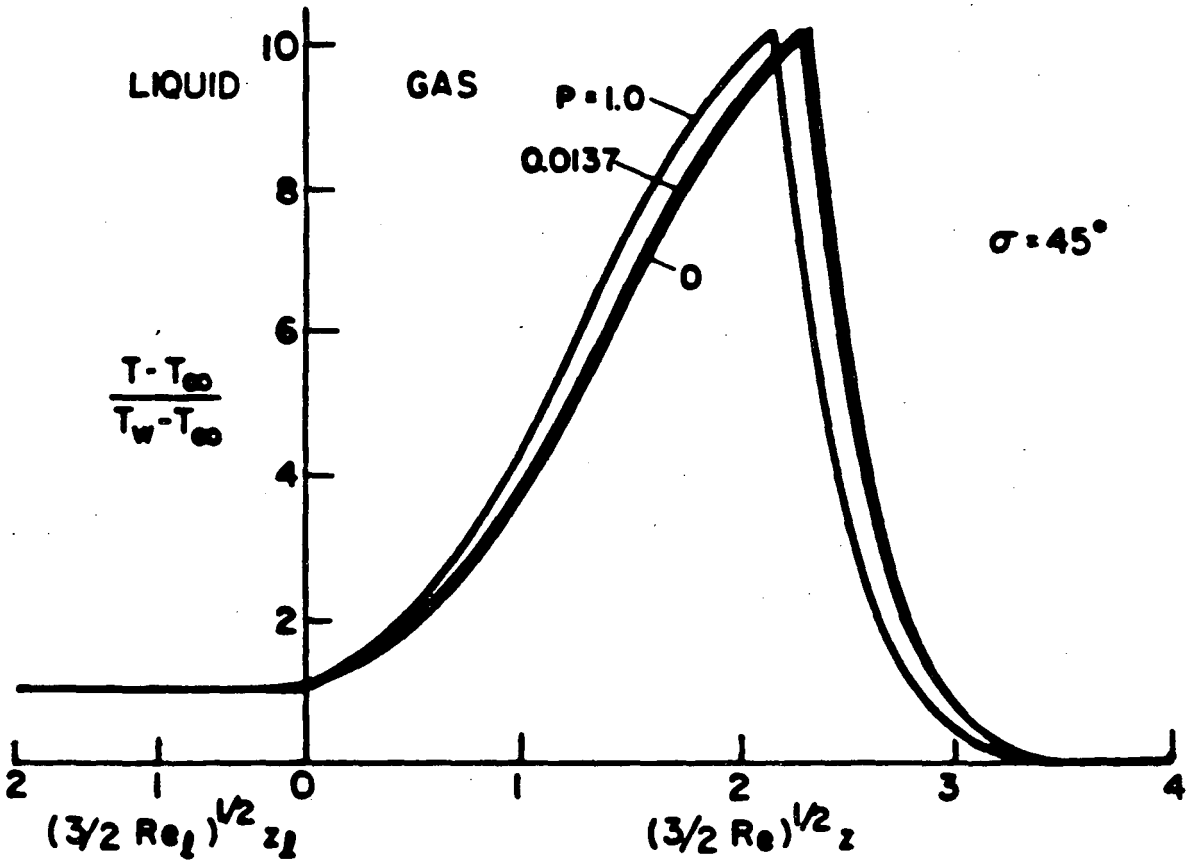
LIQUID
GAS
P = 1.0
0.0137
0
σ = 45°
$\frac{T - T_\infty}{T_w - T_\infty}$
10
8
6
4
2
2
1
0
1
2
3
4
$(3/2\ Re_l)^{1/2} z_l$
$(3/2\ Re)^{1/2} z$

Fig 4.5 b

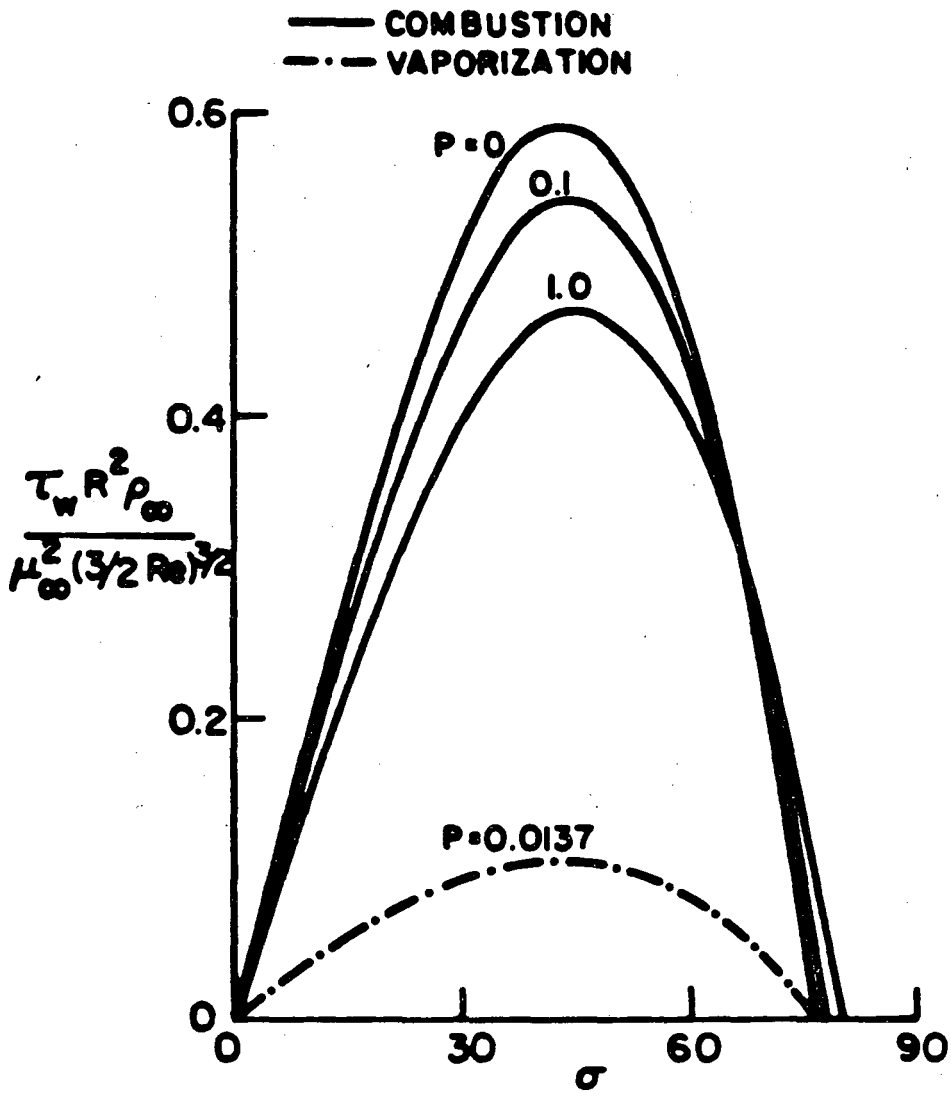
COMBUSTION
VAPORIZATION
0.6
0.4
0.2
0
P = 0
0.1
1.0
P = 0.0137
$\frac{\tau_w R^2 \rho_\infty}{\mu_\infty^2 (3/2\, Re)^{3/2}}$
0
30
60
90
σ

Fig 4.6a

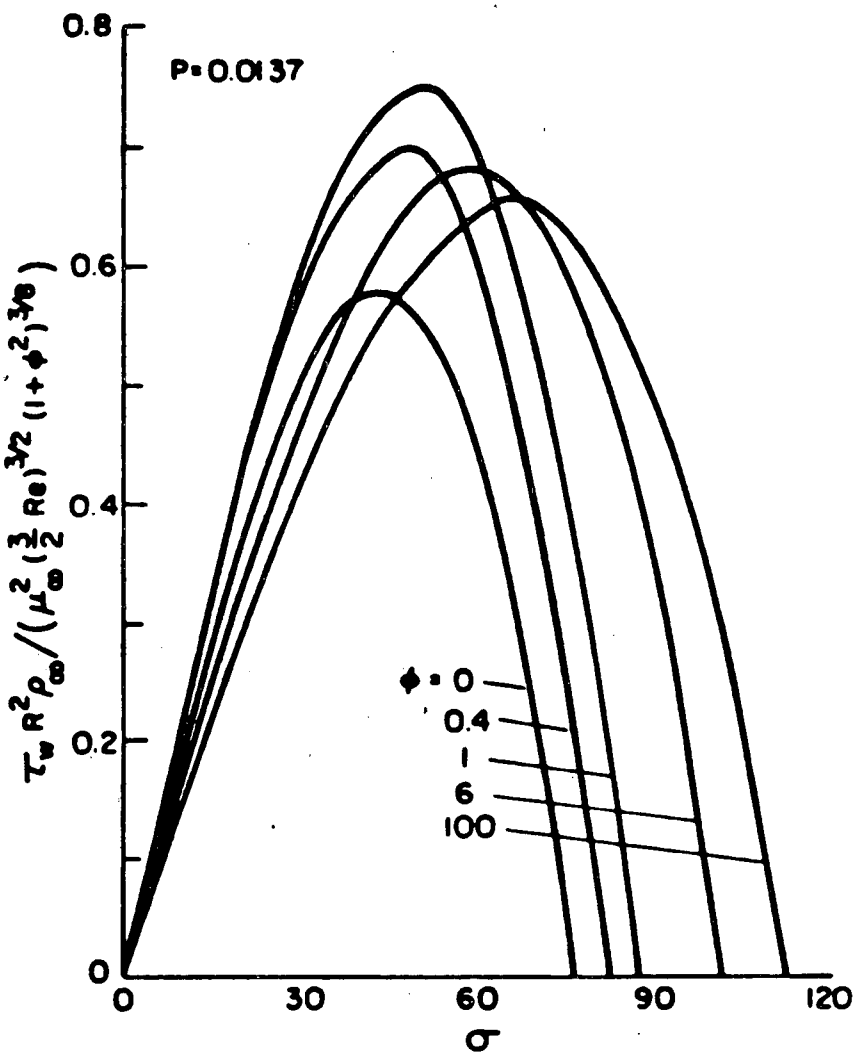
P=0.0137
0.8
0.6
0.4
0.2
0
0
30
60
90
120
σ
$\tau_w R^2 \rho_\infty / (\mu_\infty^2 (\frac{3}{2} Re)^{3/2} (1+\phi^2)^{3/8})$
φ = 0
0.4
1
6
100

Fig 4.6b

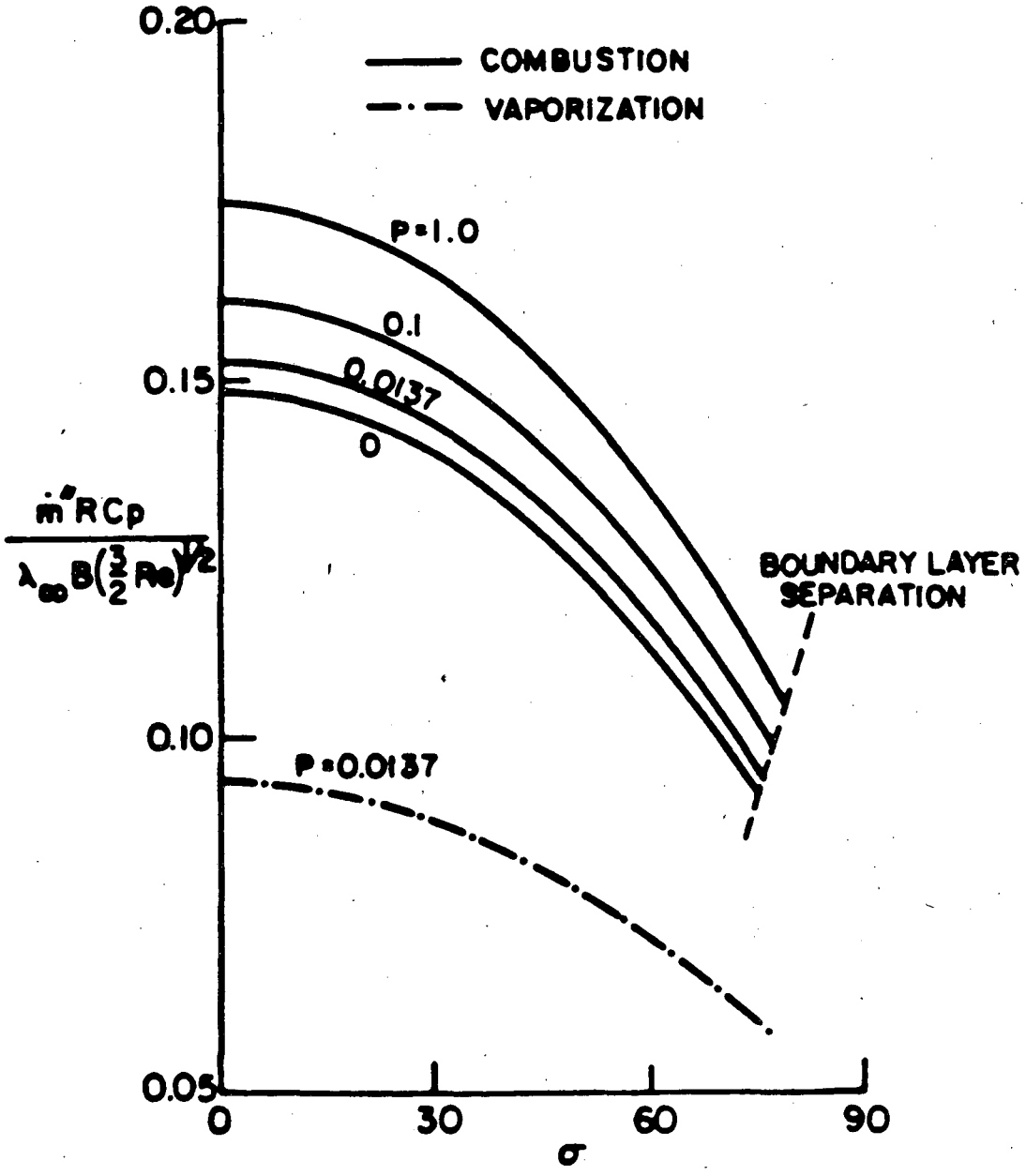
0.20
0.15
0.10
0.05
COMBUSTION
VAPORIZATION
P=1.0
0.1
0.0137
0
P=0.0137
BOUNDARY LAYER SEPARATION
$\frac{\dot{m}'' R C_p}{\lambda_\infty B (\frac{3}{2} Re)^{1/2}}$
0
30
60
90
σ

Fig 4.7a

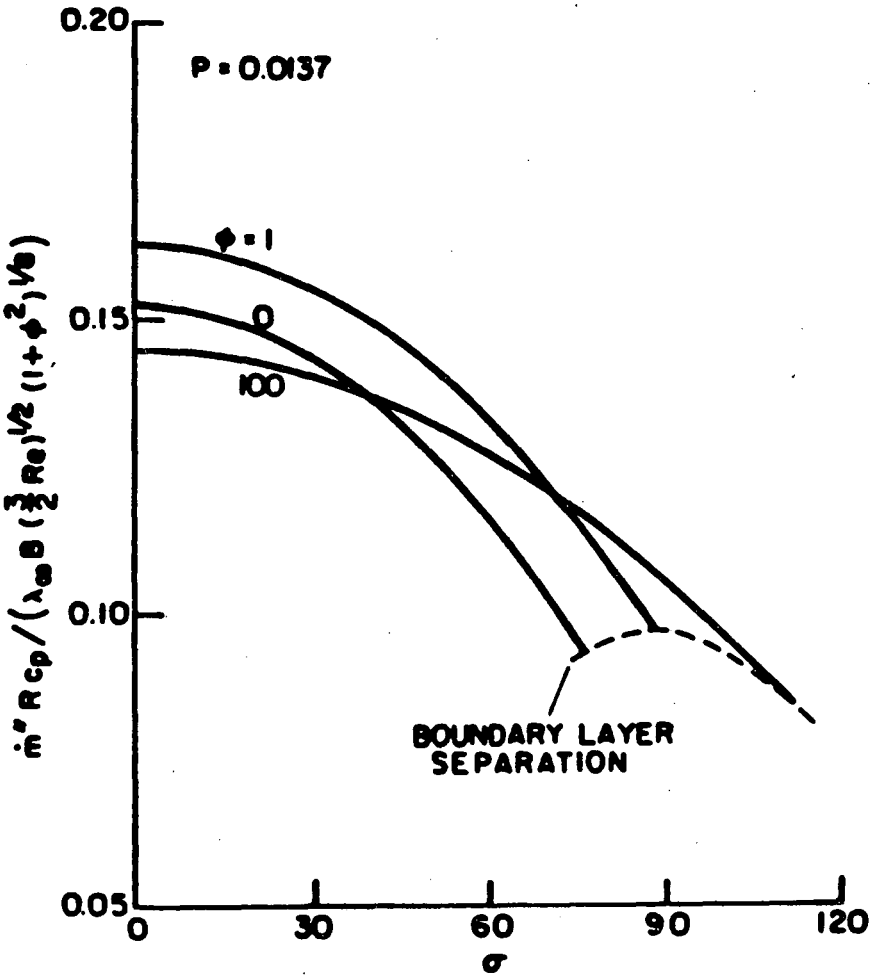
0.20
0.15
0.10
0.05
P = 0.0137
φ = 1
0
100
BOUNDARY LAYER
SEPARATION
0
30
60
90
120
σ

Fig 4.7b

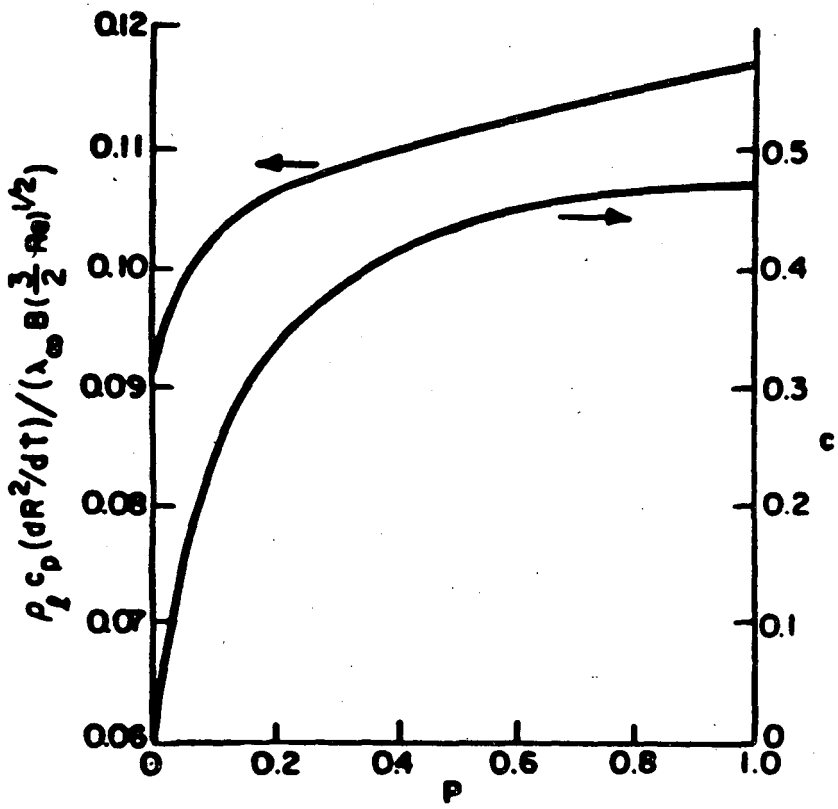

Fig 4.8a

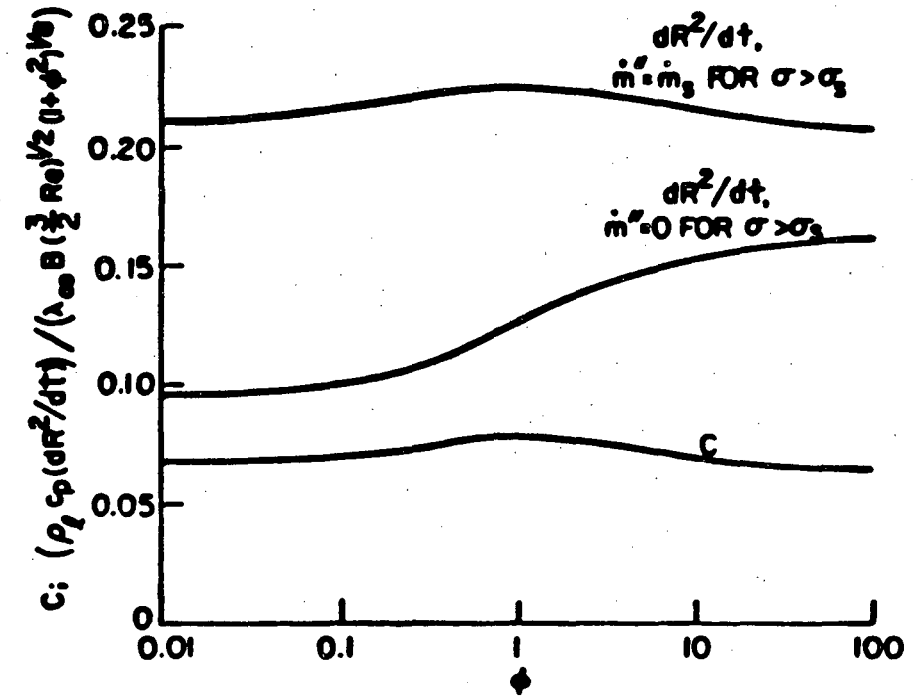
0.25
0.20
0.15
0.10
0.05
0
0.01
0.1
1
10
100
ϕ
C_i $(\rho_\ell c_p (dR^2/dt)/(\lambda_\infty B(\frac{3}{2} Re)^{1/2}(1+\phi^2)^{1/2})$
dR^2/dt,
$\dot{m}'' = \dot{m}_s$ FOR $\sigma > \sigma_s$
dR^2/dt,
$\dot{m}'' = 0$ FOR $\sigma > \sigma_s$
C

Fig 4.8b

This report was done with support from the Department of Energy. Any conclusions or opinions expressed in this report represent solely those of the author(s) and not necessarily those of The Regents of the University of California, the Lawrence Berkeley Laboratory or the Department of Energy.

Reference to a company or product name does not imply approval or recommendation of the product by the University of California or the U.S. Department of Energy to the exclusion of others that may be suitable.

LAWRENCE BERKELEY LABORATORY
TECHNICAL INFORMATION DEPARTMENT
UNIVERSITY OF CALIFORNIA
BERKELEY, CALIFORNIA 94720